ProtonVDA

TRANSFORMING PROTON THERAPY

First test of pCT in a Gantry System: Results and Challenges

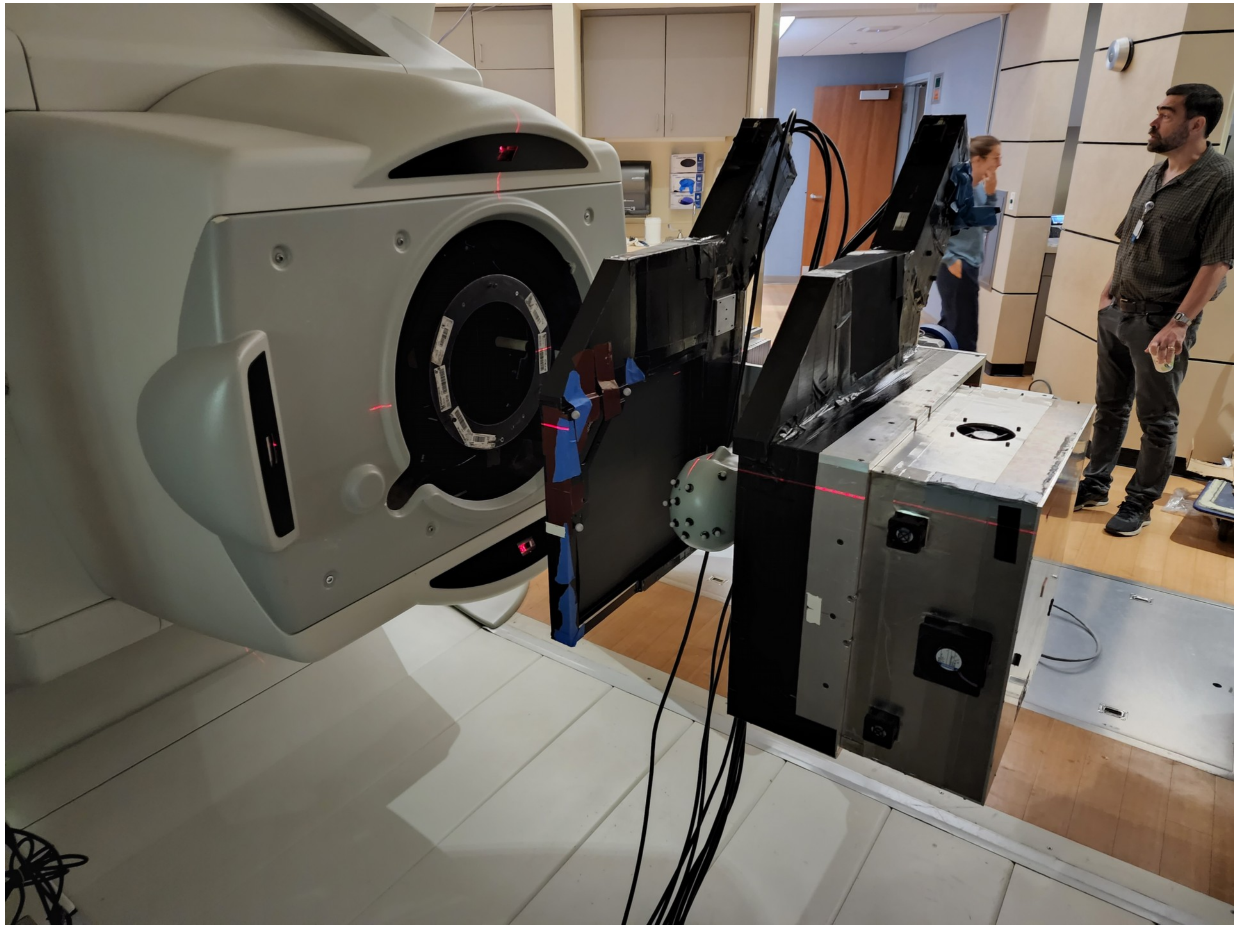

Ethan DeJongh
ProtonVDA LLC

July 18, 2022

Proton Imaging can help reduce range uncertainties by directly measuring proton stopping power

We aim to:

Develop a proton imaging system based on well-established fast scintillator technology.

1. → High-performance, low-cost measurements of proton range.
2. Achieve lower dose to the patient relative to equivalent x-ray images.
3. Produce spatially sharp images.
4. Images free of artifacts from high-Z implants.

Multidisciplinary team of detector physicists, medical physicists, computer scientists, and radiation oncologists:

- ProtonVDA: Fritz DeJongh, Ethan DeJongh, Victor Rykalin
- Loyola Stritch School of Medicine: James Welsh
- Northwestern Medicine Chicago Proton Center: Mark Pankuch, Brad Kreydick
- Northern Illinois University, Dept. of Computer Science: Nick Karonis, Cesar Ordonez, John Winans, Kirk Duffin. Dept. of Physics: George Coutrakon, Christina Sarosiek
- Loma Linda University: Reinhard Schulte

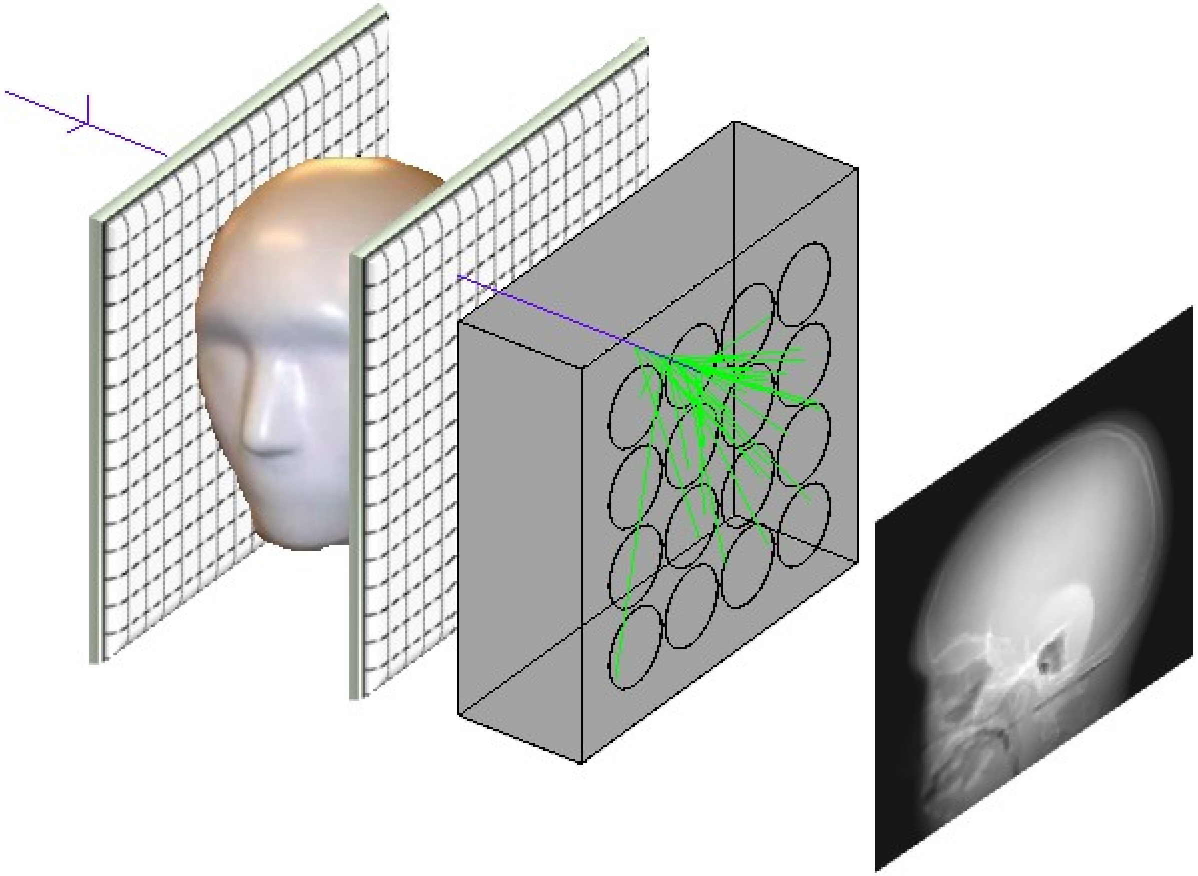

- X-Y tracking planes upstream and downstream

- Multiplexed fiber readout
  - 32 digitized channels per tracking plane
  - position ambiguities resolved using pencil beam targeting information
  - reduces amount of electronics needed

- 40 x 40 x 13 cm block of scintillator for range detector
  - 4 x 4 array of PMTs
  - Output digitized into four channels: E, U, V,C

- Individual protons tracked at up 10 MHz
- > 99% tracking efficiency
- WEPL resolution ~ 3 mm per proton
- 40 x 40 cm image field size
- Fast (<1 min) image reconstruction for radiograph

Fiber layout cross-section for one tracking plane:

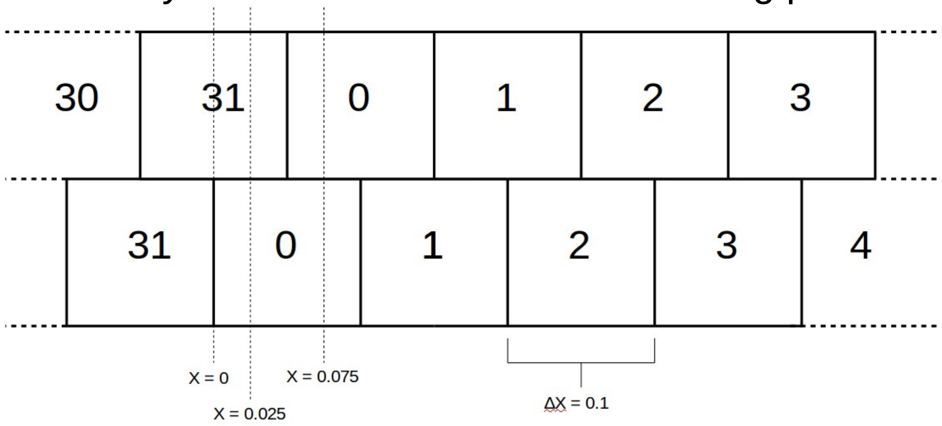

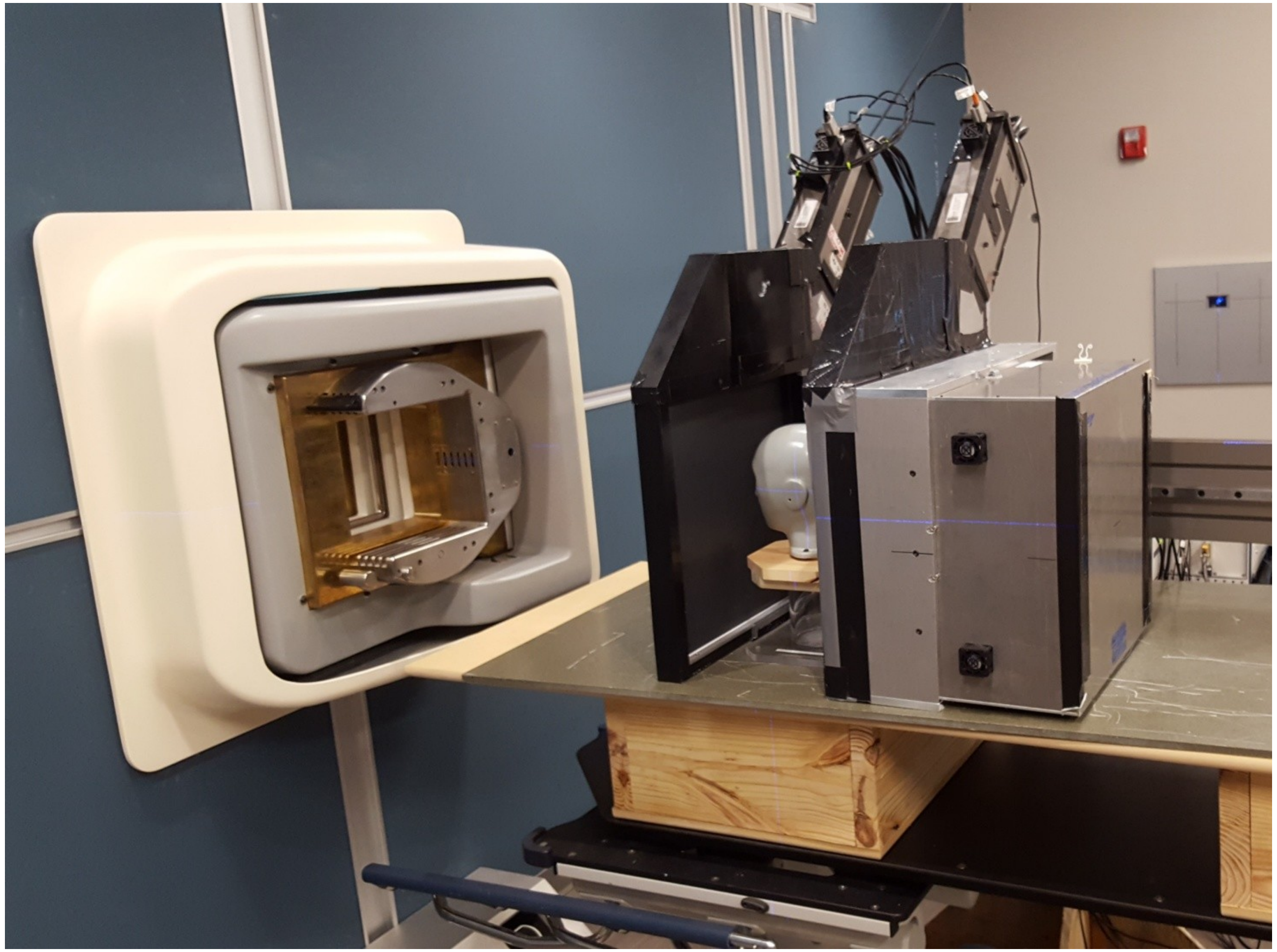

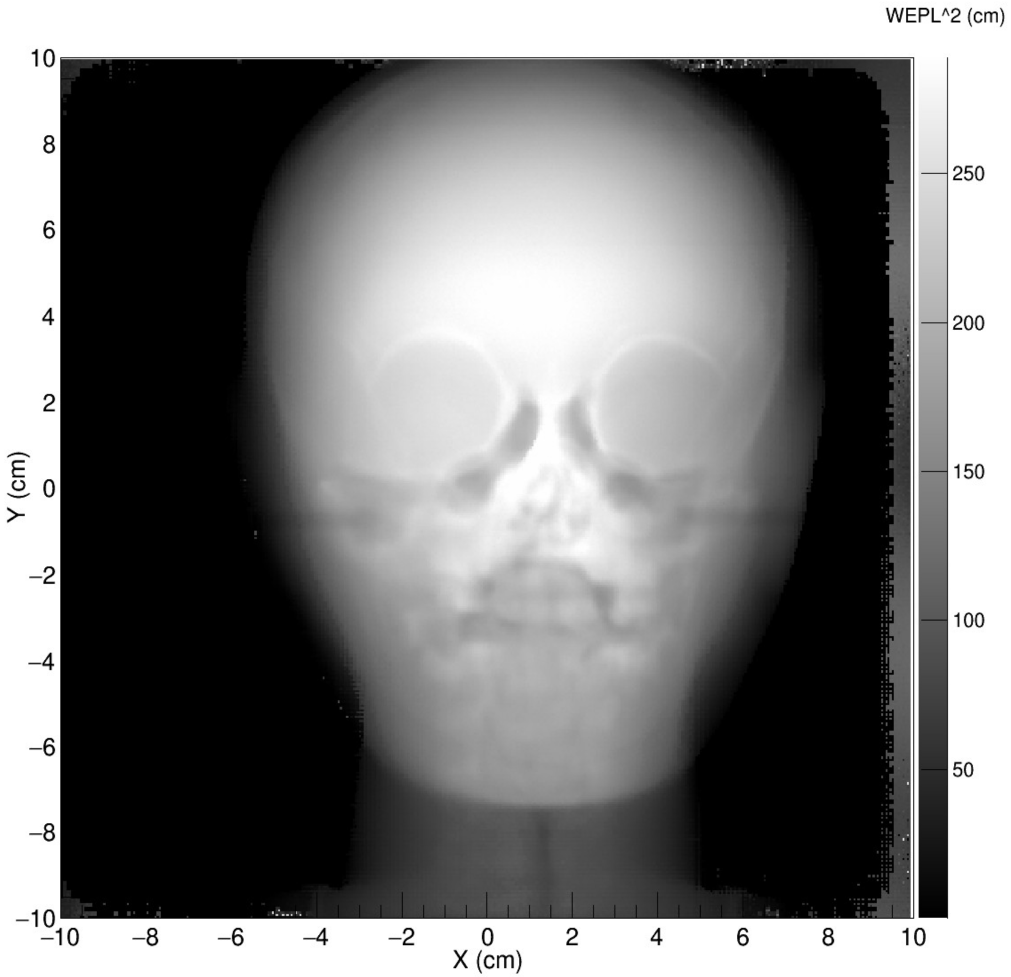

WEPL^2 (cm)
Y (cm)
X (cm)
10
8
6
4
2
0
−2
−4
−6
−8
−10
250
200
150
100
50

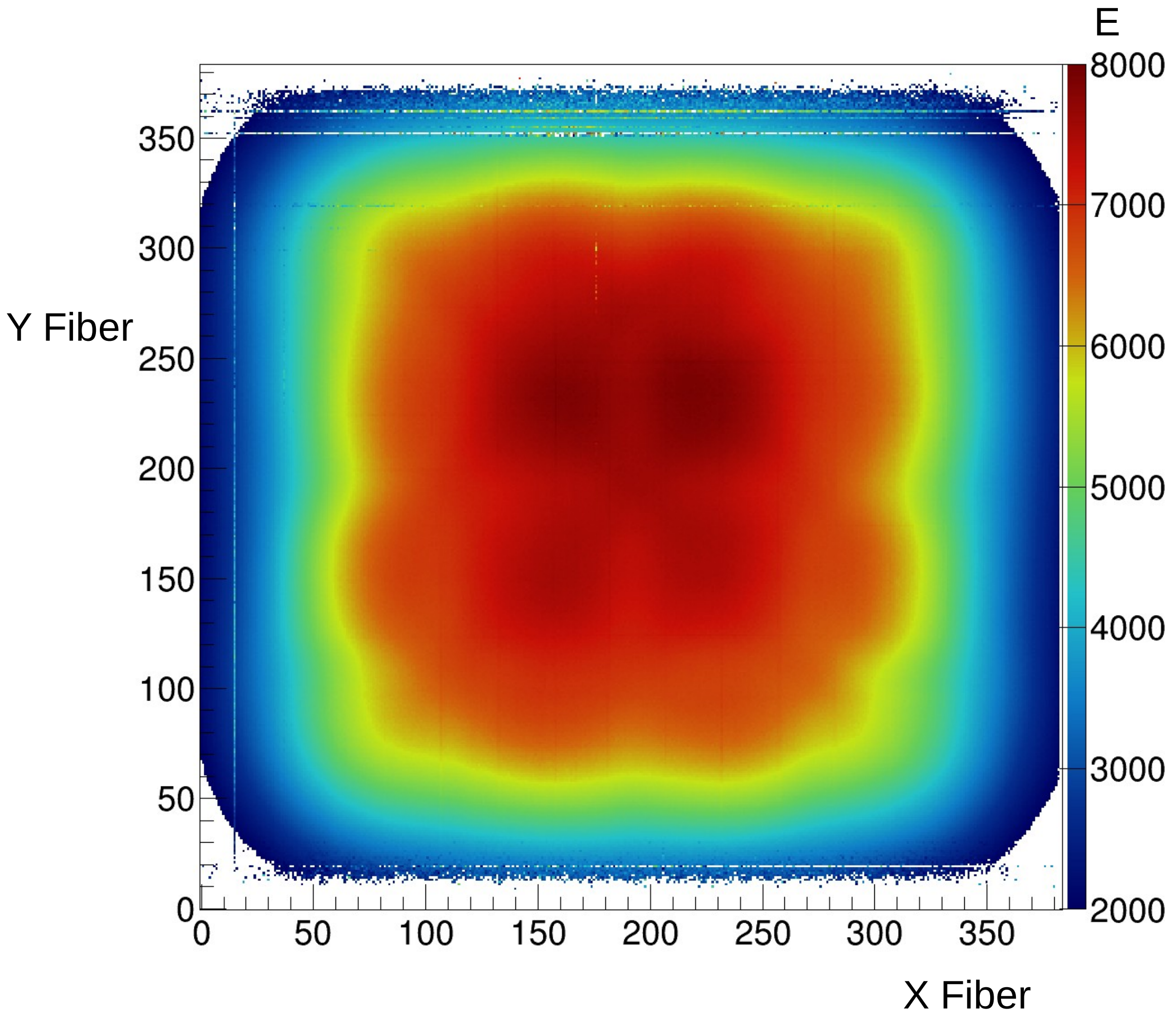

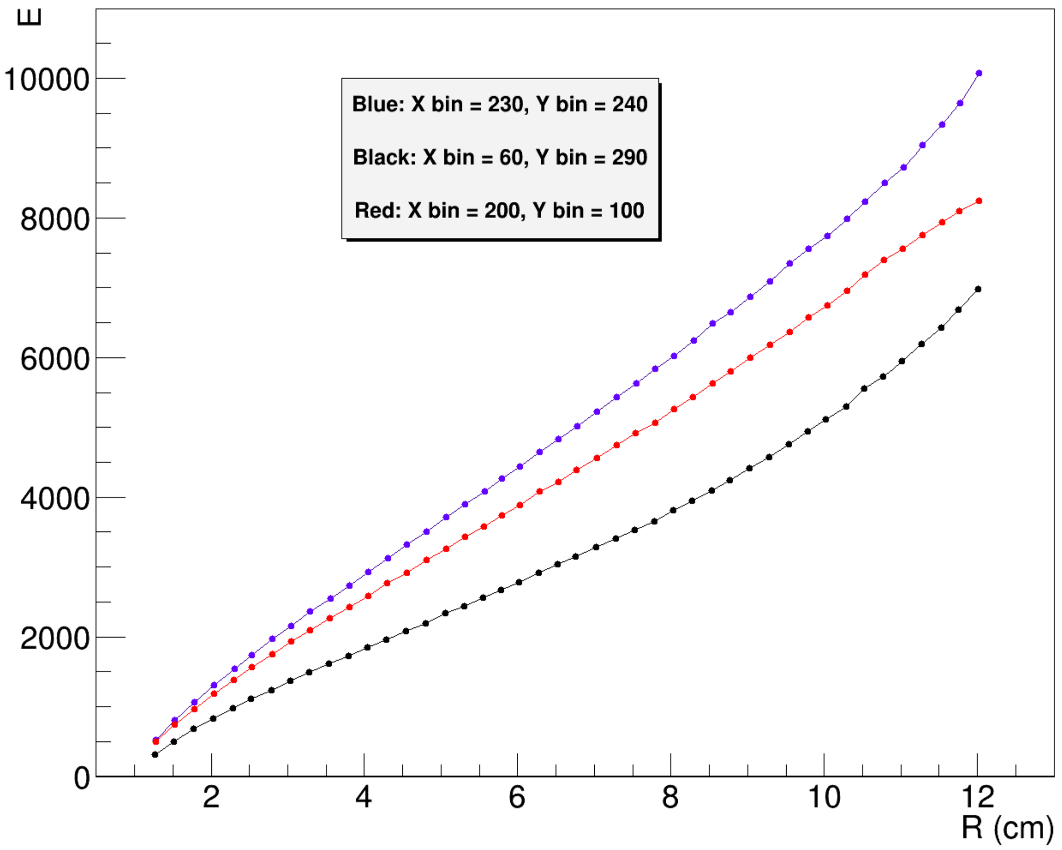

- Linear detector response vs. range gives very good range sensitivity

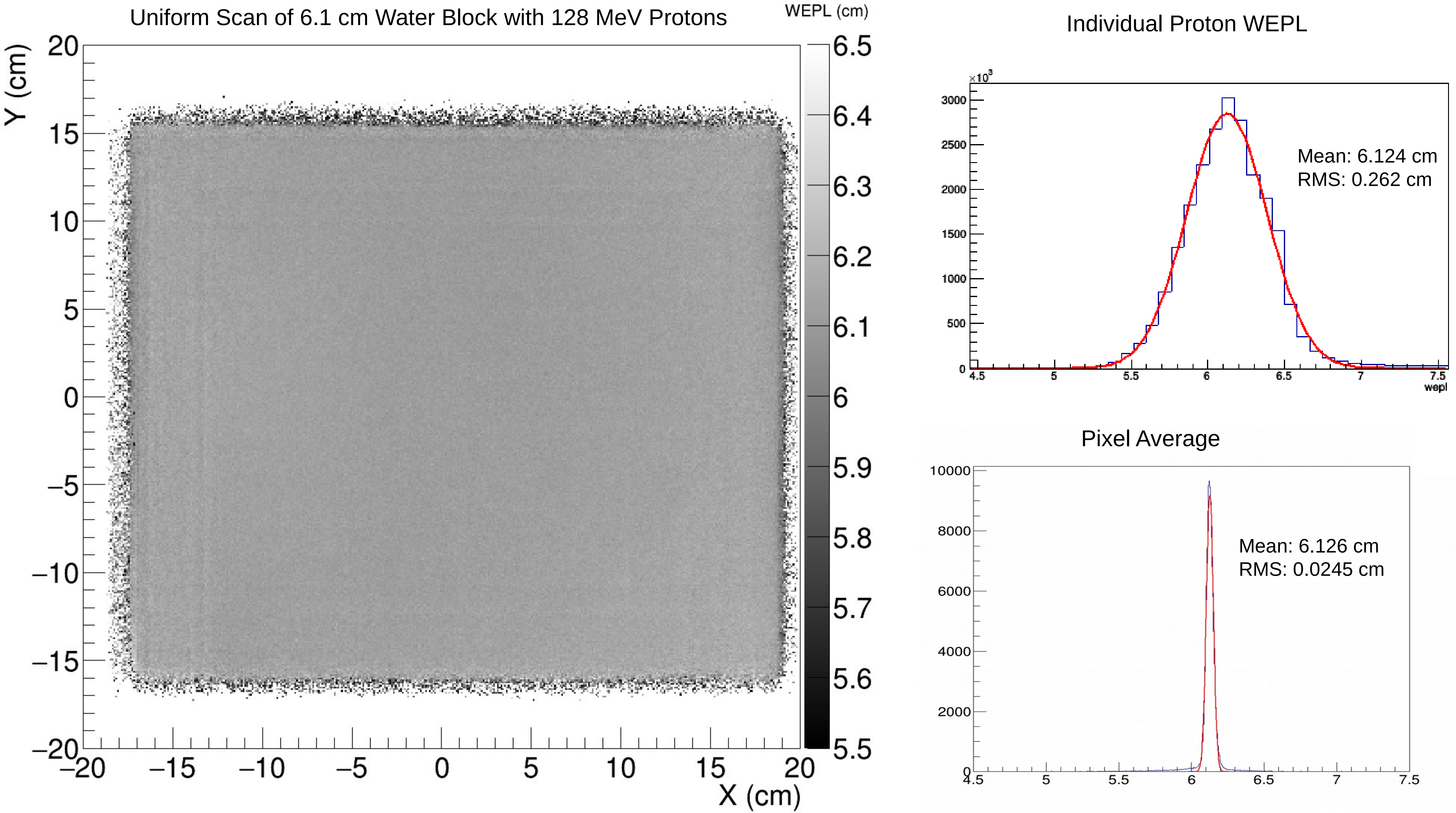
Uniform Scan of 6.1 cm Water Block with 128 MeV Protons
WEPL (cm)
Y (cm)
X (cm)
Individual Proton WEPL
×10³
wepl
Mean: 6.124 cm
RMS: 0.262 cm
Pixel Average
Mean: 6.126 cm
RMS: 0.0245 cm

Imaging with Multiple Proton Energies – Pediatric Head Phantom

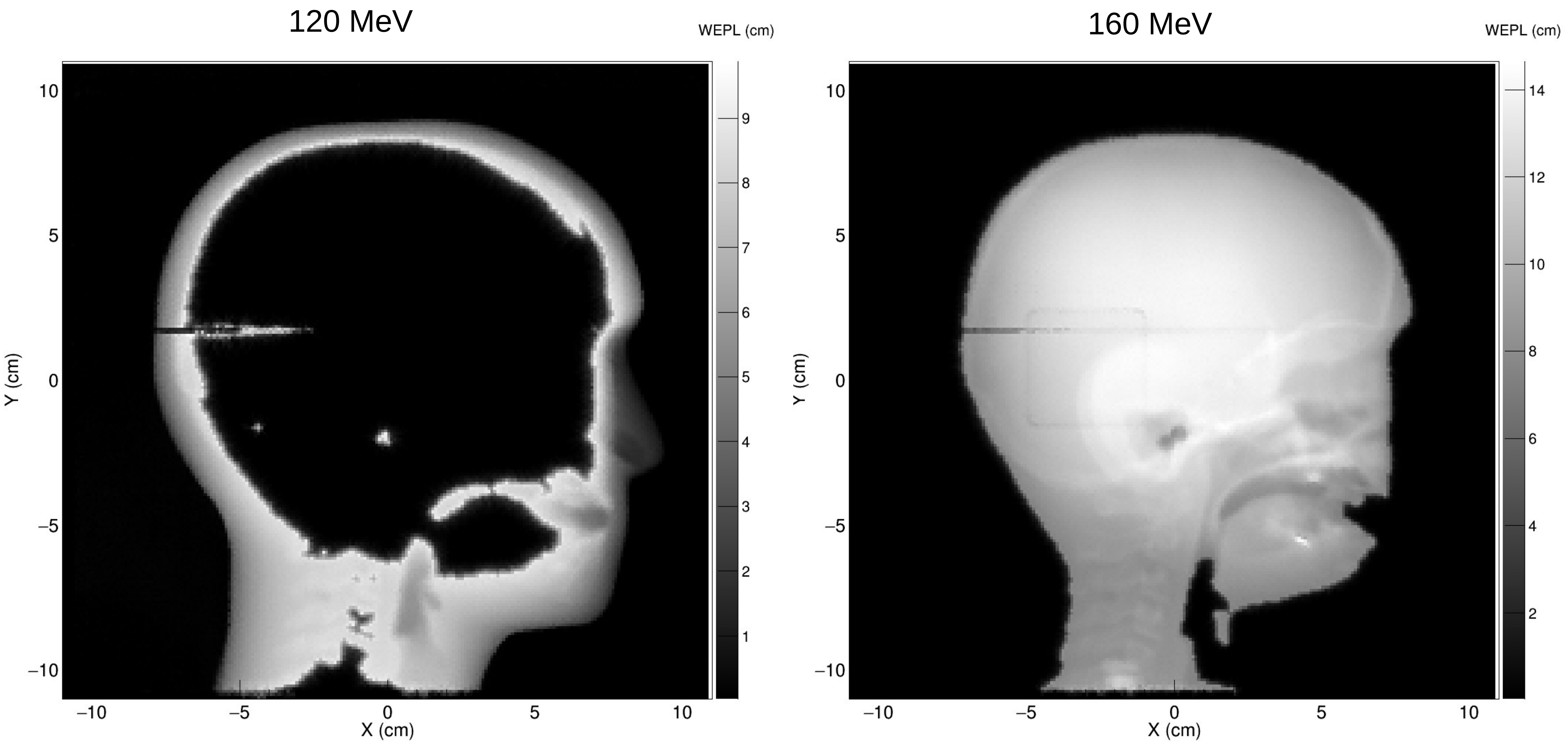

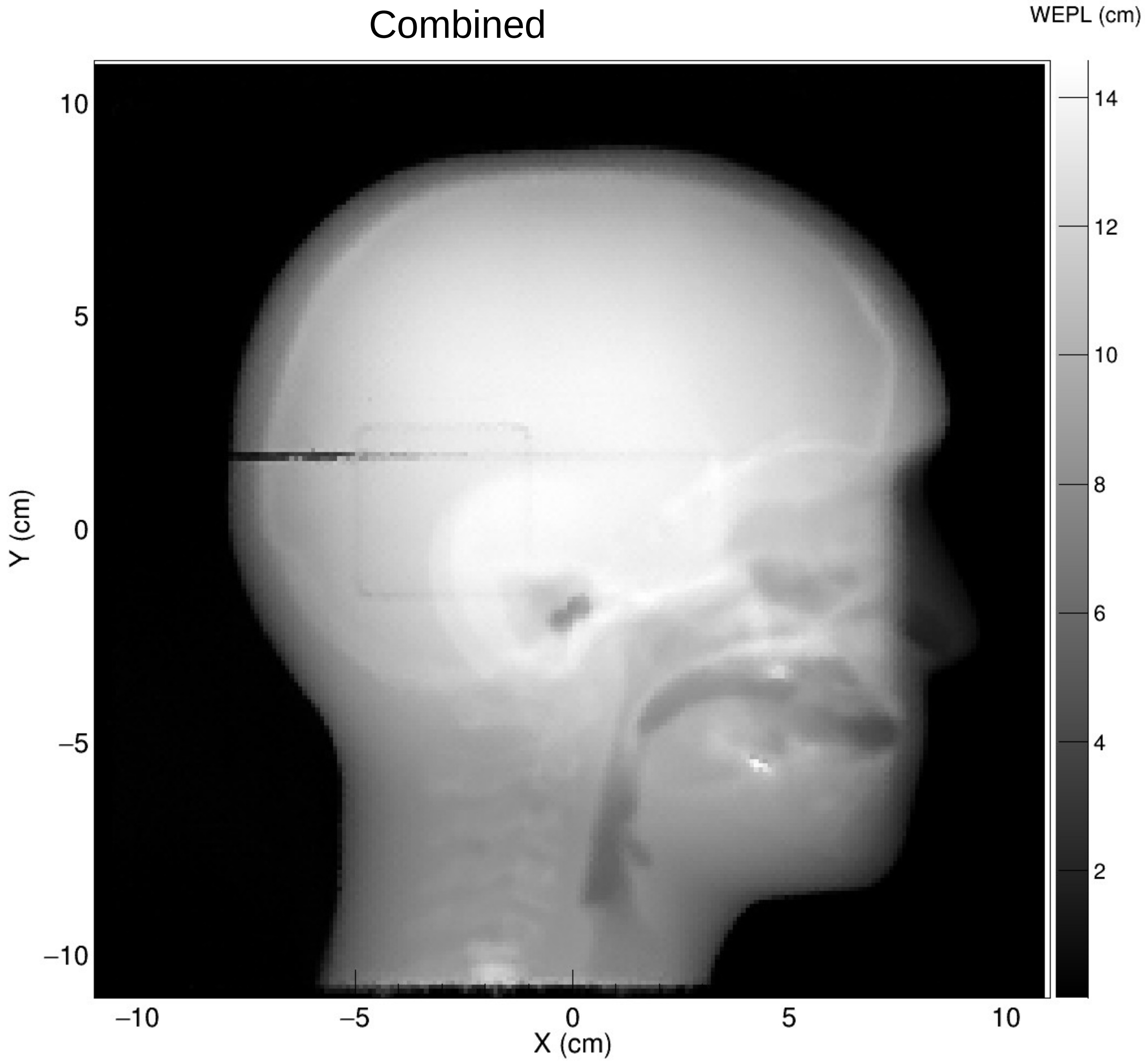

Combined
WEPL (cm)
Y (cm)
X (cm)
10
5
0
−5
−10
14
12
10
8
6
4
2

pCT of fresh pig's head

- 4 energies, data taken in 4 degree intervals
- Vertical CT taken for comparison

Proton radiographs taken every 4 degrees

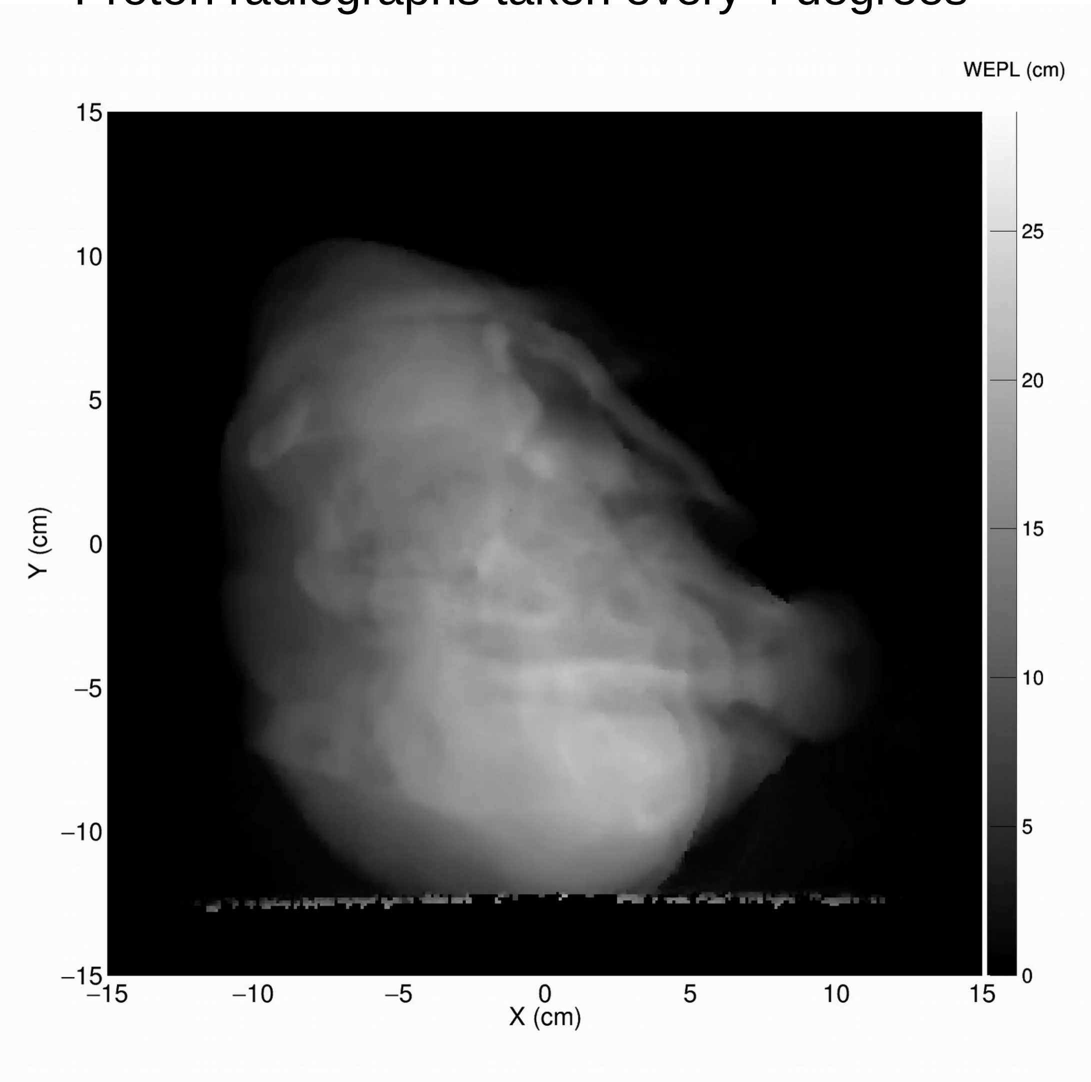

Horizontal pCT slices – 1 mm

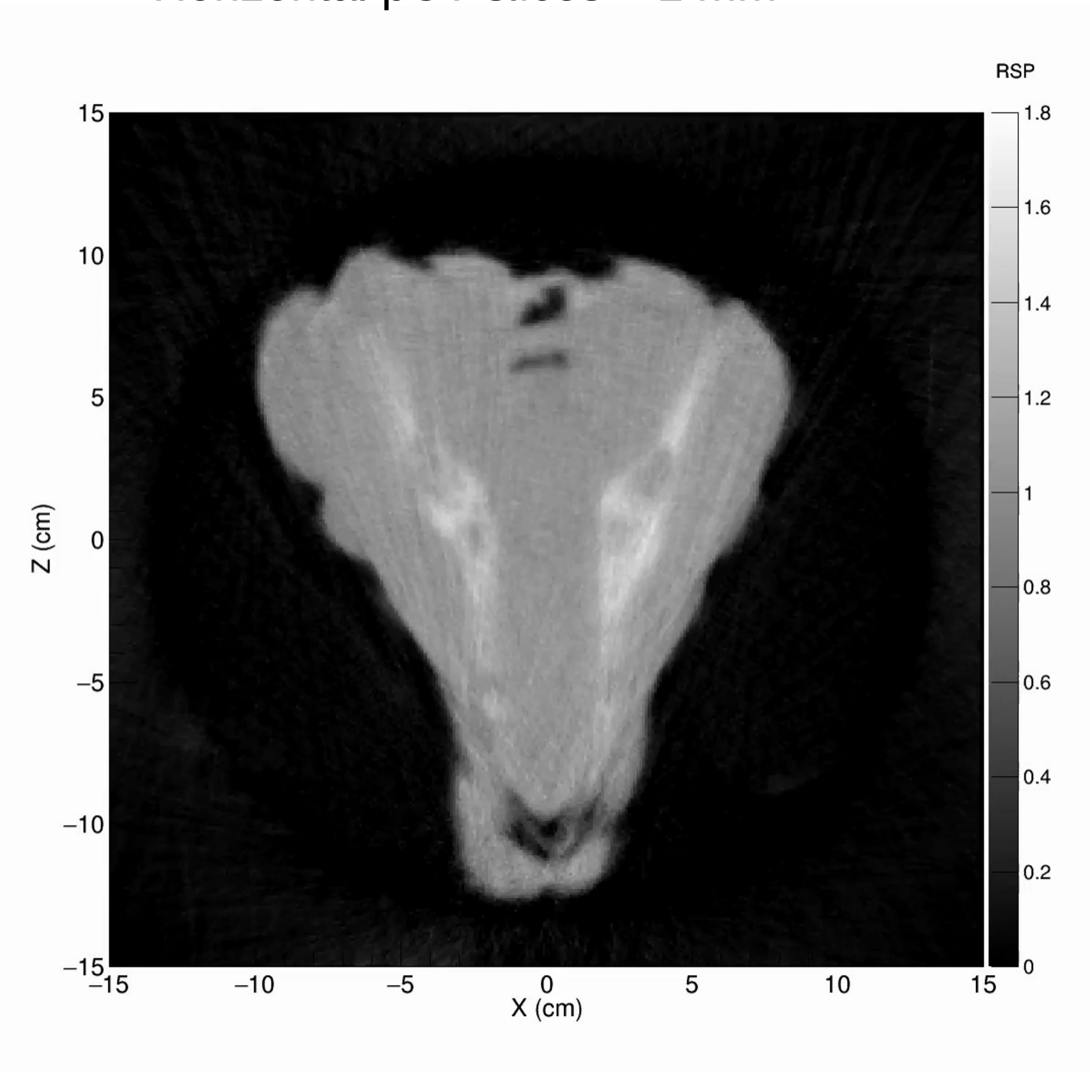

Contours: tympanic bullae

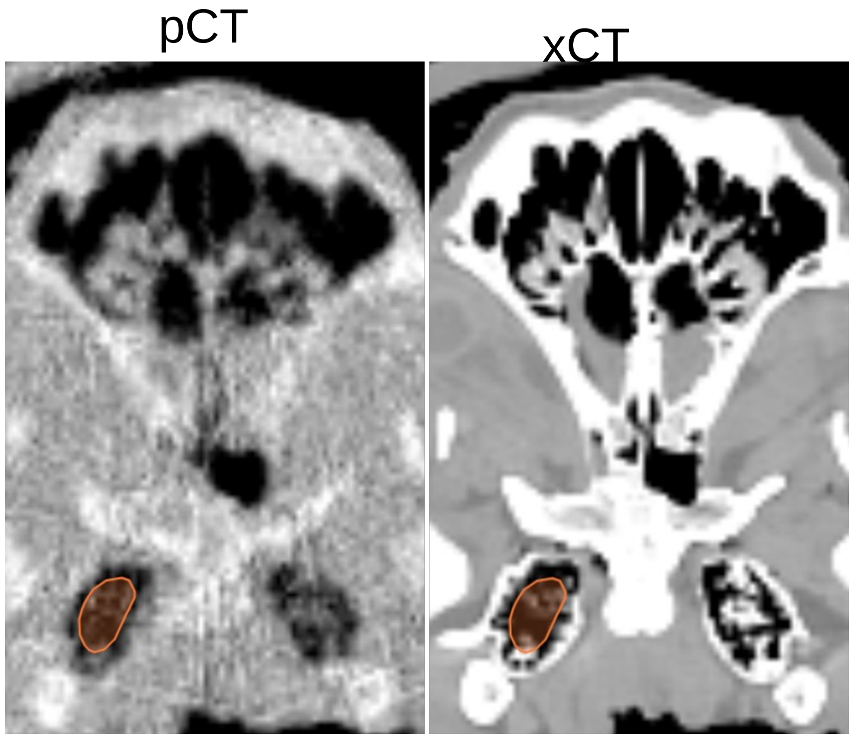

Region	Volume (cm³)	pCT RSP Mean	SD	SE(%)	Hor CT[a] RSP	Diff (%)	Hor CT[b] RSP	Diff (%)	Vert CT RSP	Diff (%)
Bullae	0.8	0.491	0.24	1.7	0.684	-39.3	0.690	-40.5	0.634	-29.1
Adipose	3.7	0.950	0.14	0.2	0.961	-1.2	0.962	-1.3	0.954	-0.4
Muscle	2.0	1.033	0.16	0.3	1.058	-2.4	1.059	-2.5	1.052	-1.8
Tongue	9.4	1.047	0.23	0.2	1.035	1.1	1.036	1.1	1.031	1.5
Brain Stem	0.7	0.994	0.16	0.6	1.038	-4.4	1.038	-4.4	1.016	-2.2
Brain	2.5	1.025	0.16	0.3	1.037	-1.2	1.039	-1.4	1.031	-0.6
Lens	0.1	1.099	0.12	1.6	1.078	1.9	1.080	1.7	1.076	2.1
Eye Left	0.5	1.015	0.13	0.5	1.015	0.0	1.017	-0.2	1.018	-0.3
Eye Right	0.8	1.011	0.15	0.5	1.021	-1.0	1.021	-1.0	1.014	-0.3
Skull	0.5	1.266	0.12	0.4	1.297	-2.4	1.303	-2.9	1.320	-4.3
Mandible	0.5	1.540	0.16	0.5	1.559	-1.2	1.565	-1.6	1.562	-1.4
Sinus Air	0.1	0.067	0.12	17	0.057	15	0.058	13	0.039	42

[a] Low dose protocol
[b] High dose protocol

Proton Radiograph

X-Ray CT DRR – converted to WET

pCT DRR

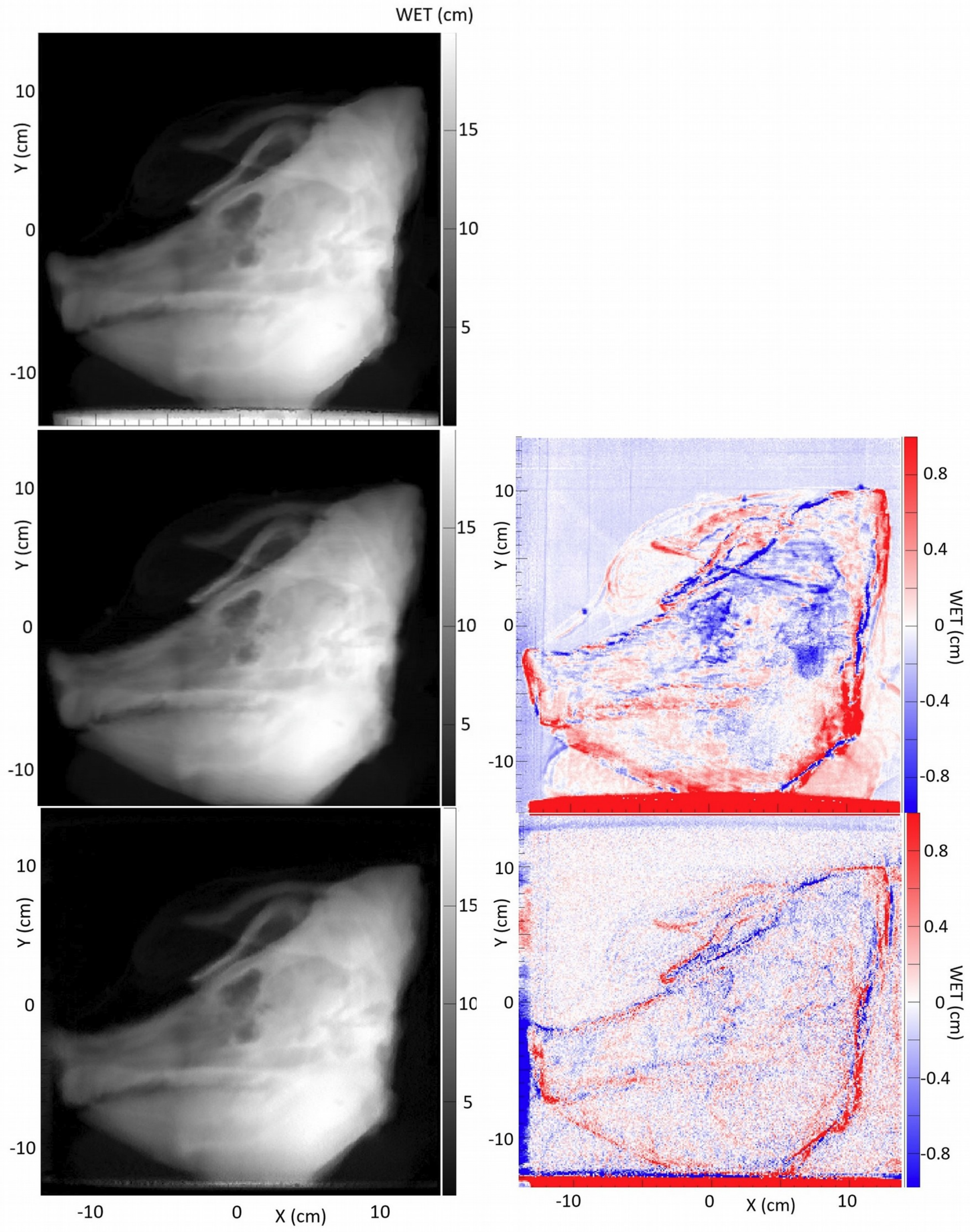

Difference – pRad vs. xCT

Difference – pRad vs. pCT

Using pRad to align the patient – see talk by Joe Piet

X-Ray DRR – registered alignment

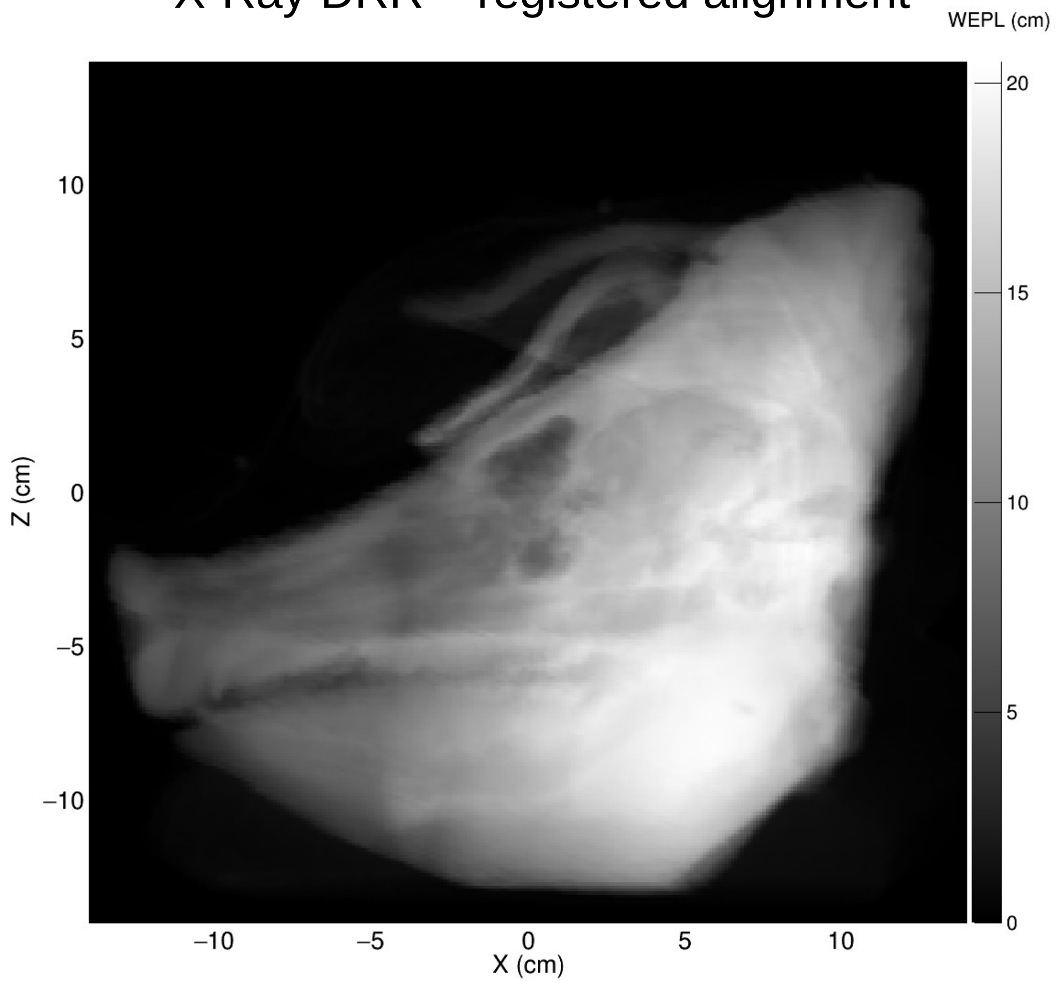

Difference – pRad vs DRR

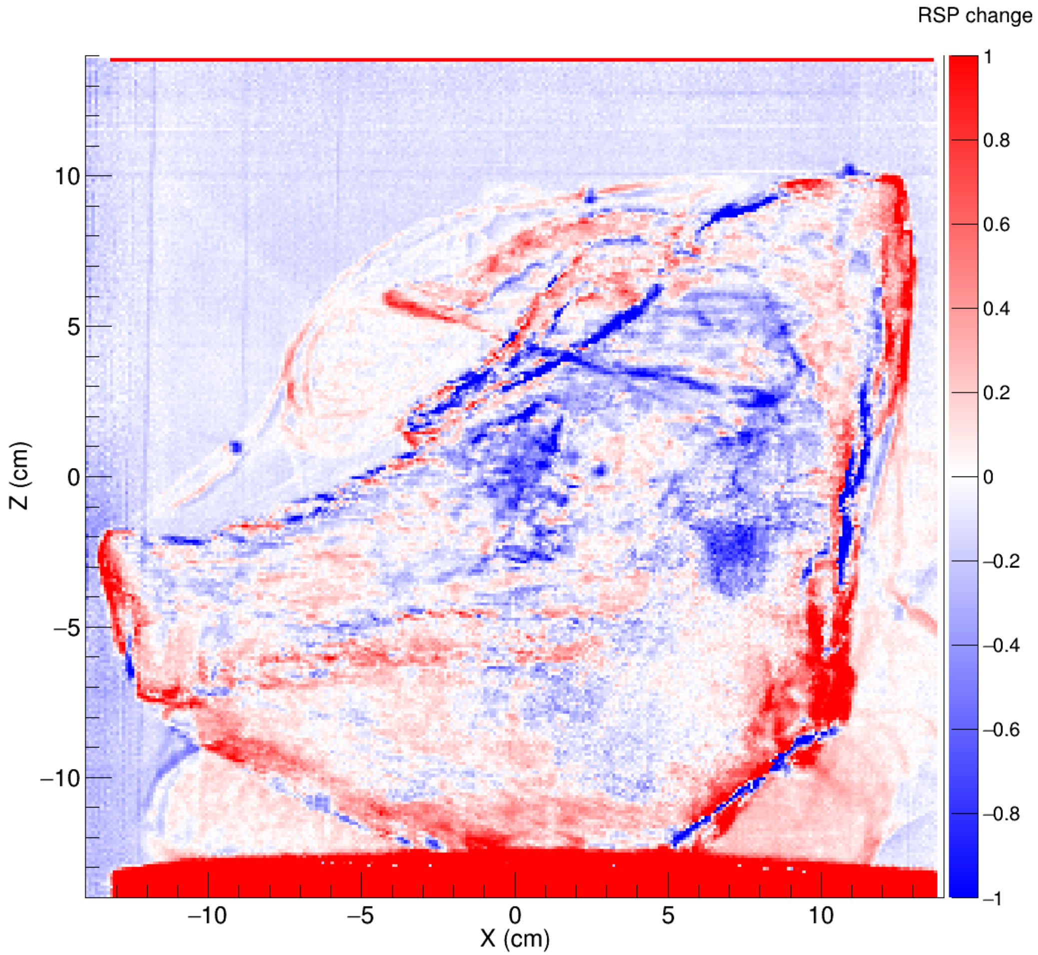

Using pRad to align the patient – see talk by Joe Piet

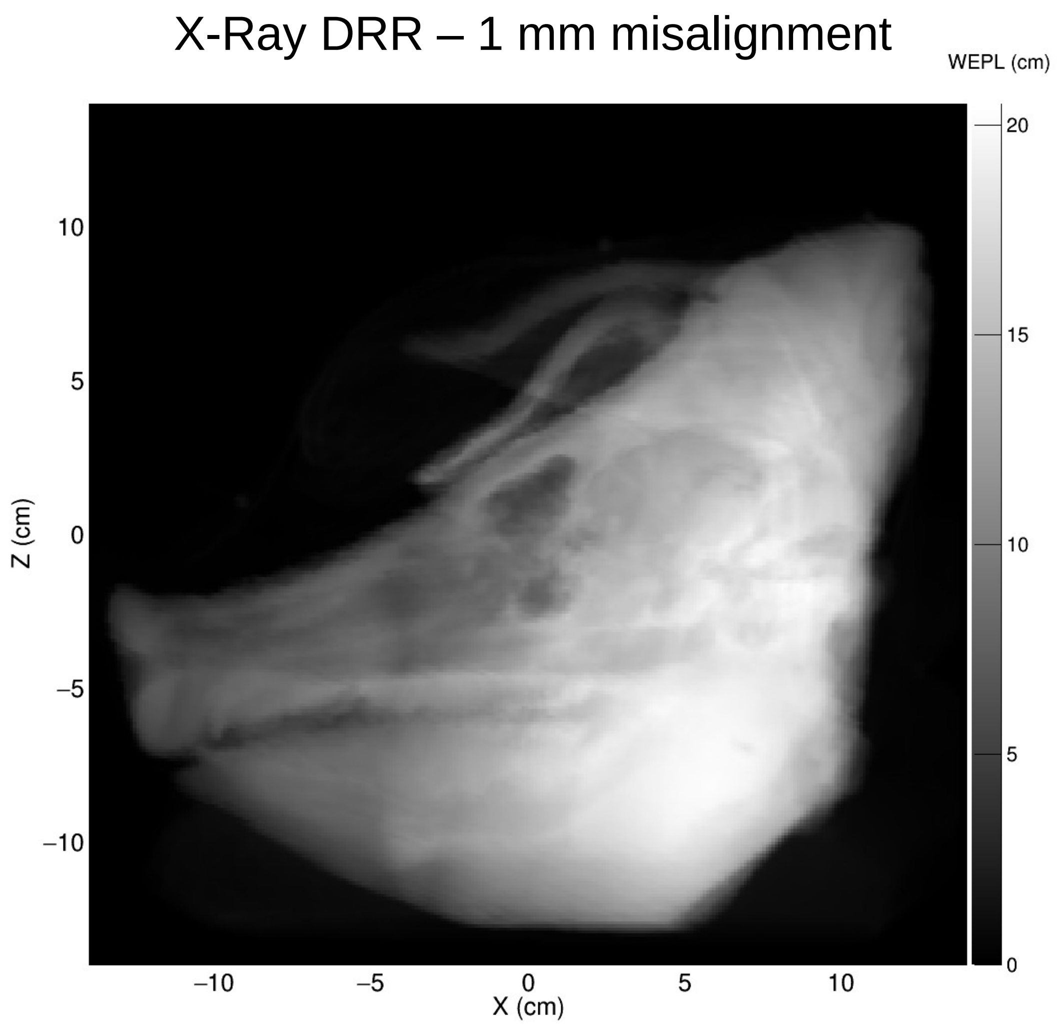

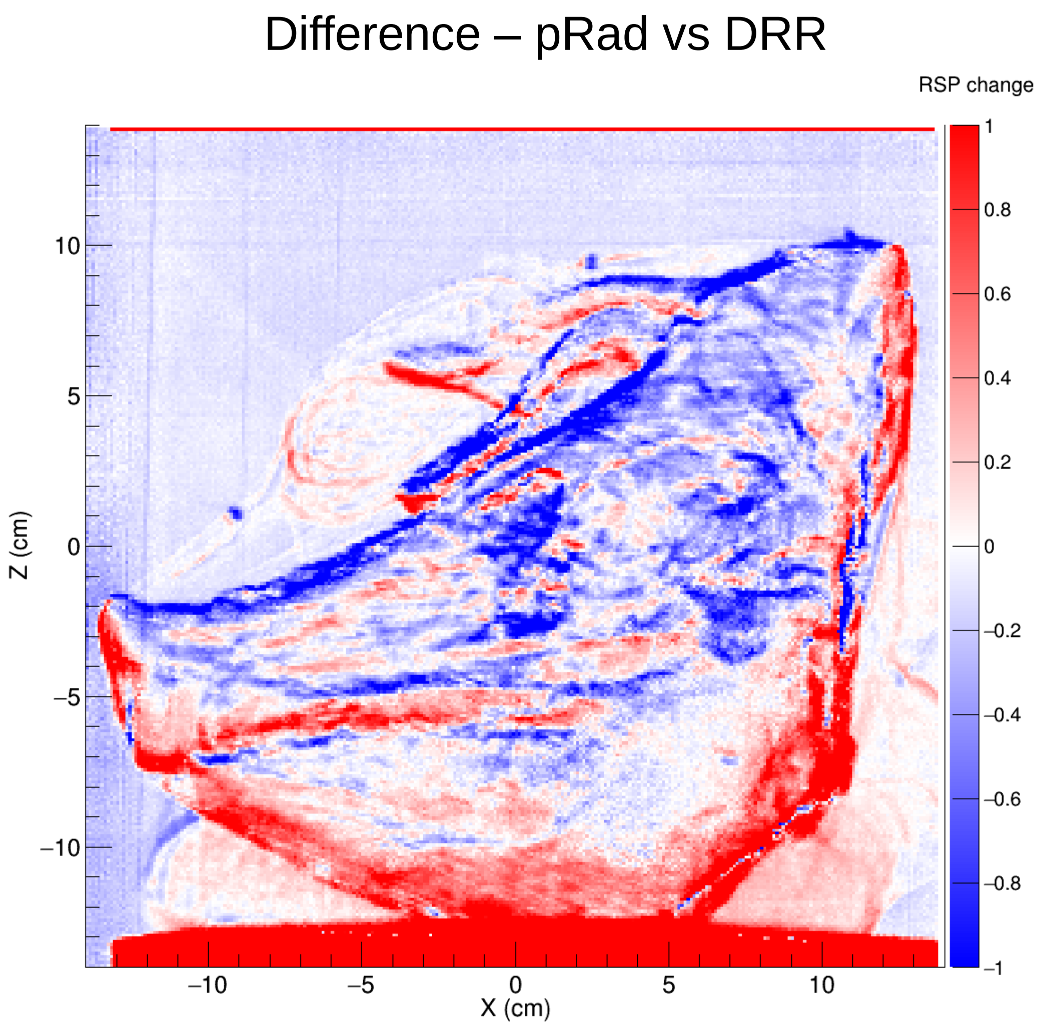

Using pRad to align the patient – see talk by Joe Piet

X-Ray DRR – 2 mm misalignment

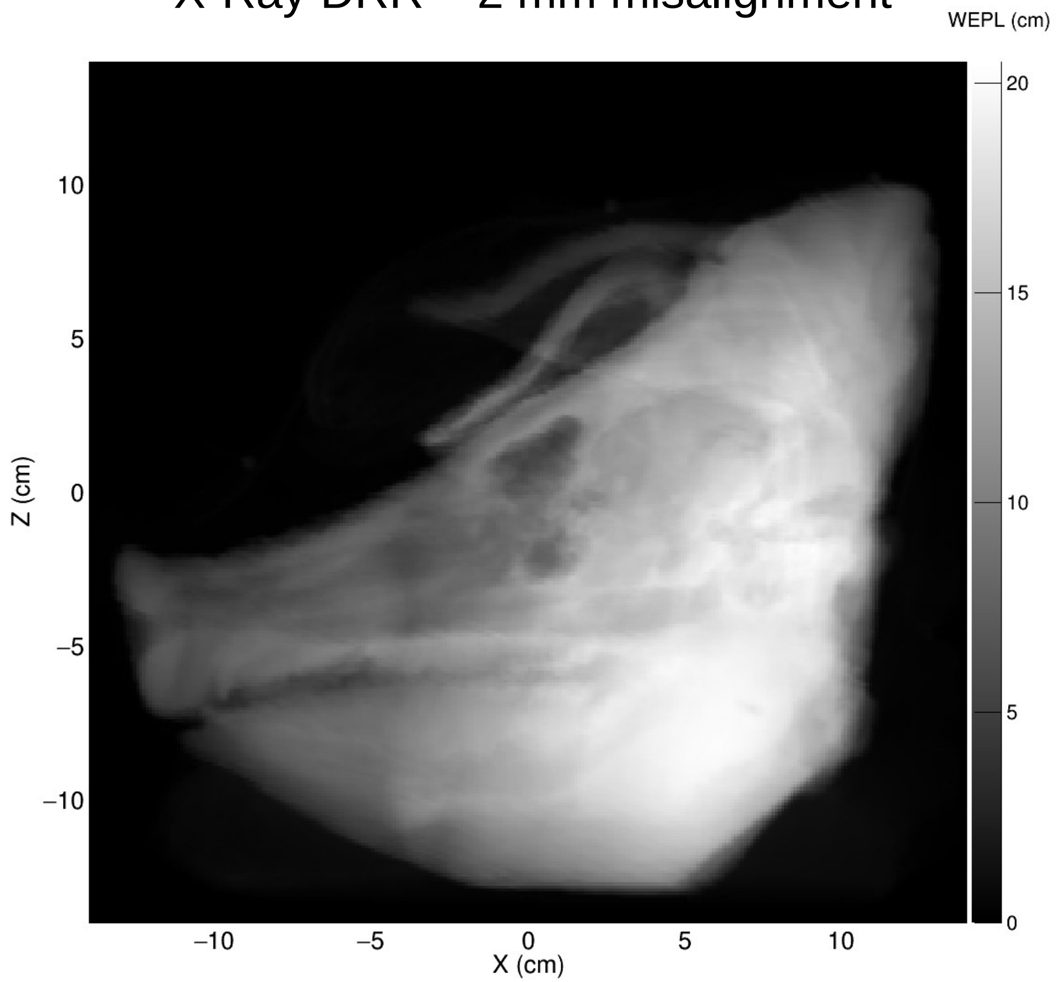

Difference – pRad vs DRR

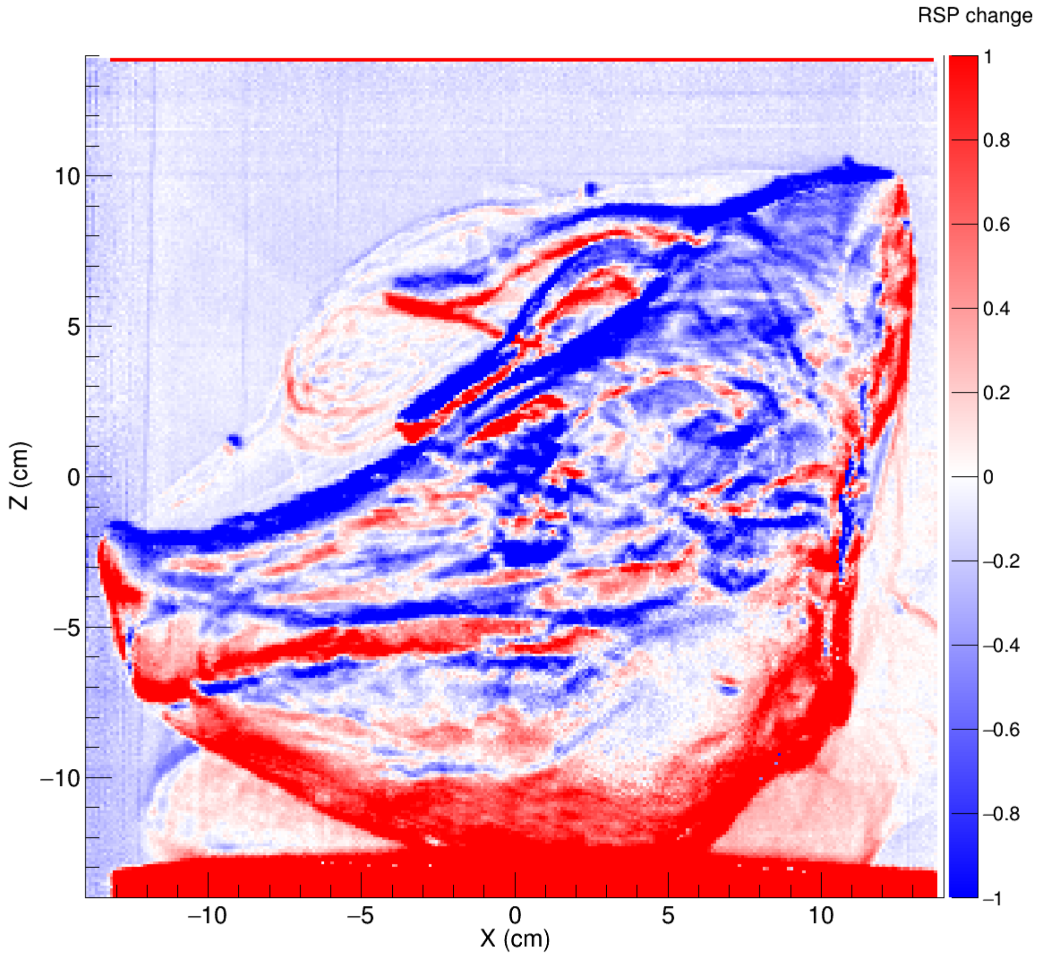

Our Reconstruction
Algorithm: the DV method

$$d_p = Ax - b$$

$$d_v = \bar{A}^T d_p$$

$$\bar{A}^T = V^{-1} A^T$$

$$V^{-1} = diag\left(\frac{1}{\sum_j \alpha_{ij}^T}\right)$$

$$x_{k+1} = x_k - \lambda_k \, d_{vk}$$

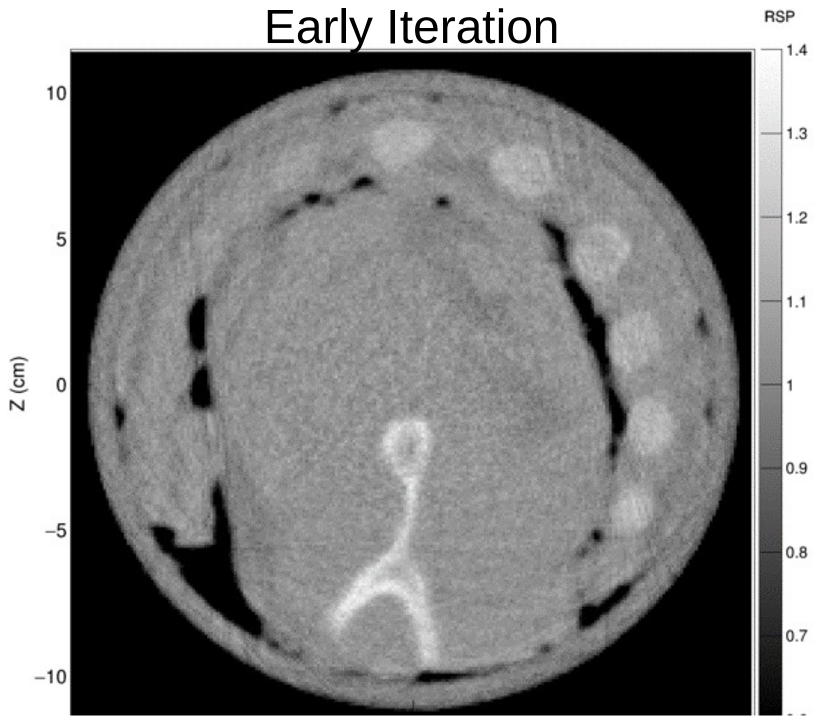

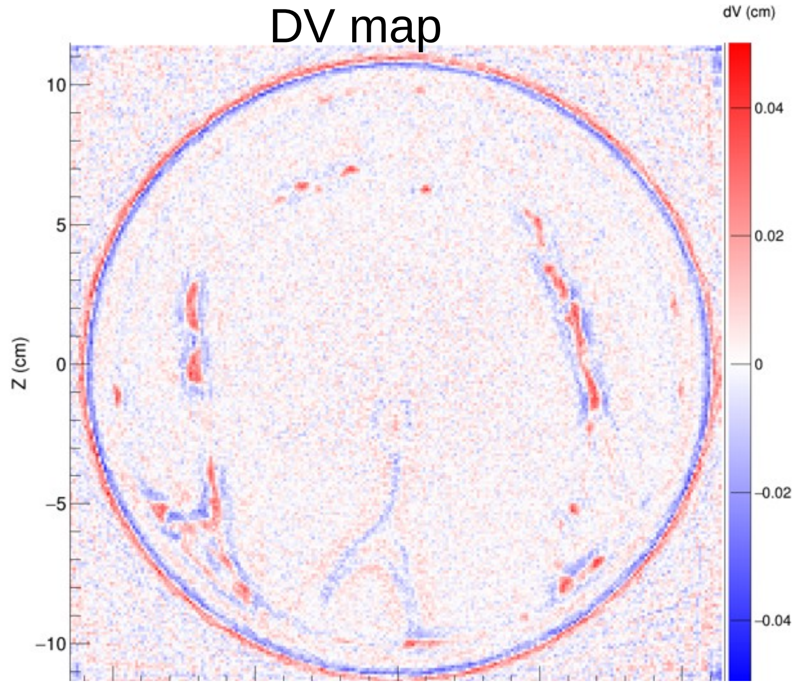

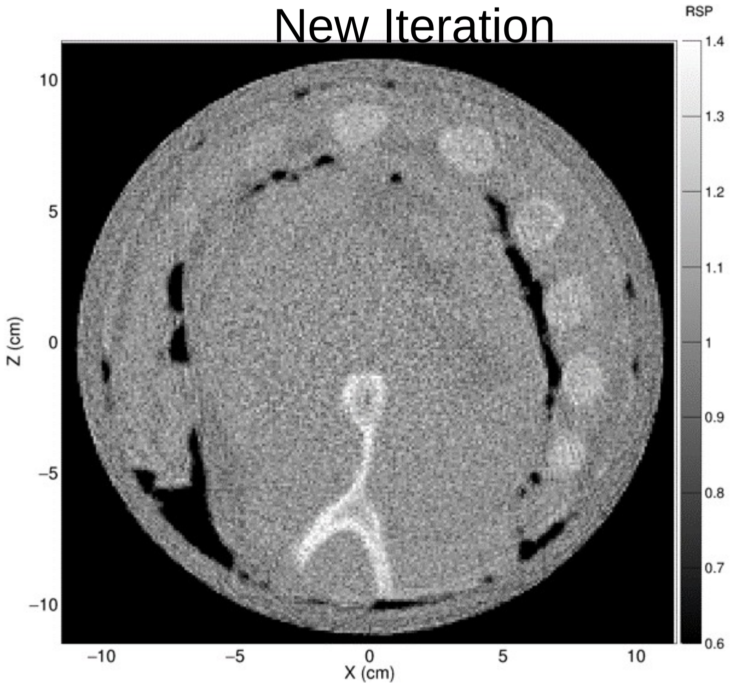

Optimization of λ_k

$$d_{pk} = Ax_k - b$$
$$d_{vk} = \bar{A}^T d_{pk}$$
$$x_{k+1} = x_k - \lambda_k \, d_{vk}$$
$$d_{p(k+1)} = Ax_{k+1} - b = d_{pk} - \lambda_k \, Ad_{vk}$$

$$d_{v(k+1)} = \bar{A}^T d_{p(k+1)} = d_{vk} - \lambda_k \, \bar{A}^T(Ad_{vk})$$

- One possible choice for λ_k: Minimize χ^2_{k+1}

$$\chi^2_{k+1} = d_{p(k+1)} \cdot d_{p(k+1)} = d_{pk} \cdot d_{pk} - 2\lambda_k \, d_{pk} \cdot (Ad_{vk}) + \lambda^2_k \, |Ad_{vk}|^2 = \chi^2_k - 2\lambda_k \, d_{pk} \cdot (Ad_{vk}) + \lambda^2_k \, |Ad_{vk}|^2$$

$$d\chi^2_{k+1} / d\lambda_k = -2 \, d_{pk} \cdot (Ad_{vk}) + 2\lambda_k \, |Ad_{vk}|^2 = 0$$

$$\lambda_k = d_{pk} \cdot (Ad_{vk}) \, / \, |Ad_{vk}|^2$$

- Another choice for λ_k: Minimize $d_{v(k+1)} \cdot d_{v(k+1)}$

$$\lambda_k = d_{vk} \cdot (\bar{A}^T Ad_{vk}) \, / \, |\bar{A}^T Ad_{vk}|^2$$

Stopping Criteria

WEPL uncertainty per proton:

$$\sigma_p = \sqrt{\frac{\chi_p^2}{N_p - N_v}}$$

Estimated RSP uncertainty per voxel:

$$\sigma_v = \frac{\sigma_p}{\bar{\alpha}\sqrt{N_{pv}}}$$

*See talk by Alexander Pryanichnikov

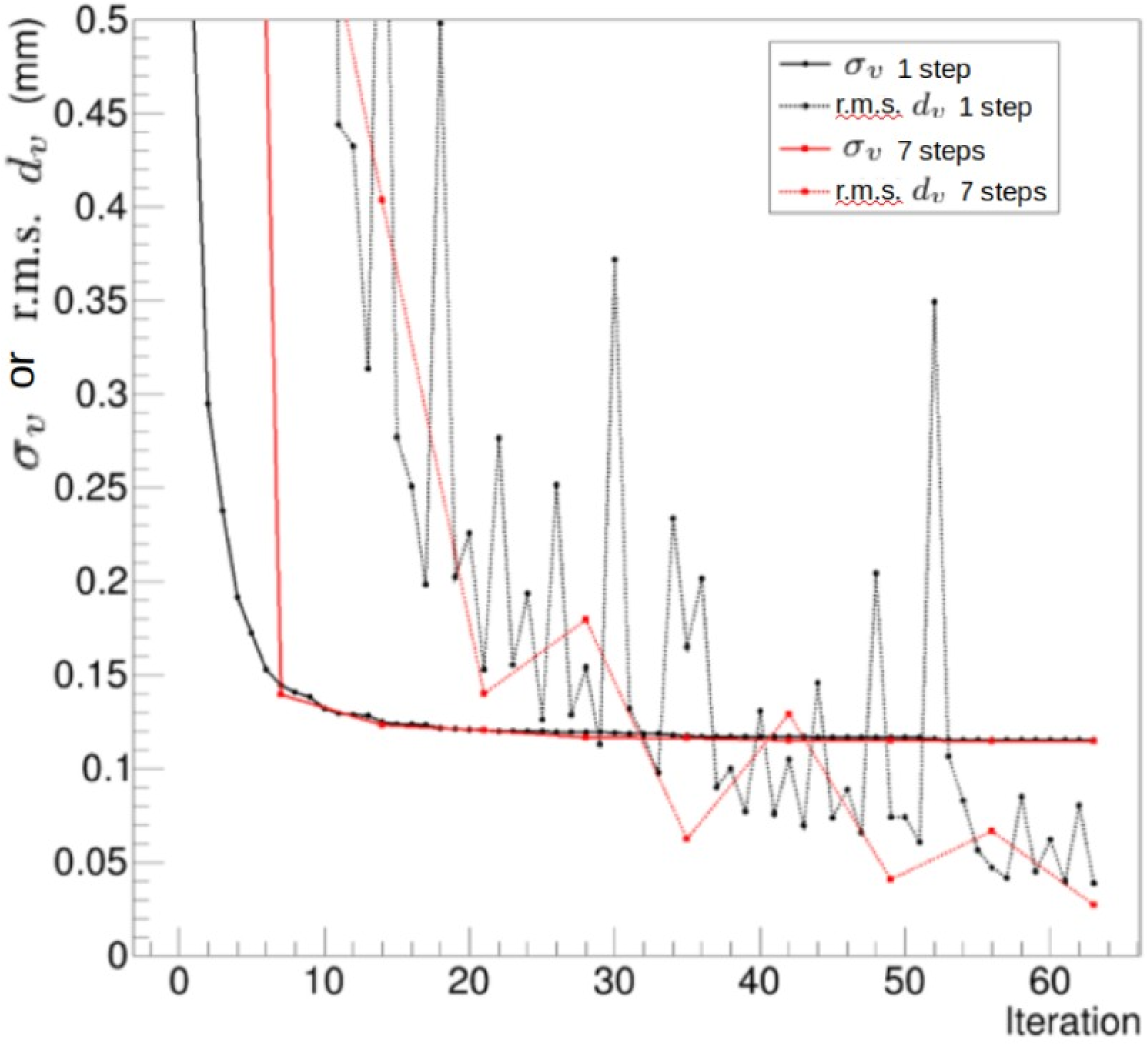

Fixed beam and imaging system, rotating patient

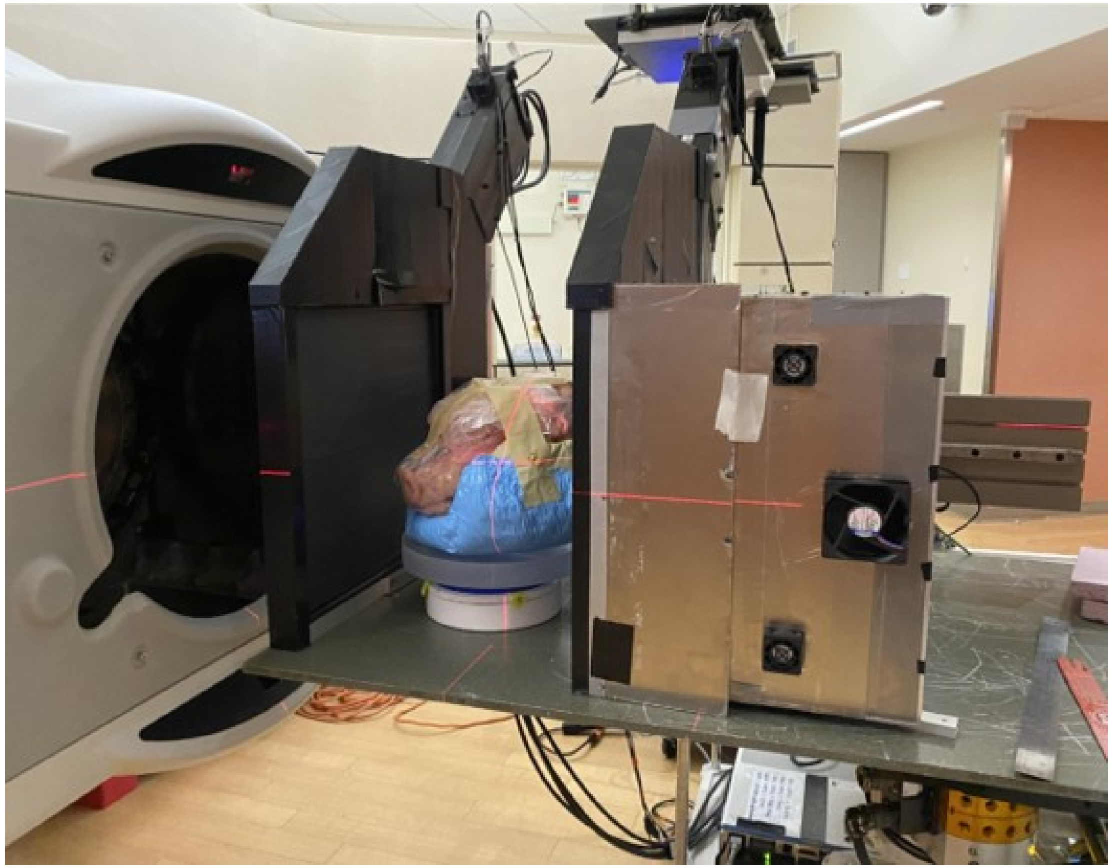

Fixed patient, rotating beam and imaging system

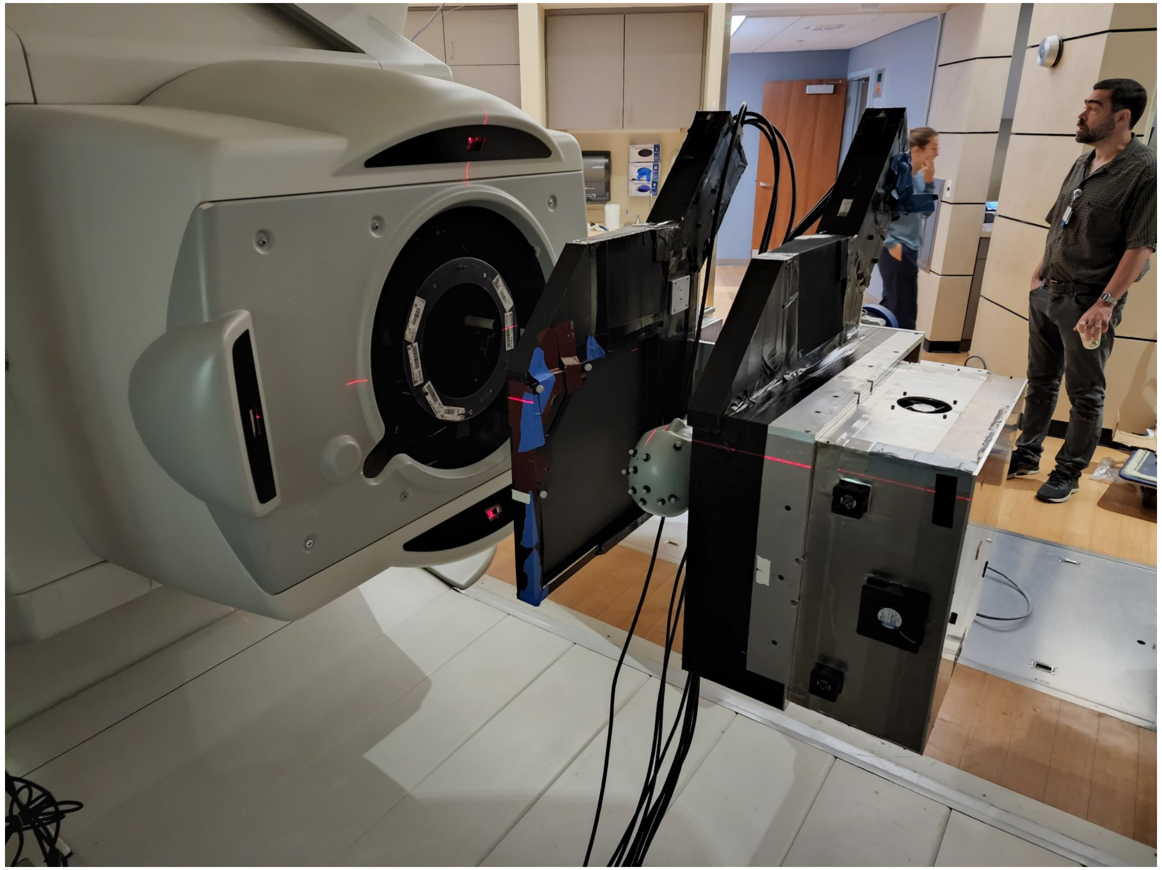

Mounting system designed and built by Cosylab

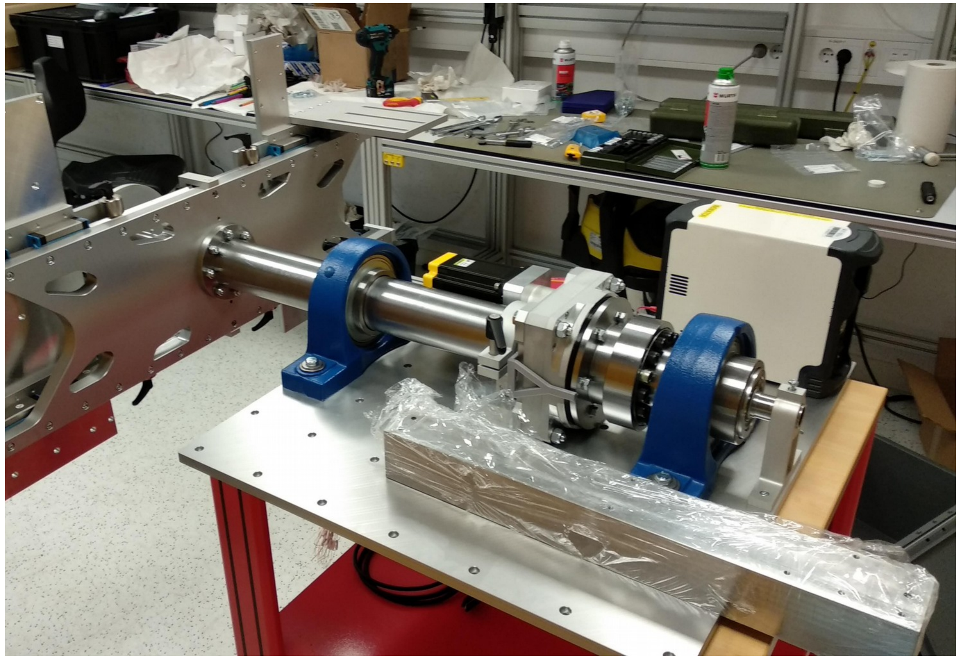

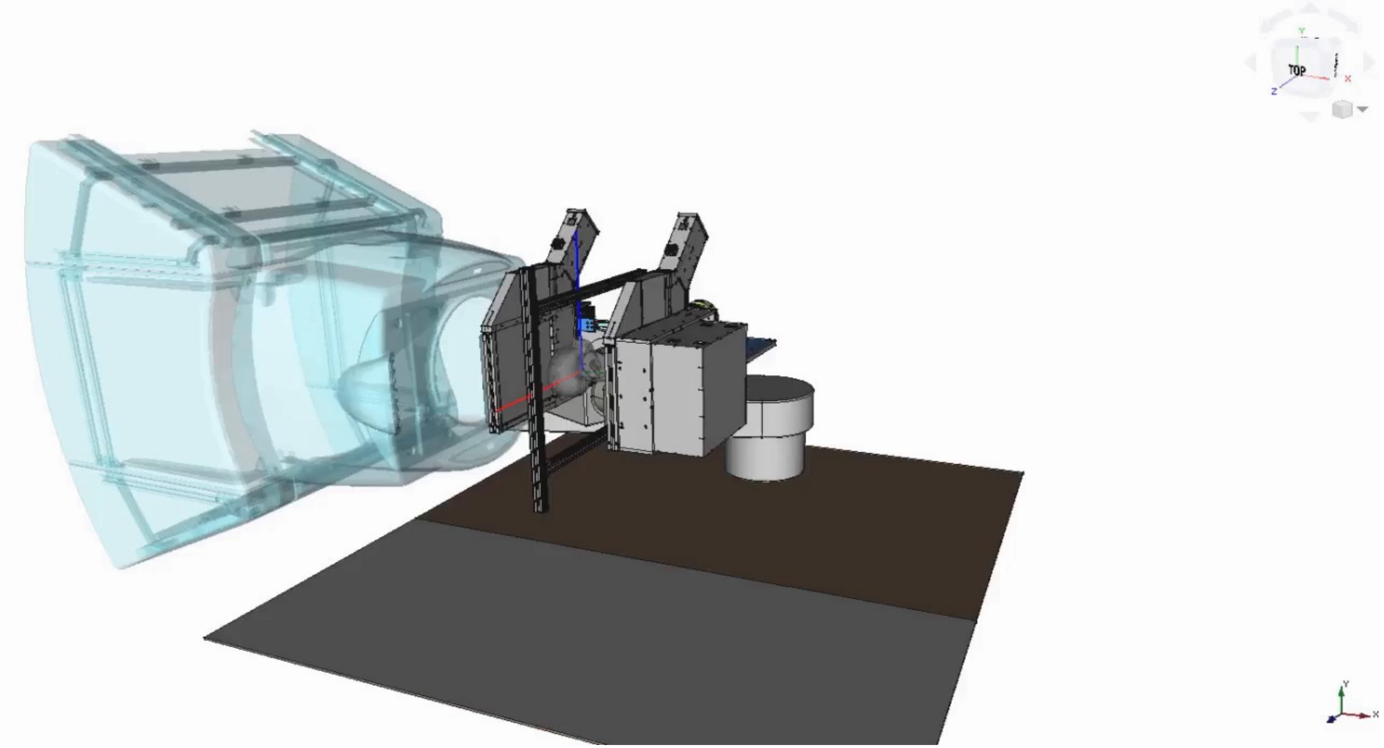

First ever pCT test in a gantry system!
June 25, 2022

We acquired proton imaging data from 45 angles for a pediatric head phantom using 3 proton energies – 120, 162, and 198 MeV.

The test took over 6 hours to complete.

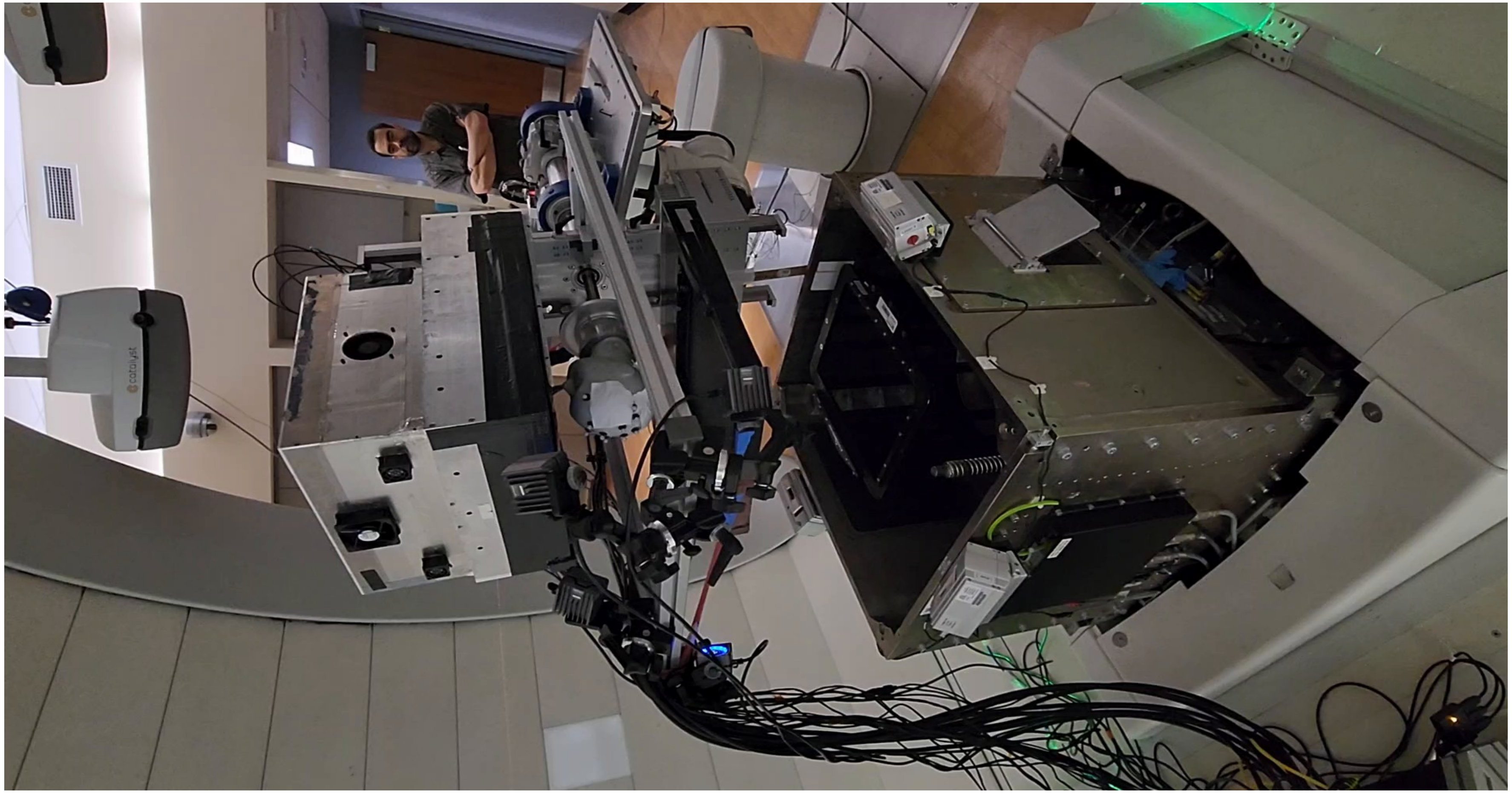

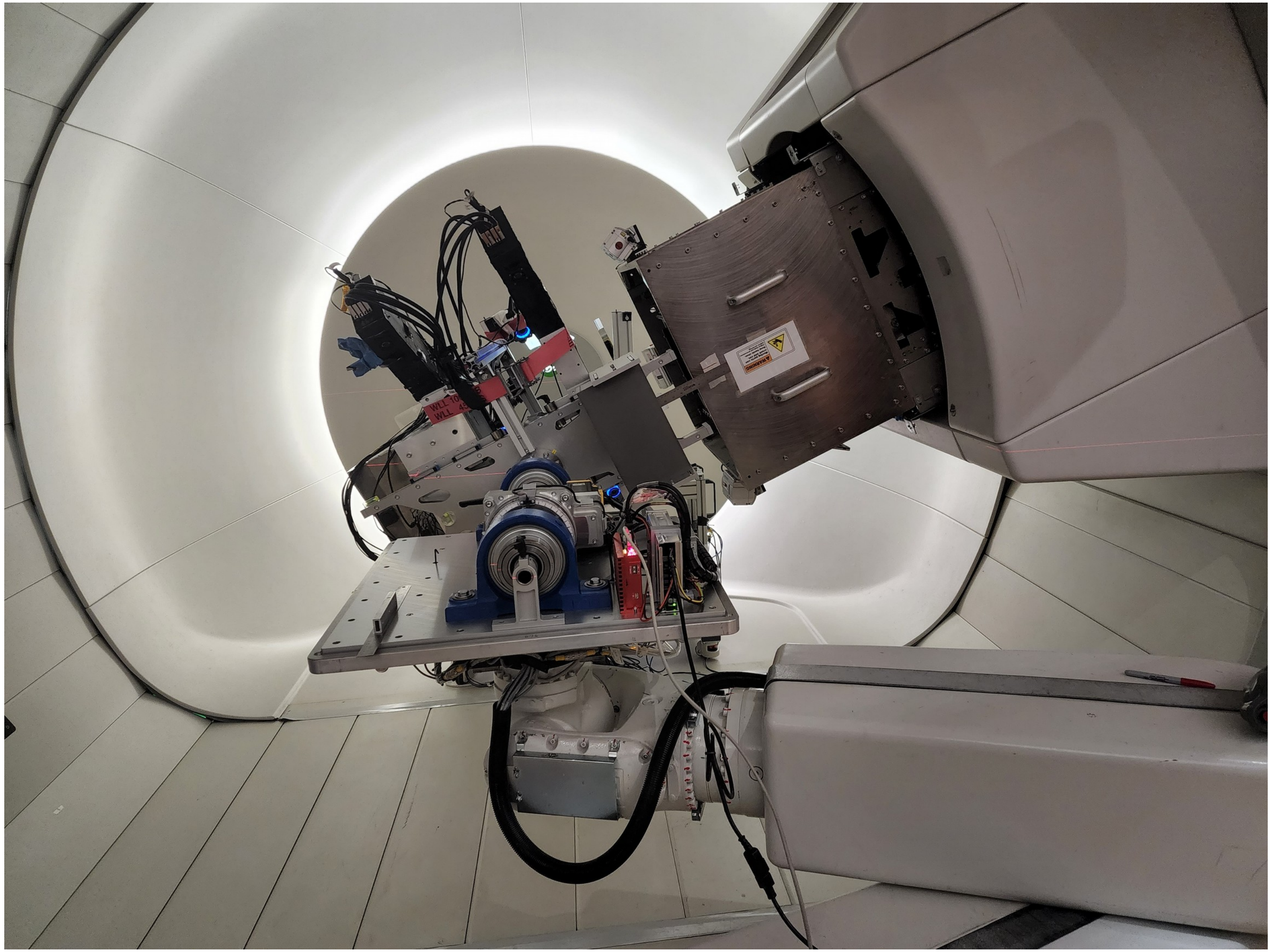

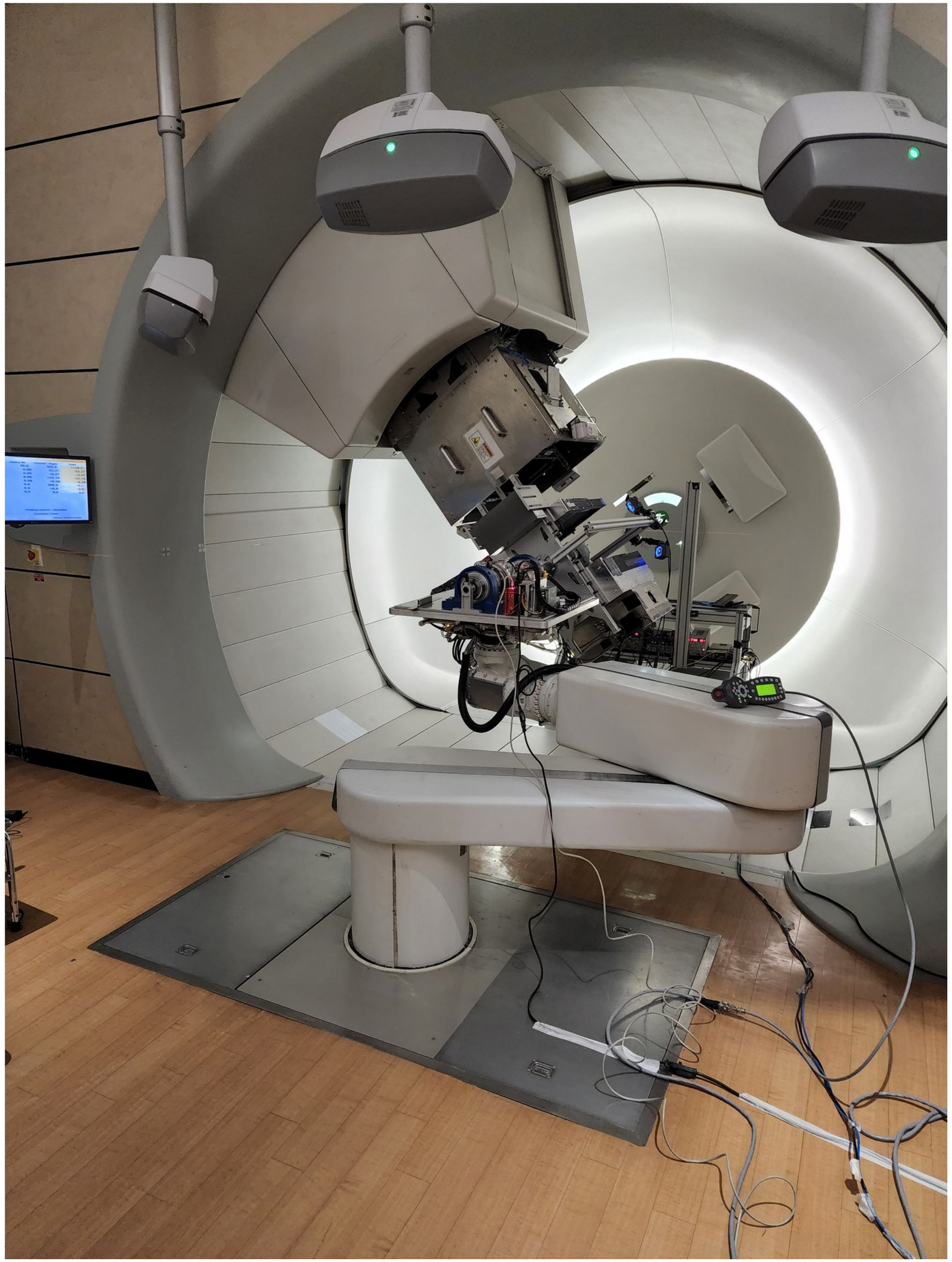

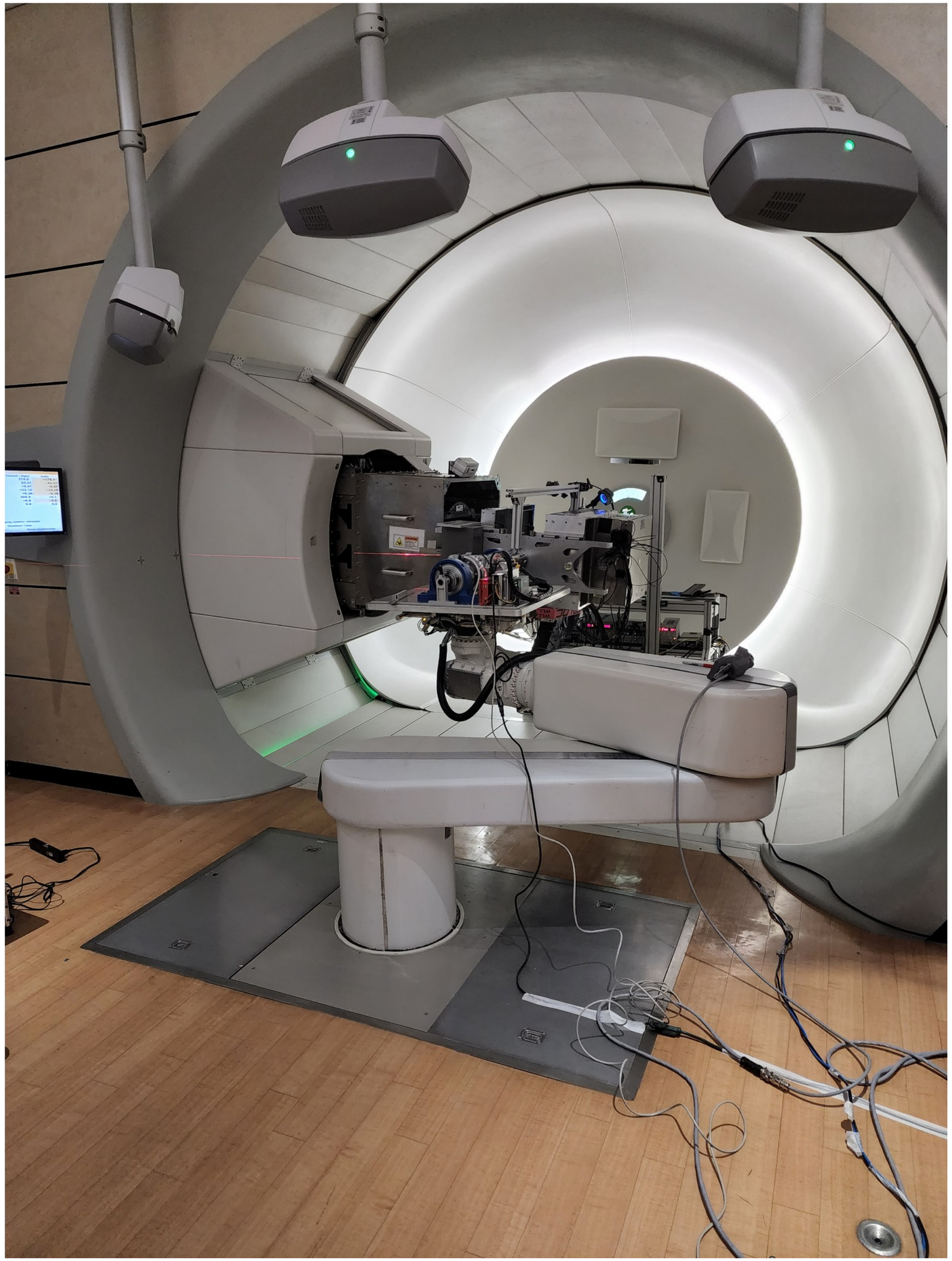

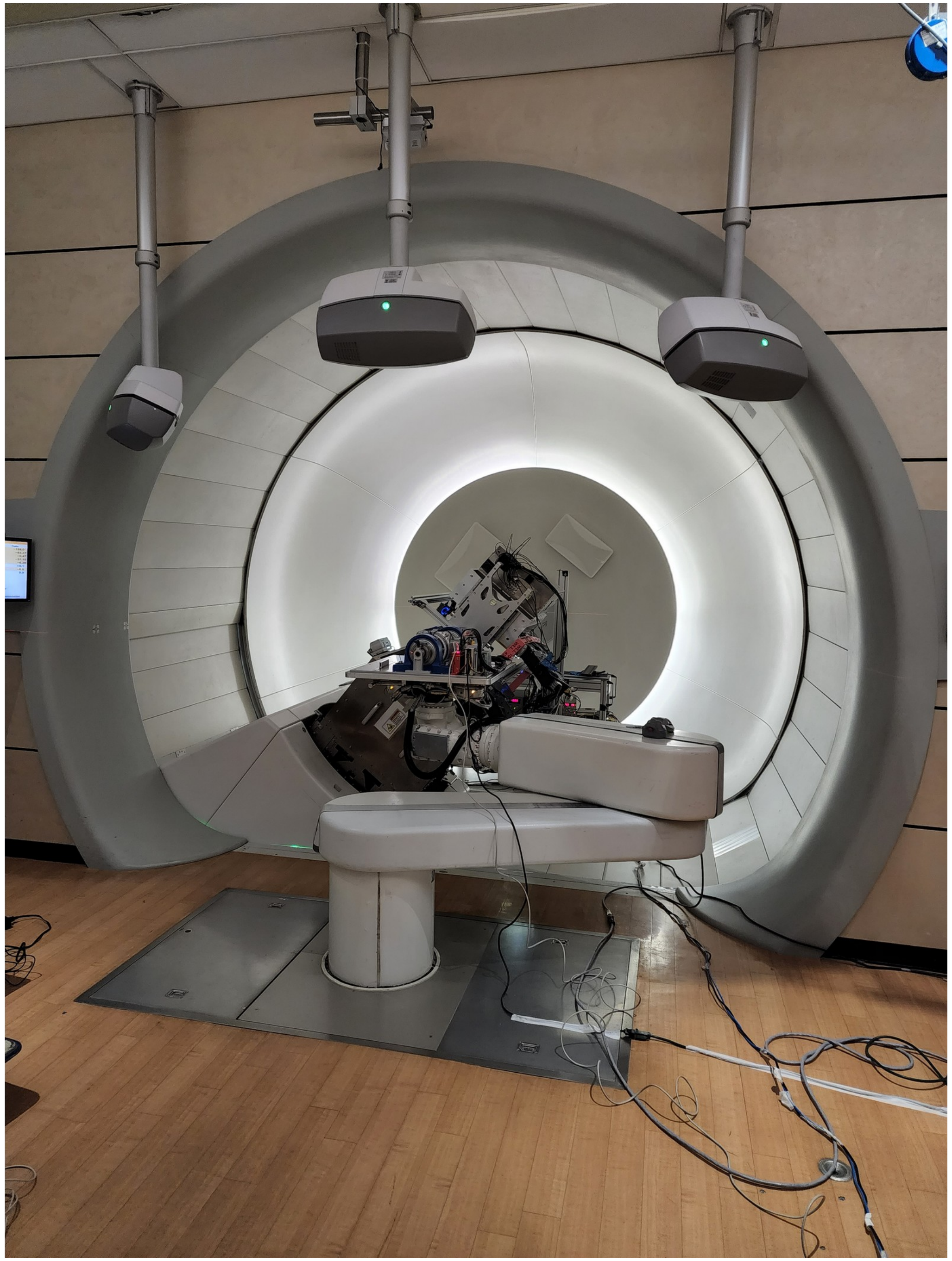

Issues affecting image reconstruction:

- Separate rotational axes for imaging system and gantry
- Shifting of detector geometry vs. angle
- Sagging of gantry vs. angle
- Change in PMT gains vs. angle
- Beam steering not well calibrated at low intensity

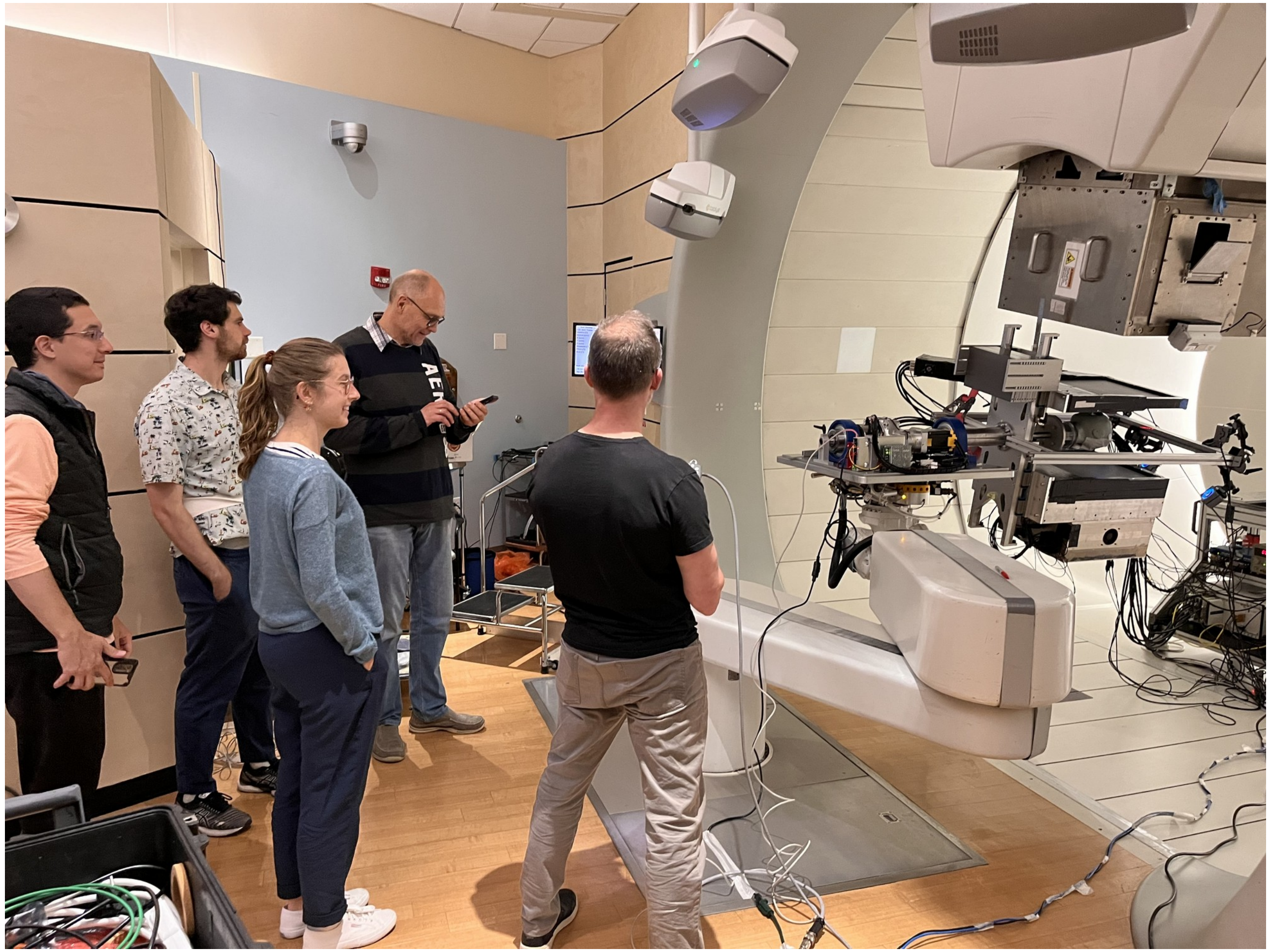

Plot of proton count vs beam spot for 120 MeV

- Each pixel represents a 5x5 mm area

- Apparent movement of head indicates scan pattern shifts up to 2 cm

- This did not occur for 198 MeV scan

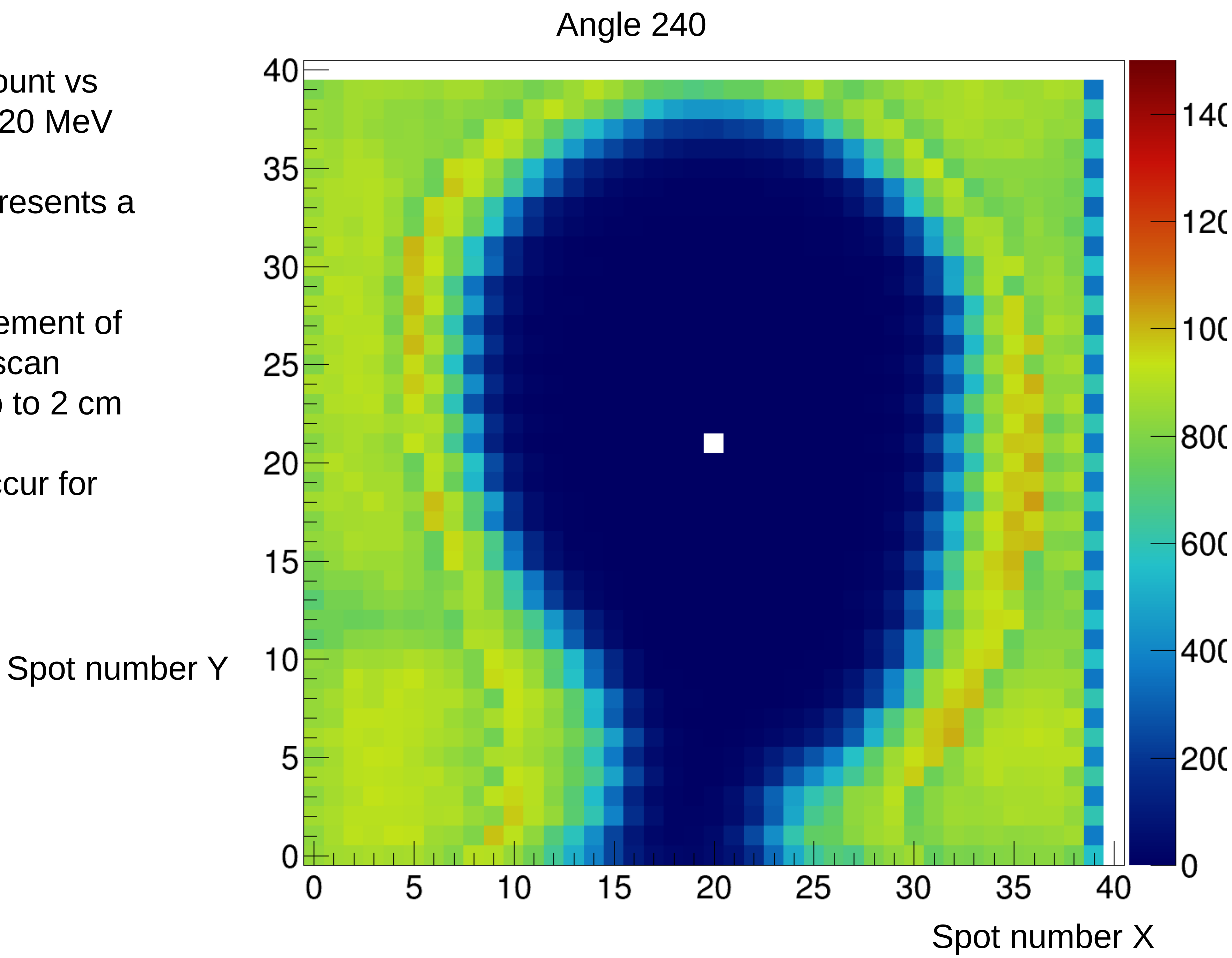

Plot of proton count vs beam spot for 120 MeV

- Each pixel represents a 5x5 mm area

- Apparent movement of head indicates scan pattern shifts up to 2 cm

- This did not occur for 198 MeV scan

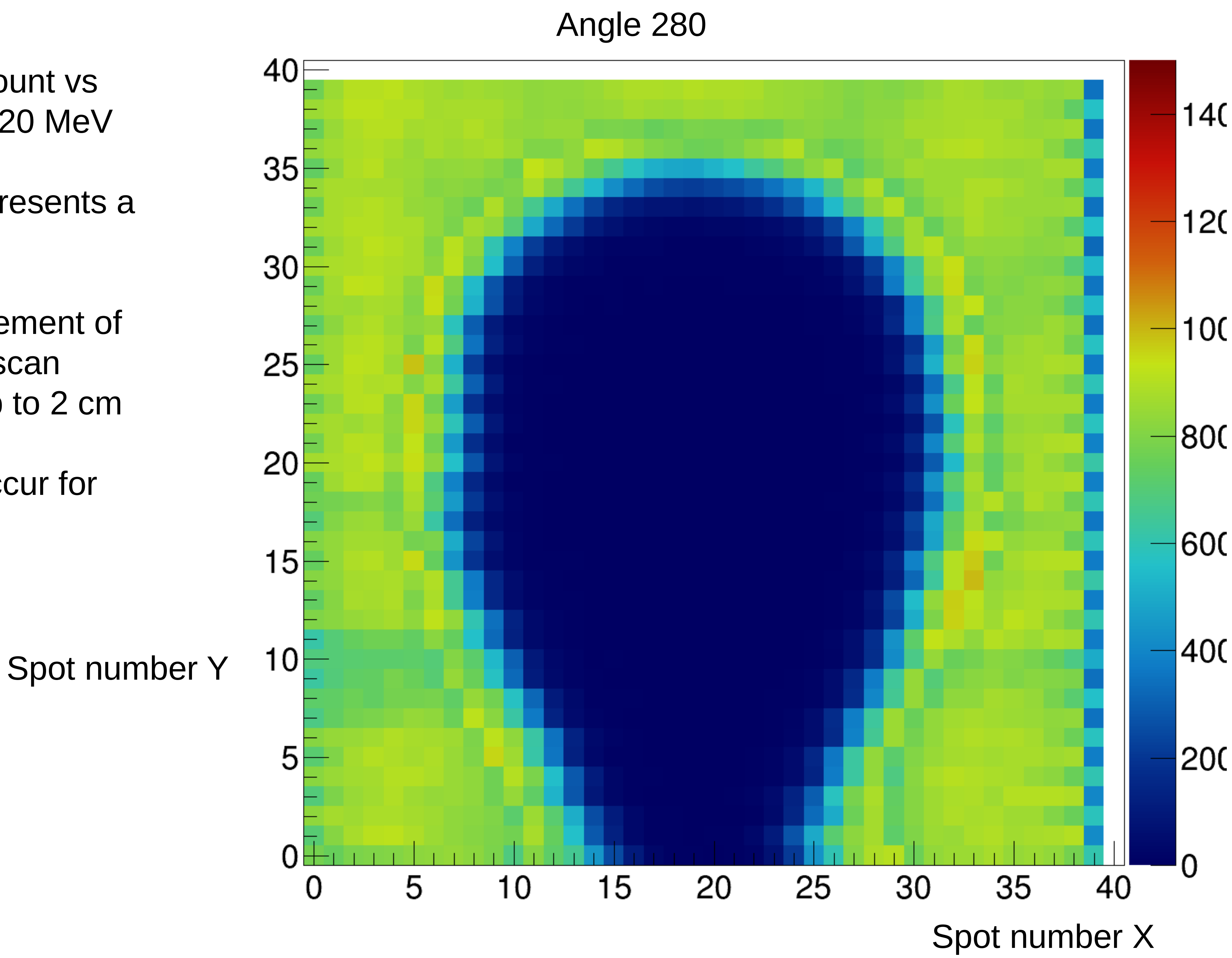

Plot of proton count vs beam spot for 120 MeV

- Each pixel represents a 5x5 mm area

- Apparent movement of head indicates scan pattern shifts up to 2 cm

- This did not occur for 198 MeV scan

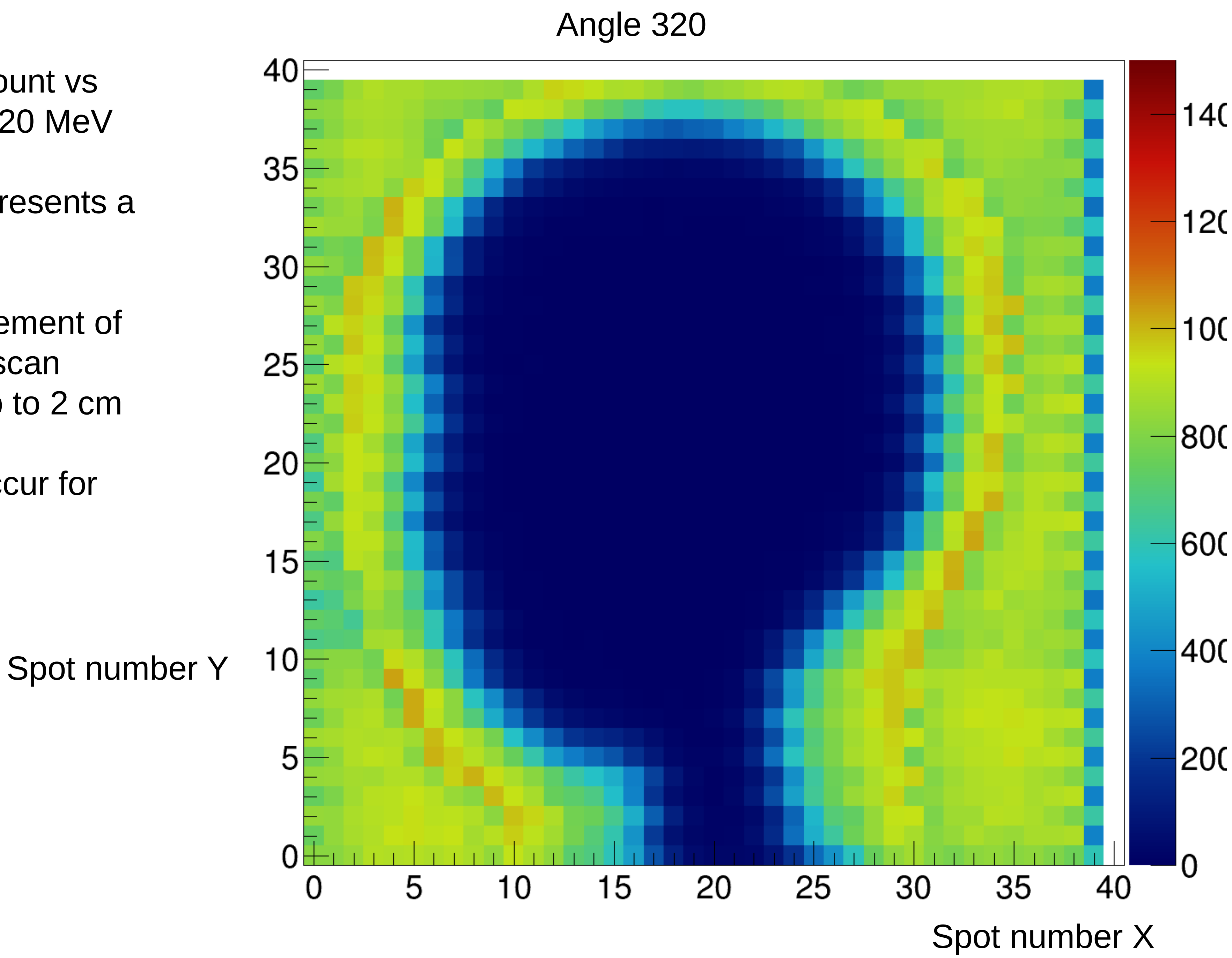

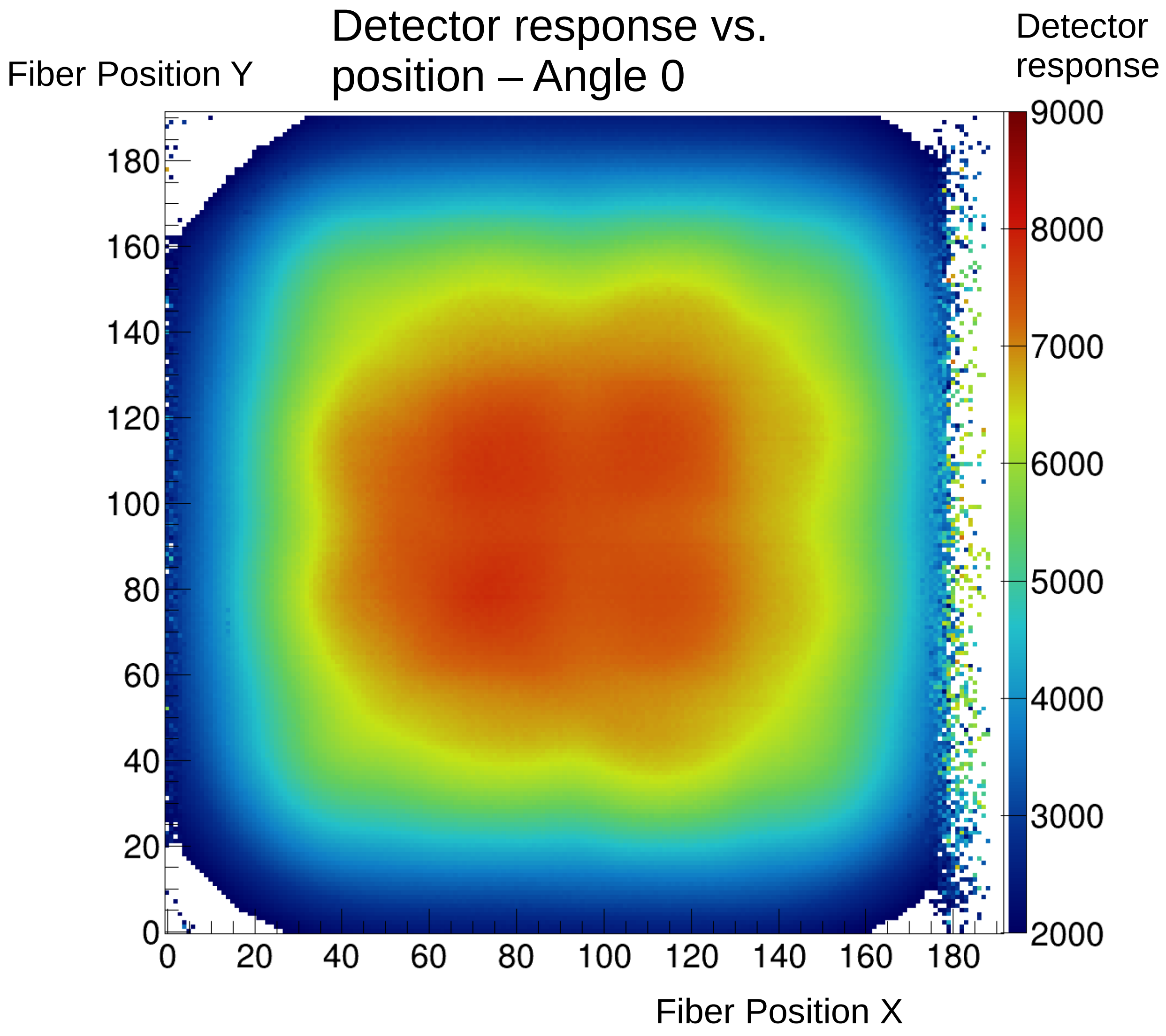

Detector response vs. position – Angle 0
Fiber Position Y
Detector response
9000
8000
7000
6000
5000
4000
3000
2000
0
20
40
60
80
100
120
140
160
180
Fiber Position X

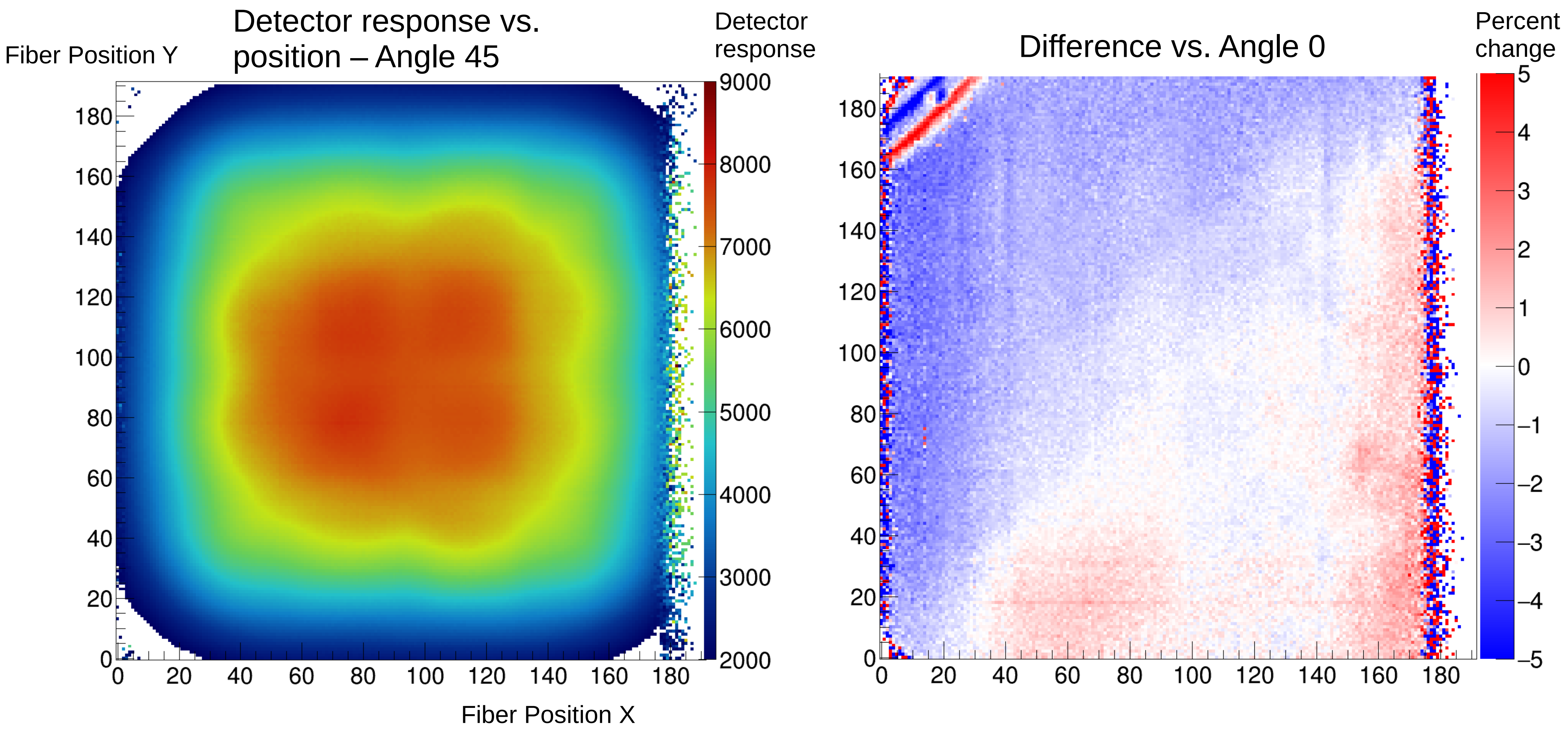

Detector response vs. position – Angle 45
Fiber Position Y
Detector response
Fiber Position X
Difference vs. Angle 0
Percent change

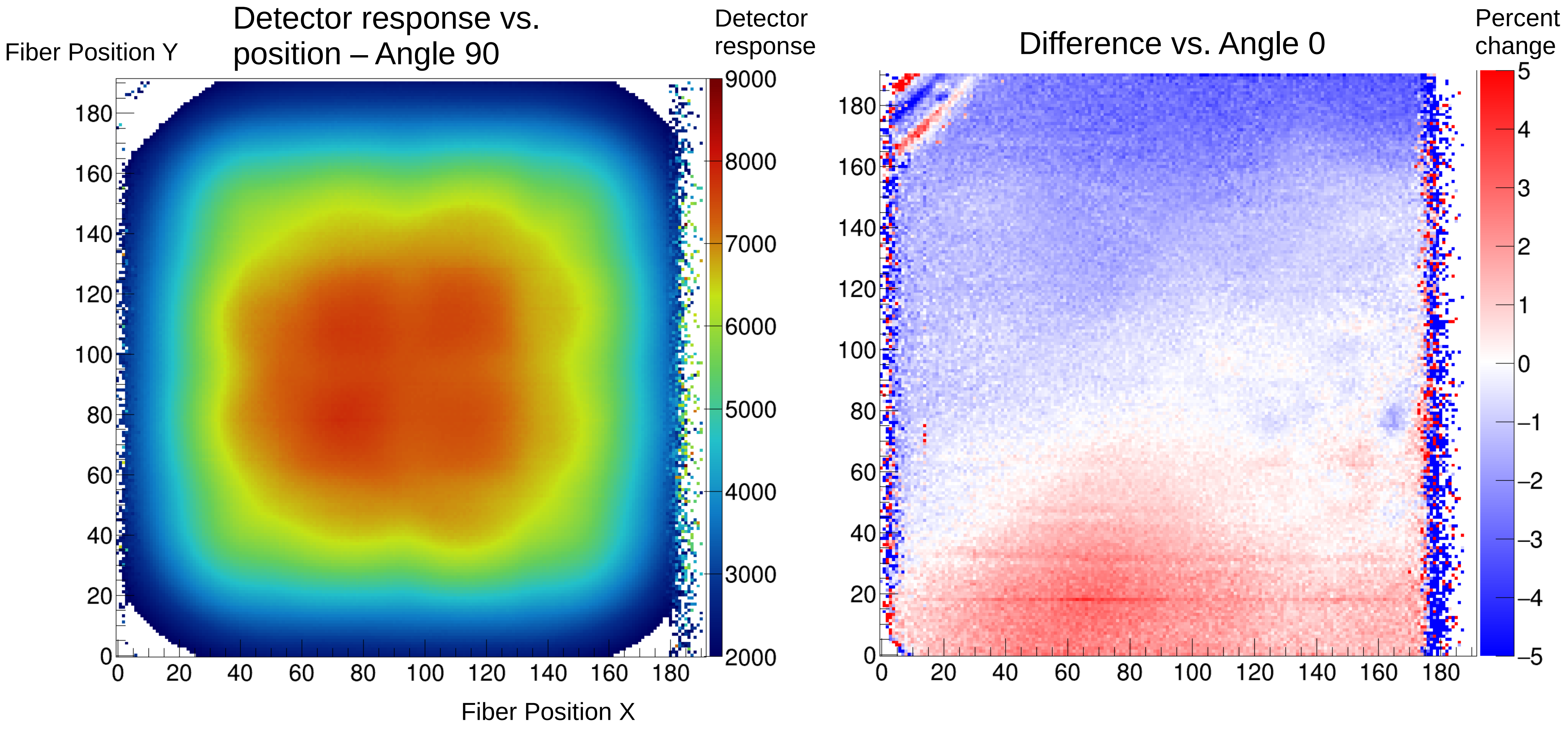
Detector response vs. position – Angle 90
Fiber Position Y
Detector response
9000
8000
7000
6000
5000
4000
3000
2000
0
20
40
60
80
100
120
140
160
180
Fiber Position X
Difference vs. Angle 0
Percent change
5
4
3
2
1
0
−1
−2
−3
−4
−5

Detector Response vs. Fiber Position for 45 gantry angles

- 162 MeV protons

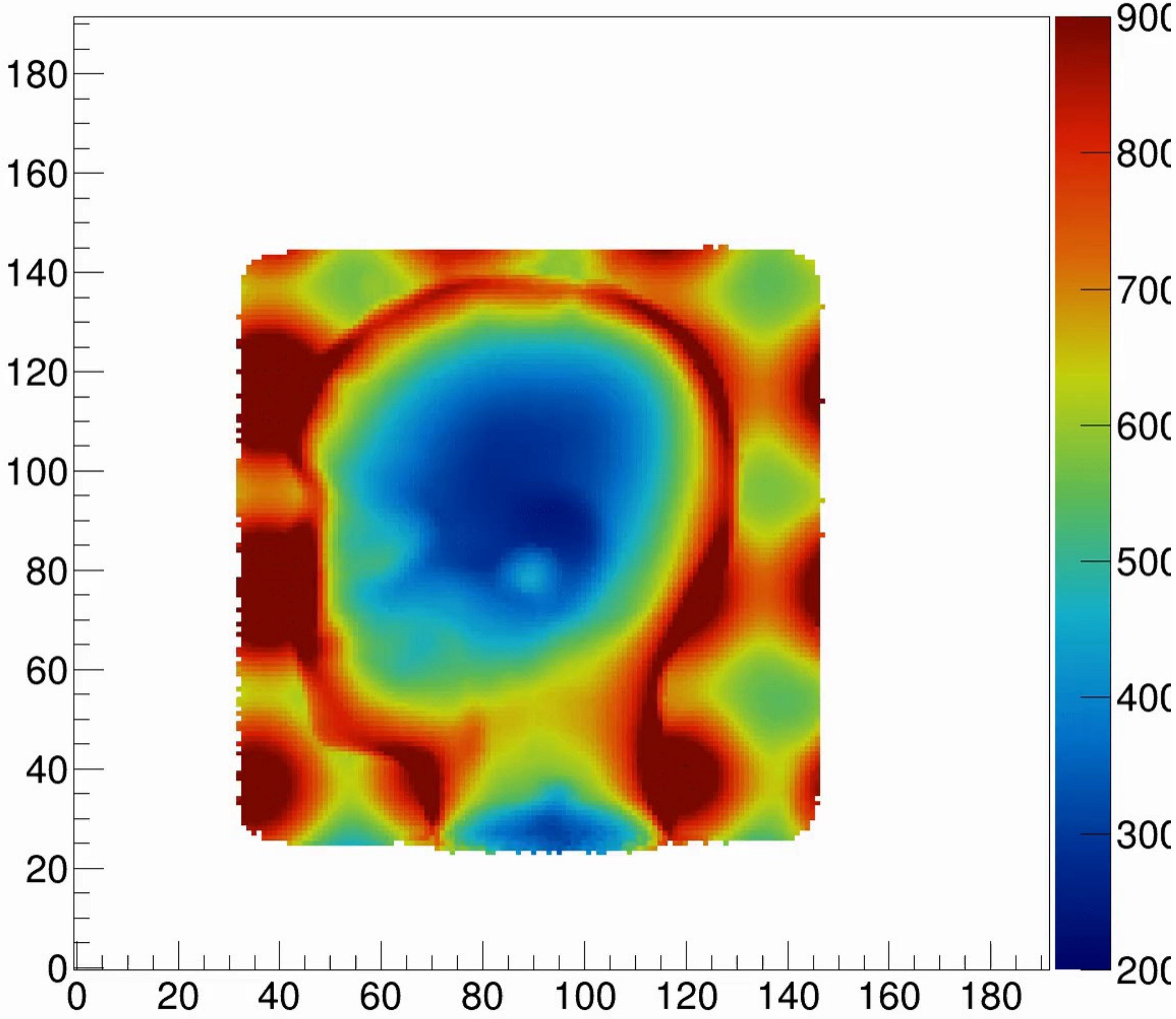

Mapping fiber positions to beam coordinates using the average fiber index of each beam spot

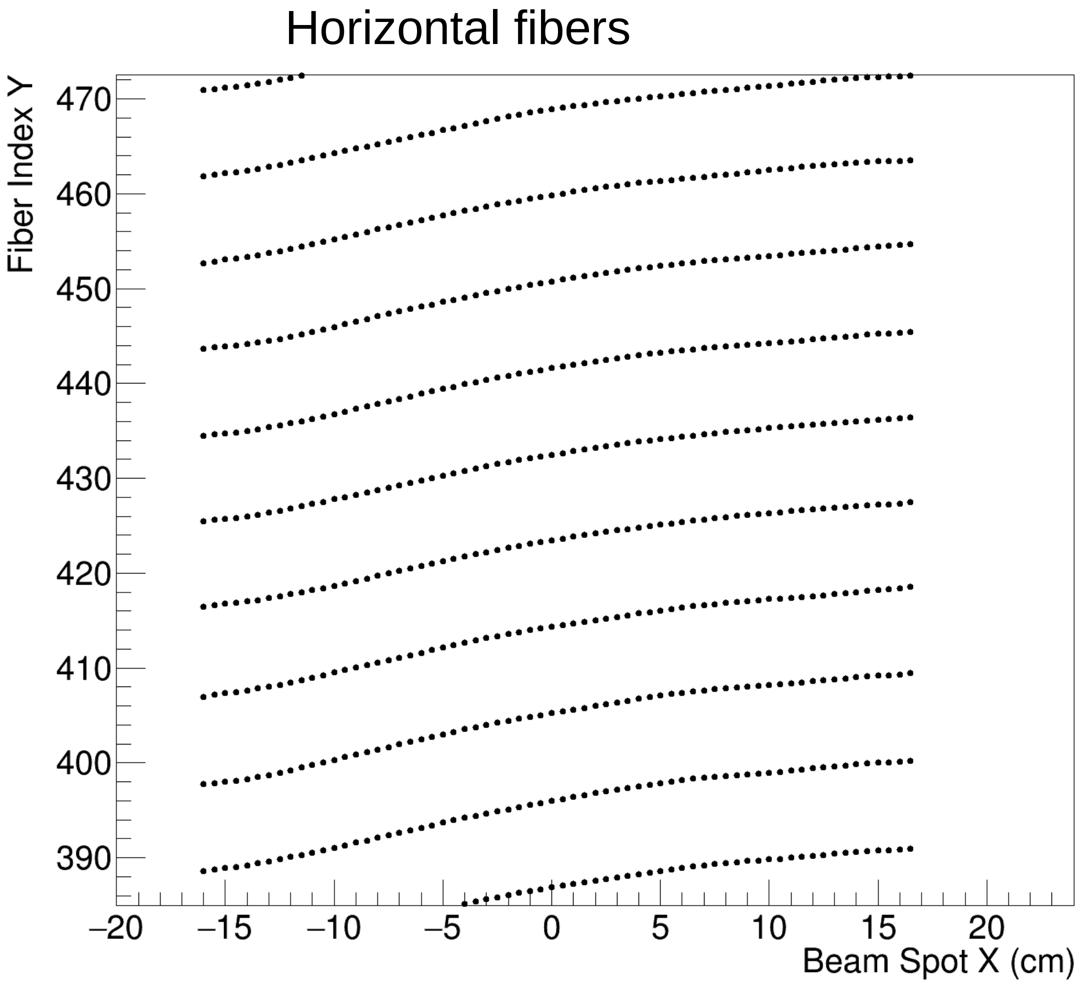

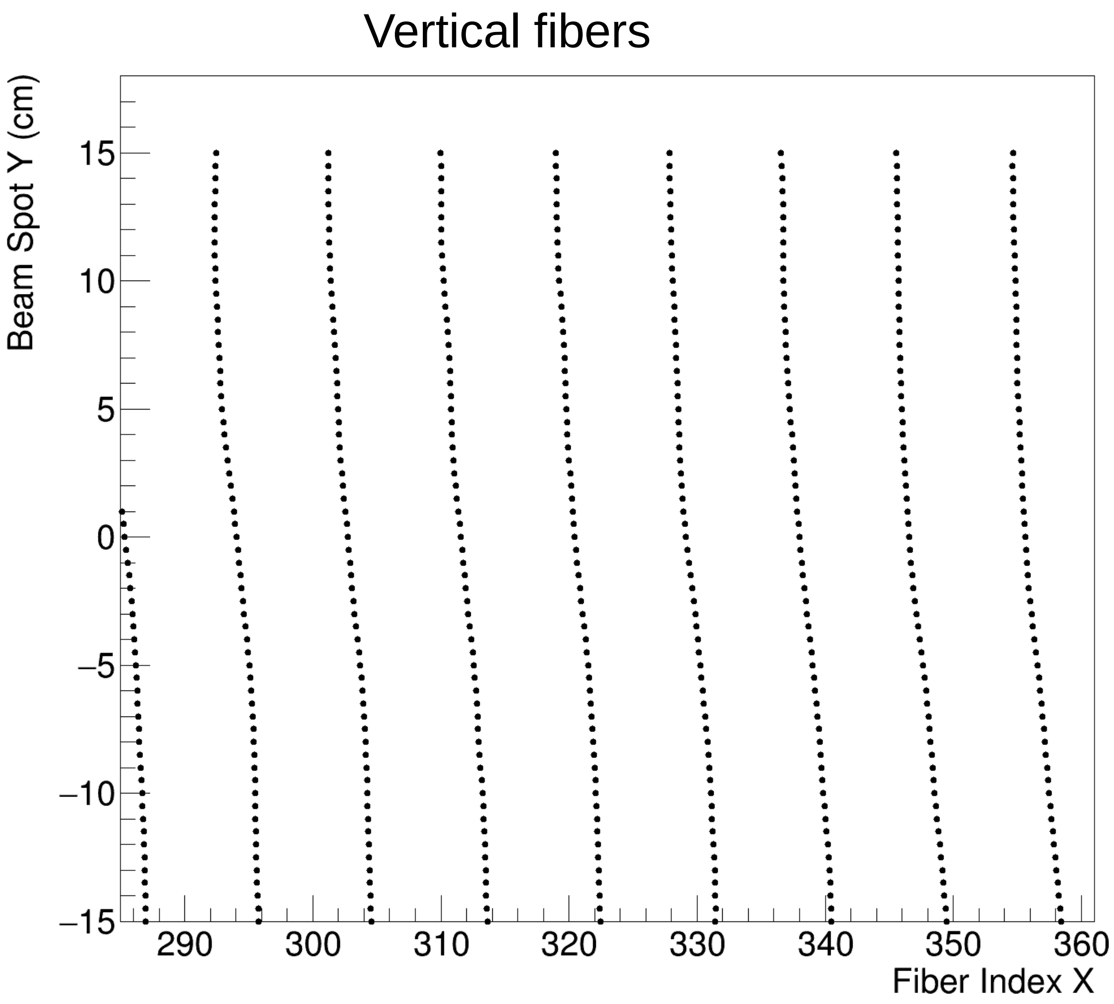

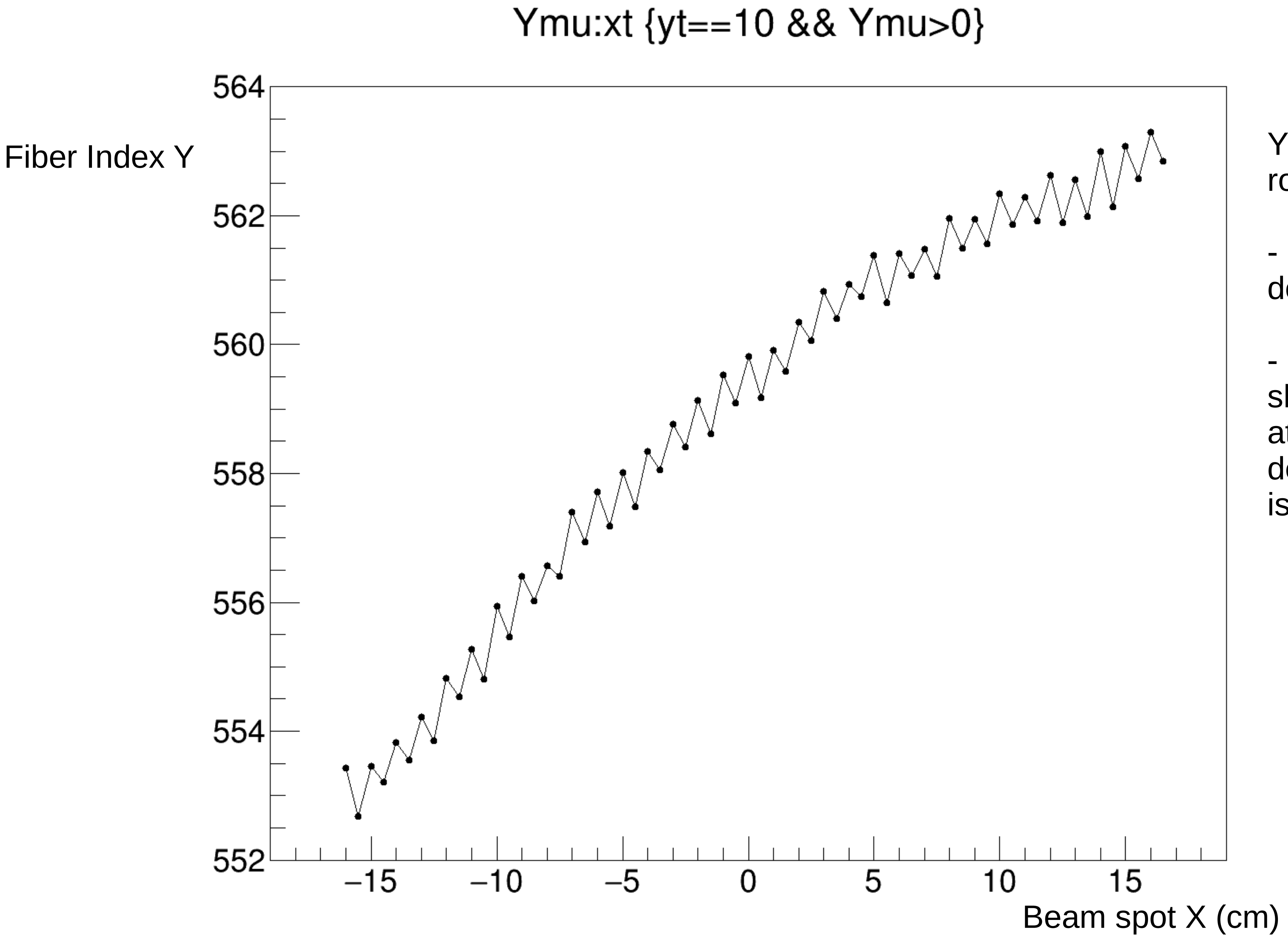

Y Fiber Positions for one row of spots

- beam scanning up and down

- oscillating pattern shows the beam stopping at different heights depending on whether it is moving up or down

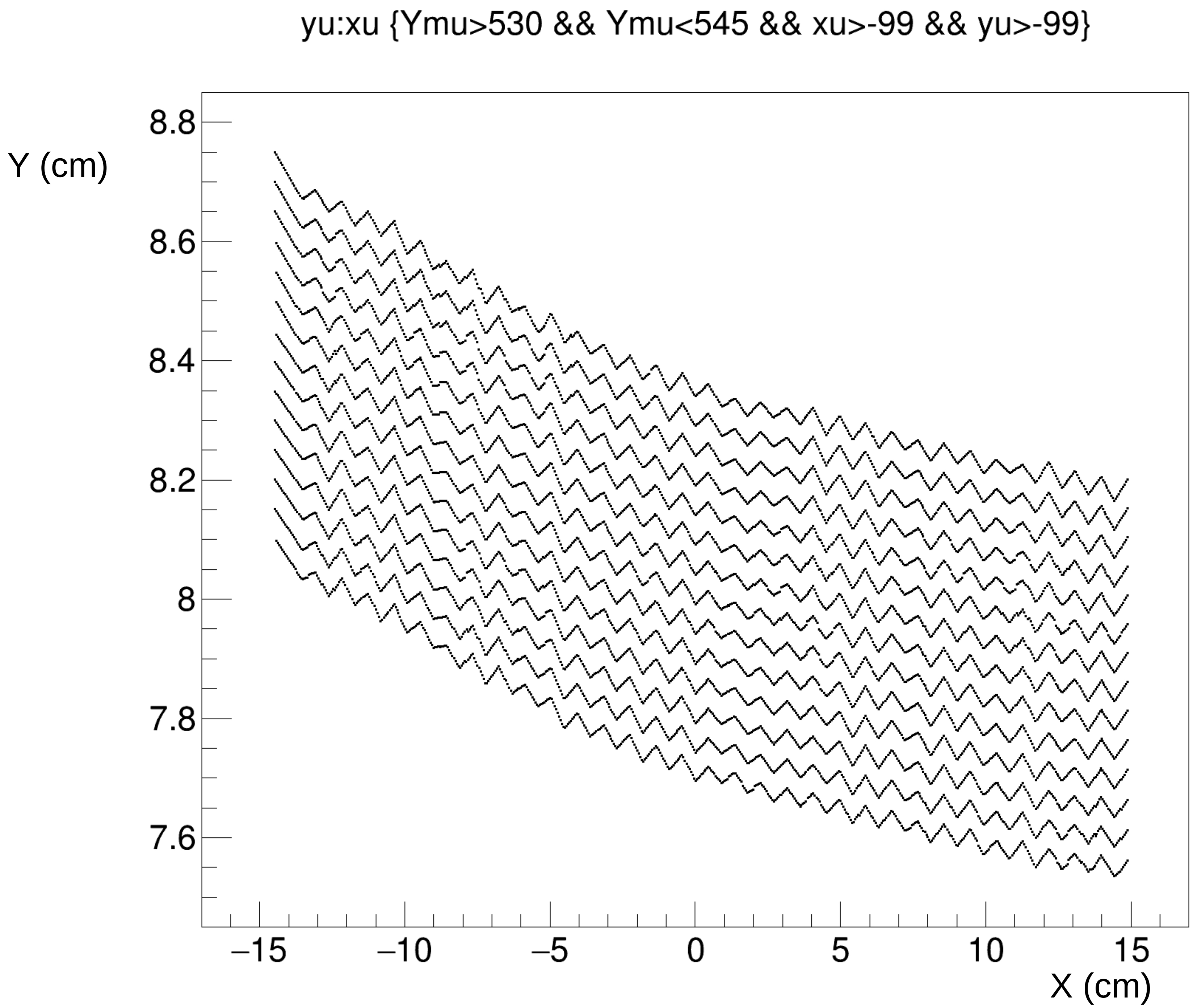

X-Y location of each fiber index combination, in beam coordinates

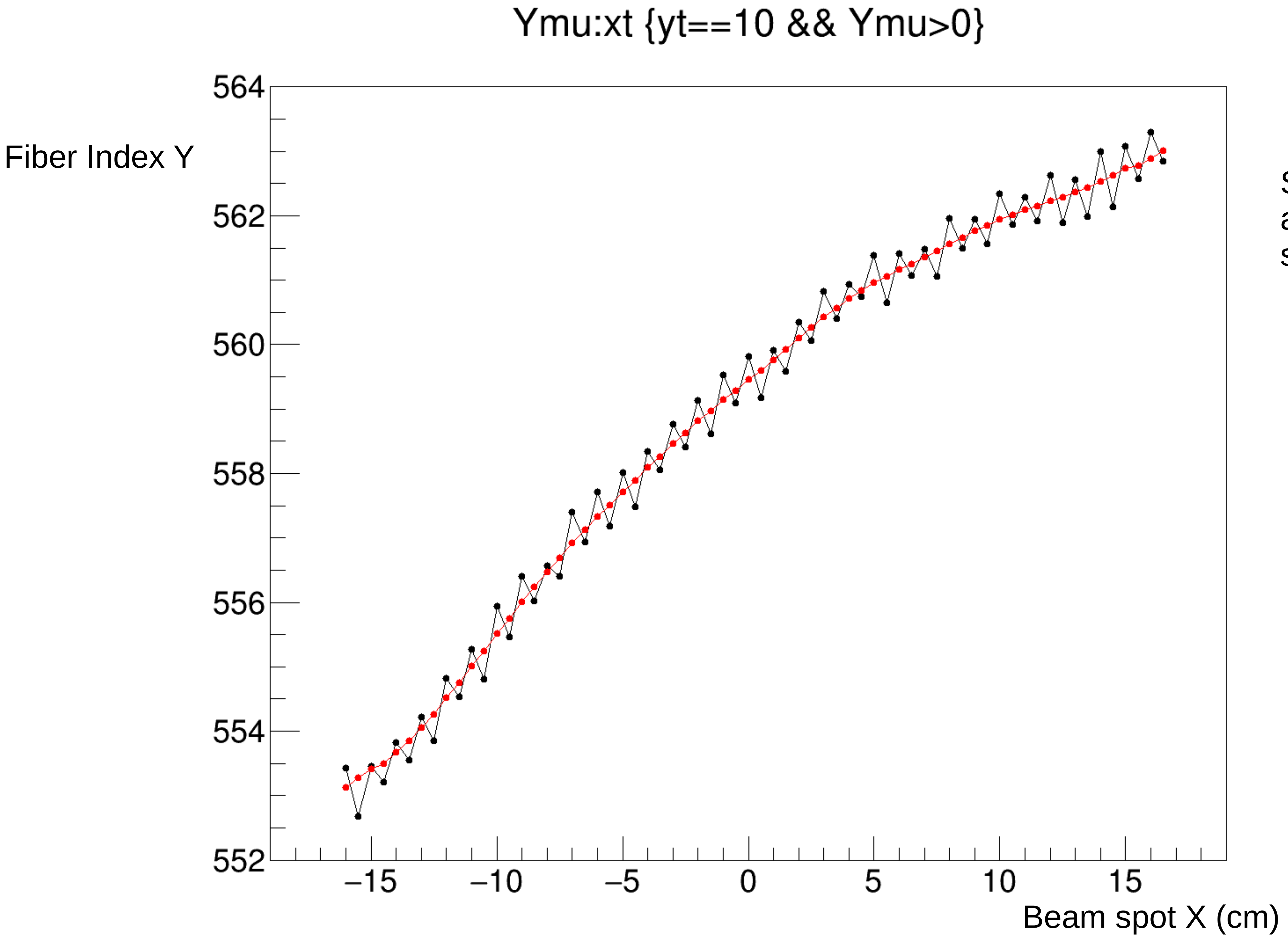

Smoothing algorithm applied to beam spot positions

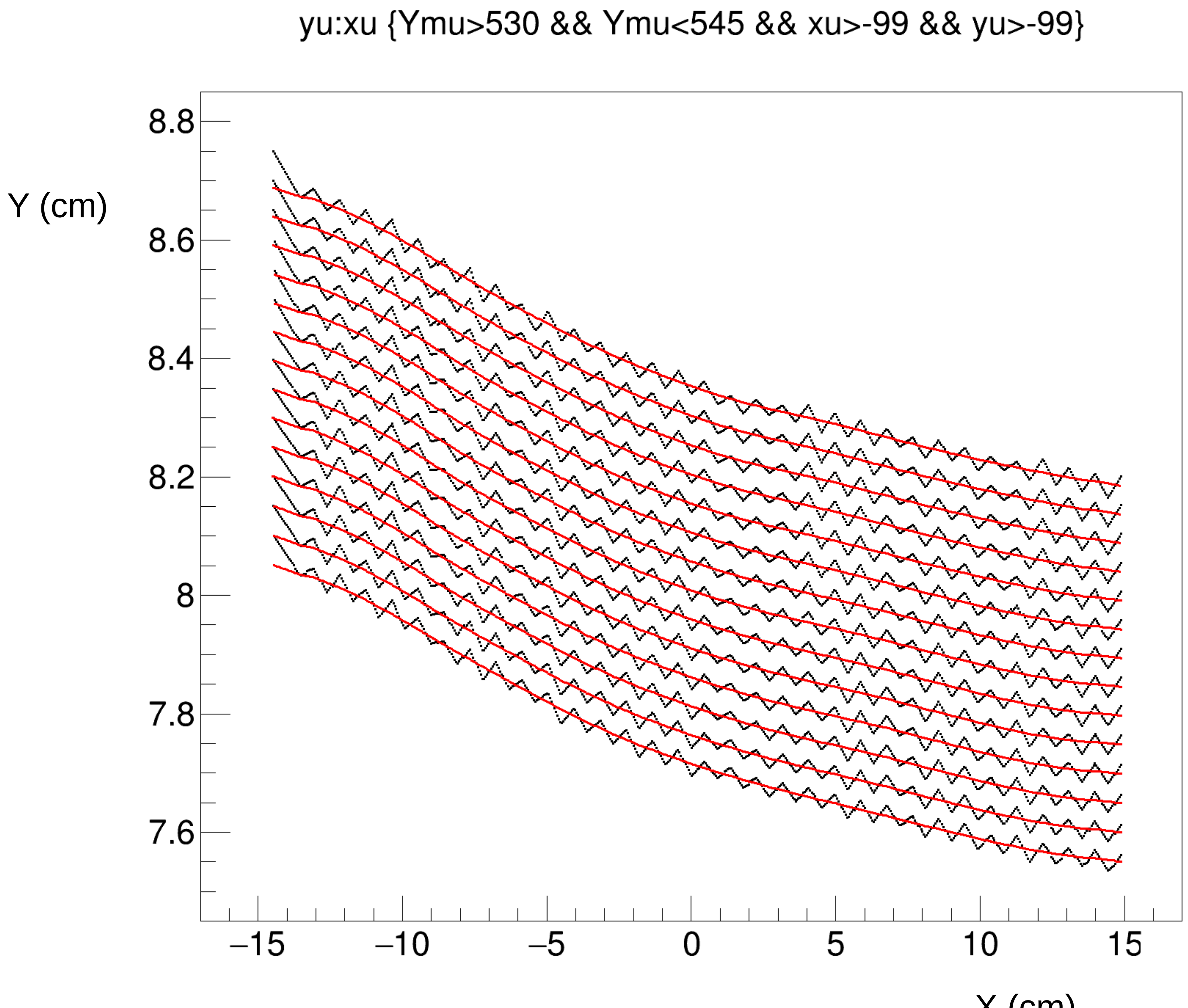

Affect of smoothing of fiber positions

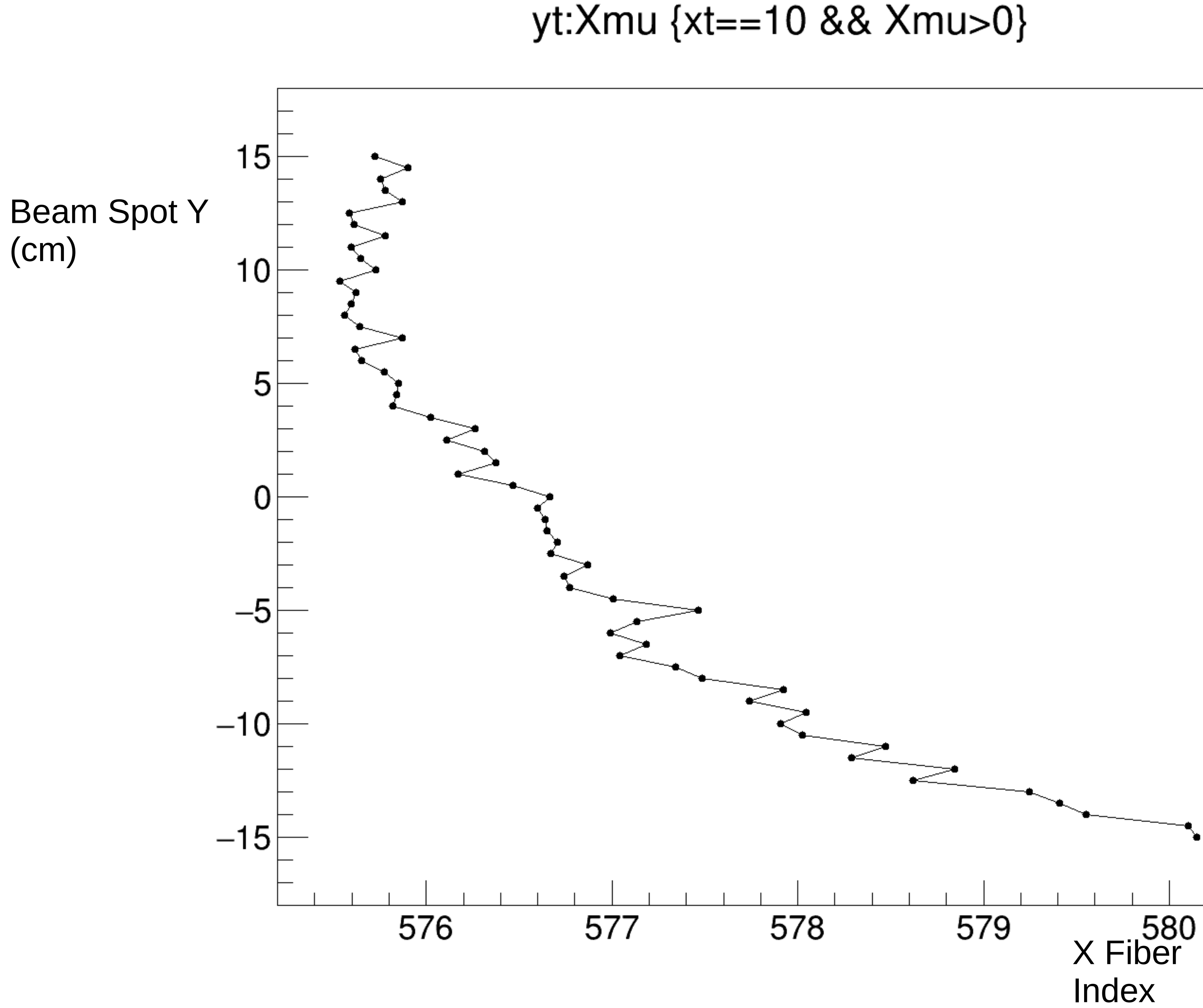

X Fiber positions
for one column of
beam spots

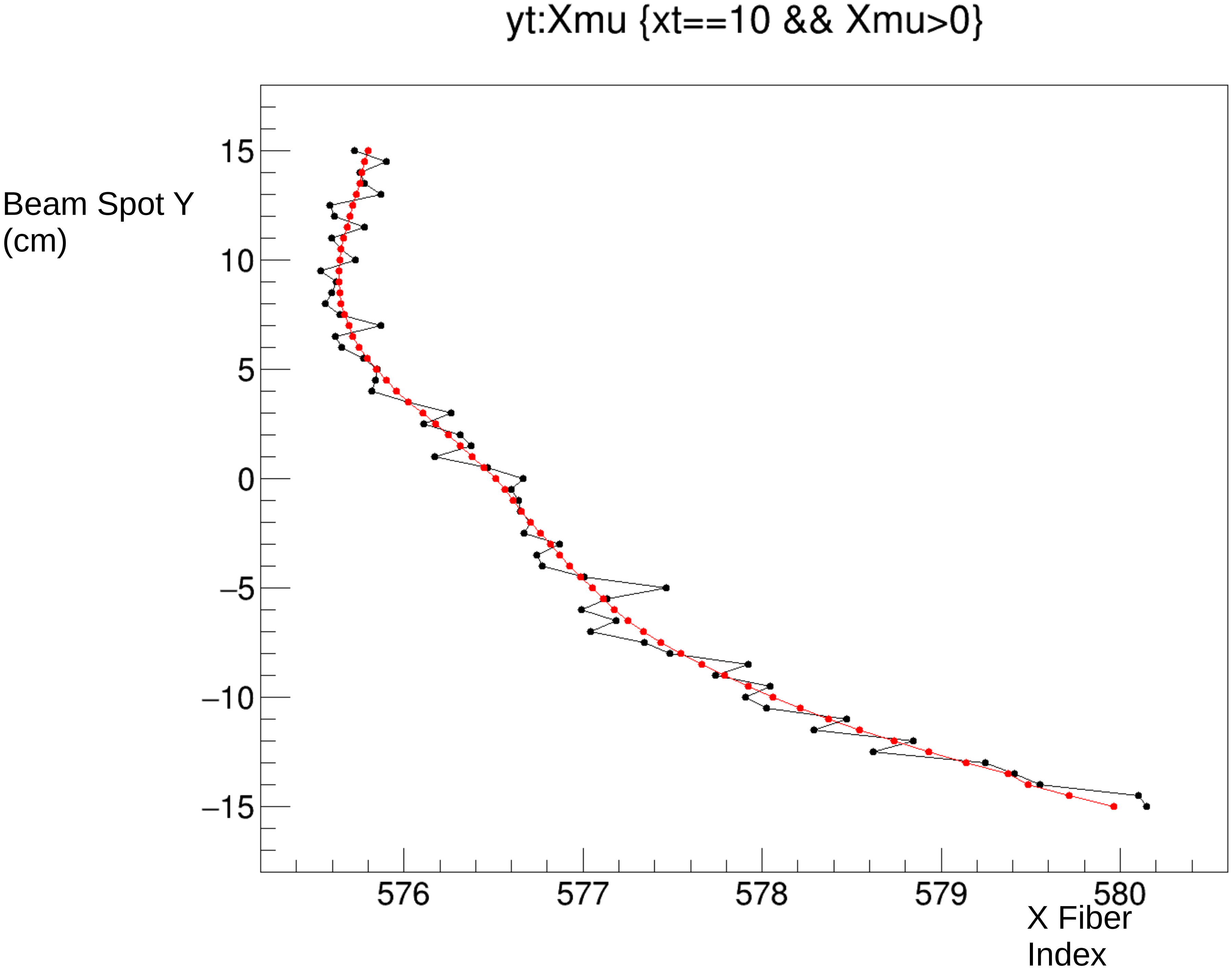
yt:Xmu {xt==10 && Xmu>0}
Beam Spot Y
(cm)
15
10
5
0
−5
−10
−15
576
577
578
579
580
X Fiber
Index

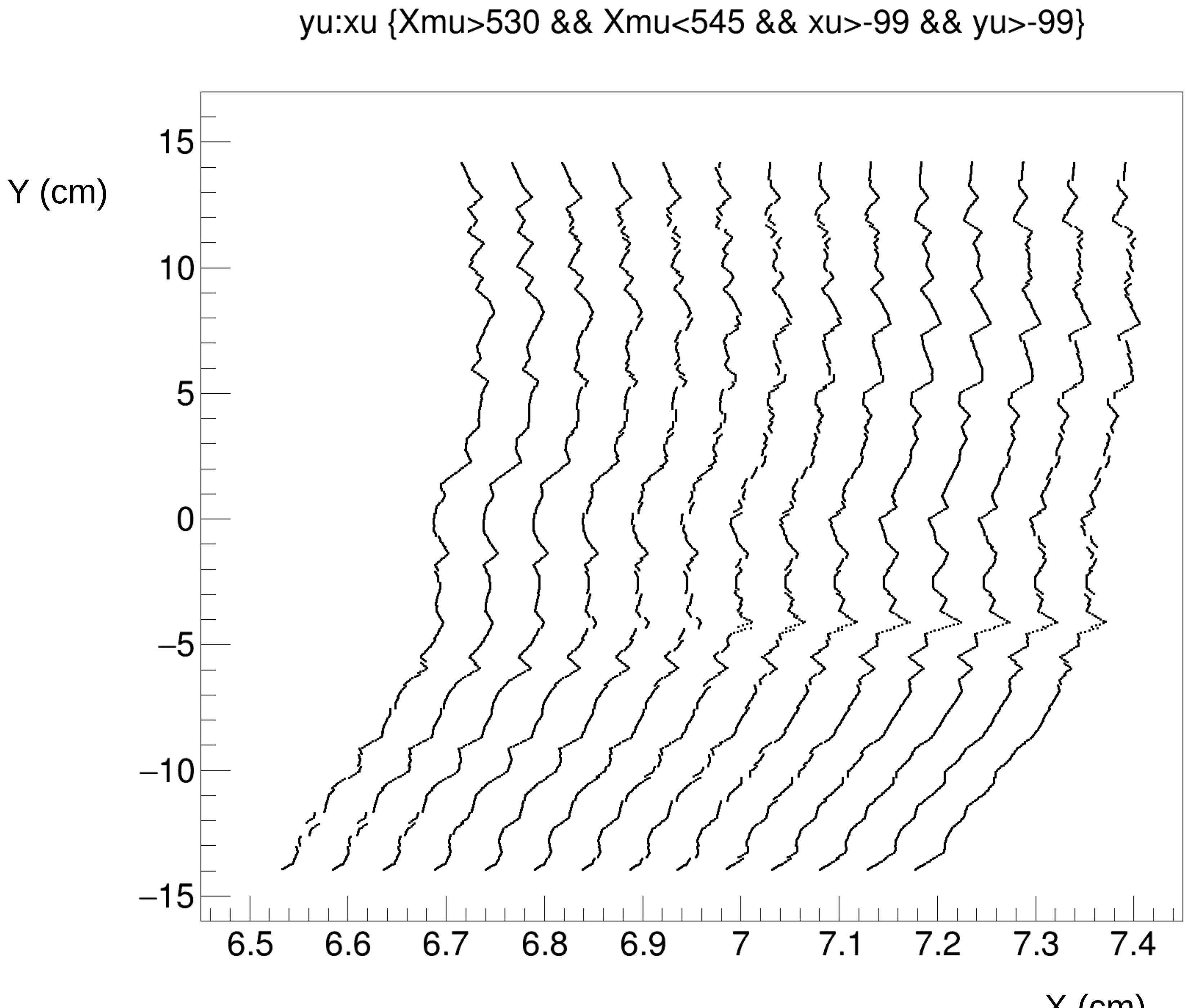

Vertical fiber positions (cm)

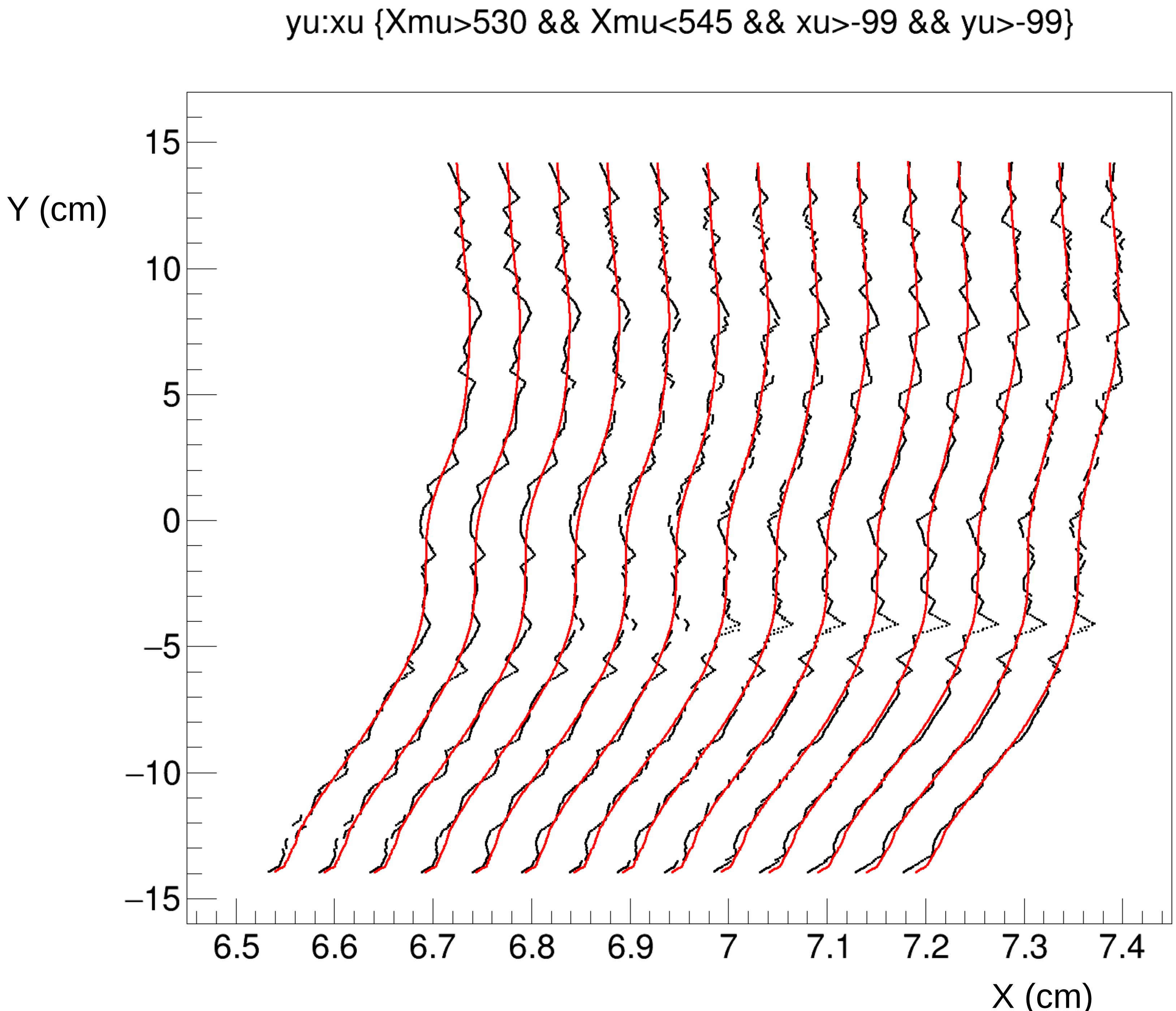

Vertical fiber positions (cm)

1 cm pCT slices – unsmoothed fibers

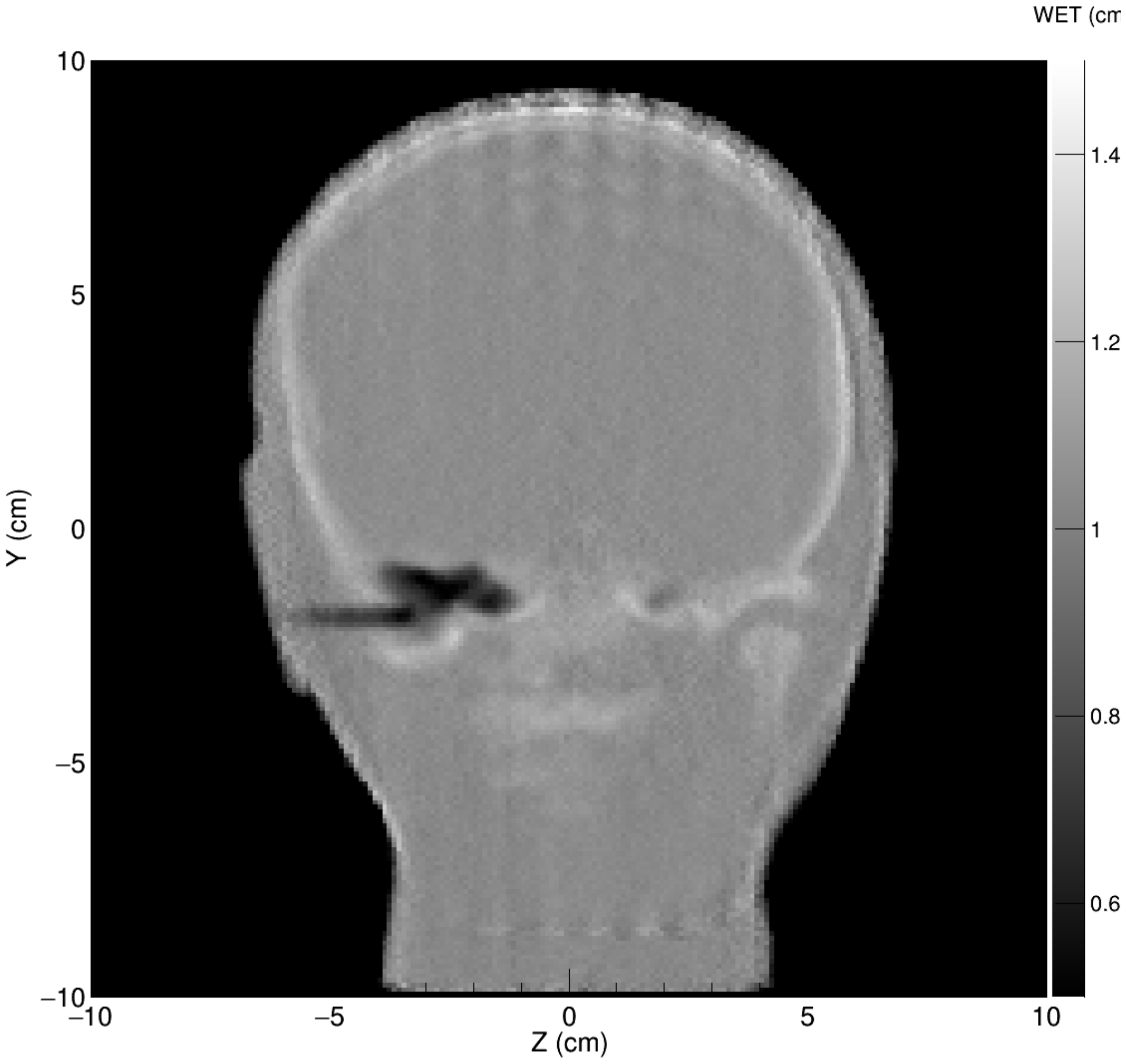

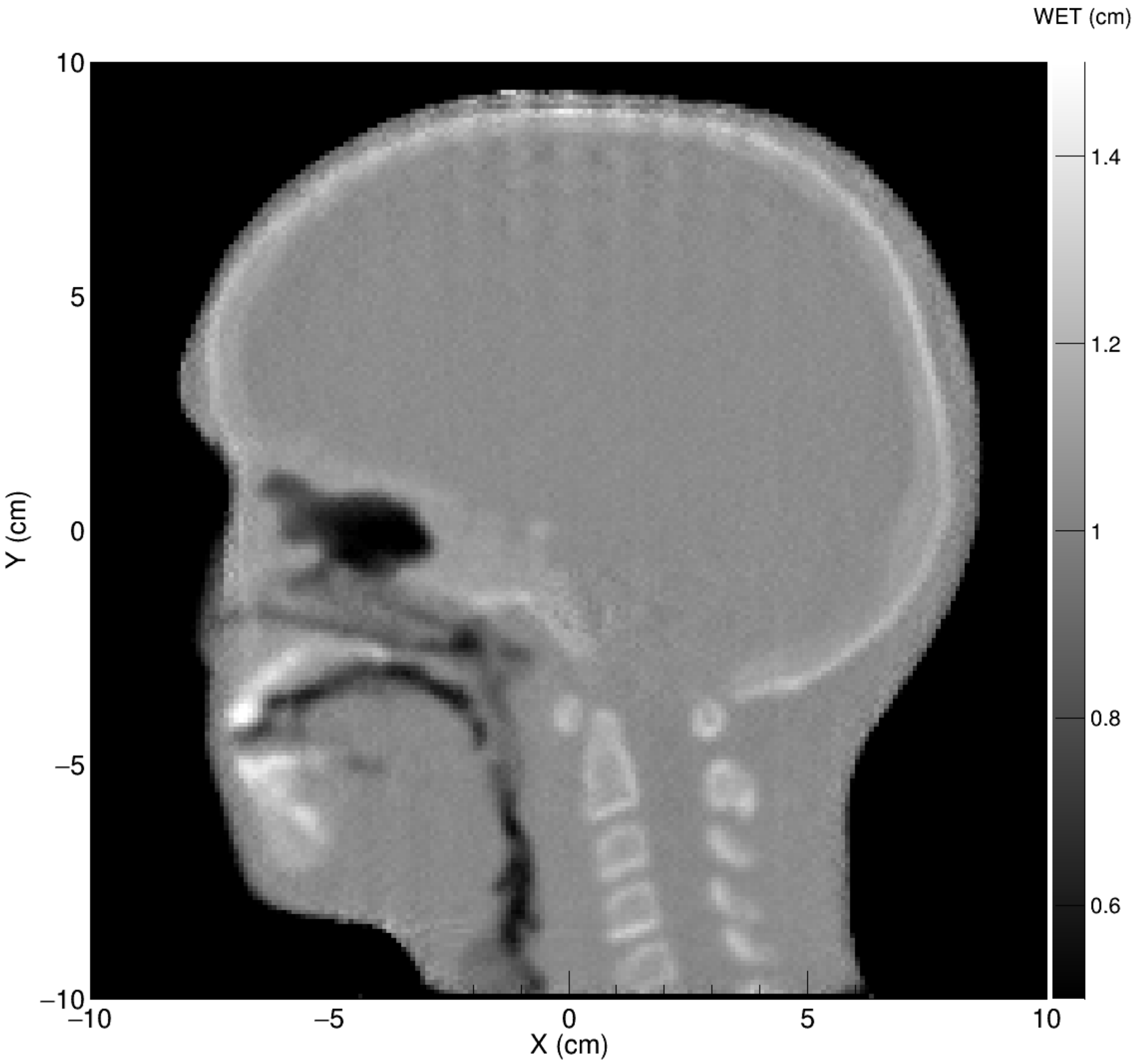

*Data taken from November 2021 fixed-beam room pCT scan

1 mm pCT slices – smoothed fibers

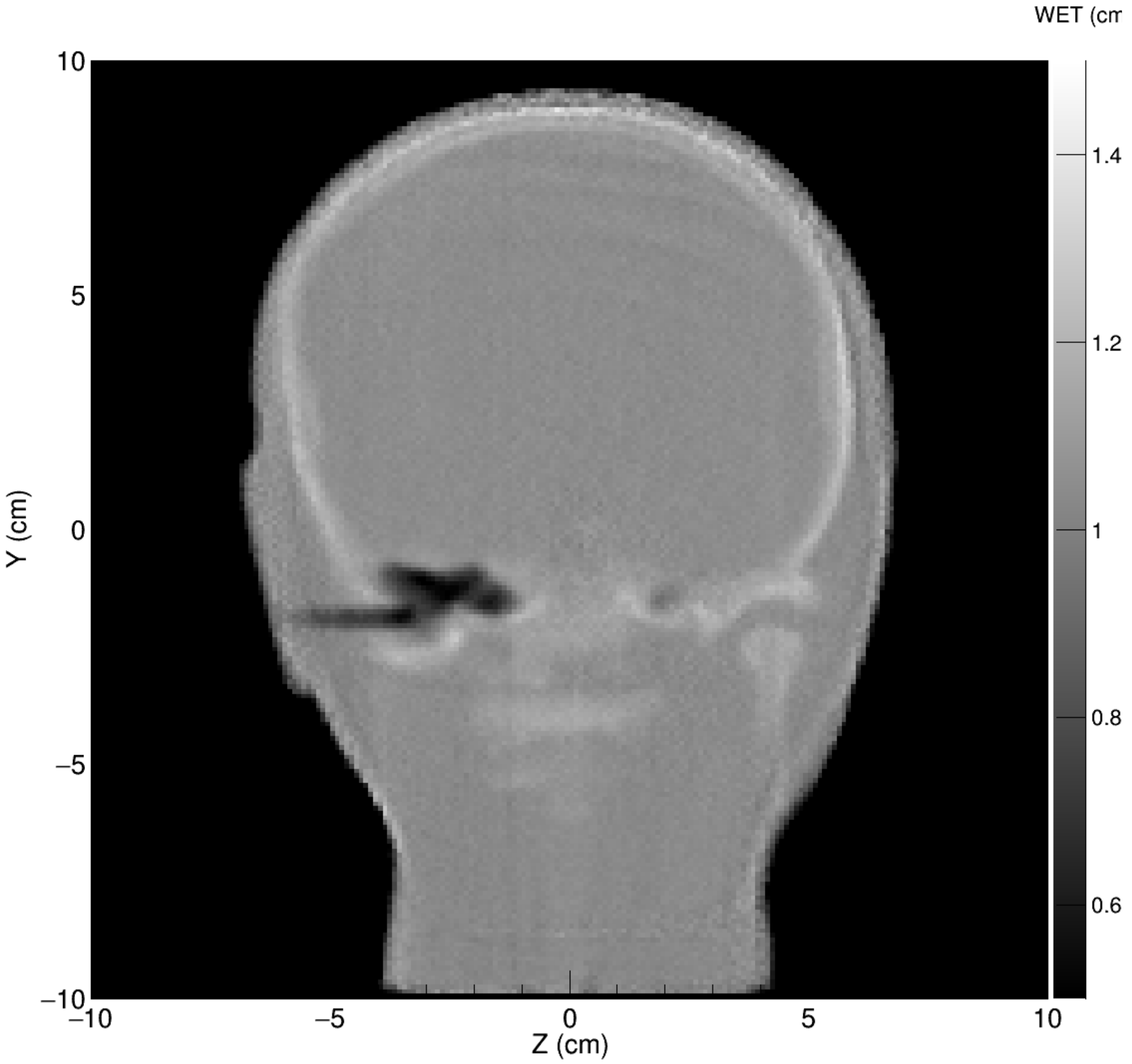

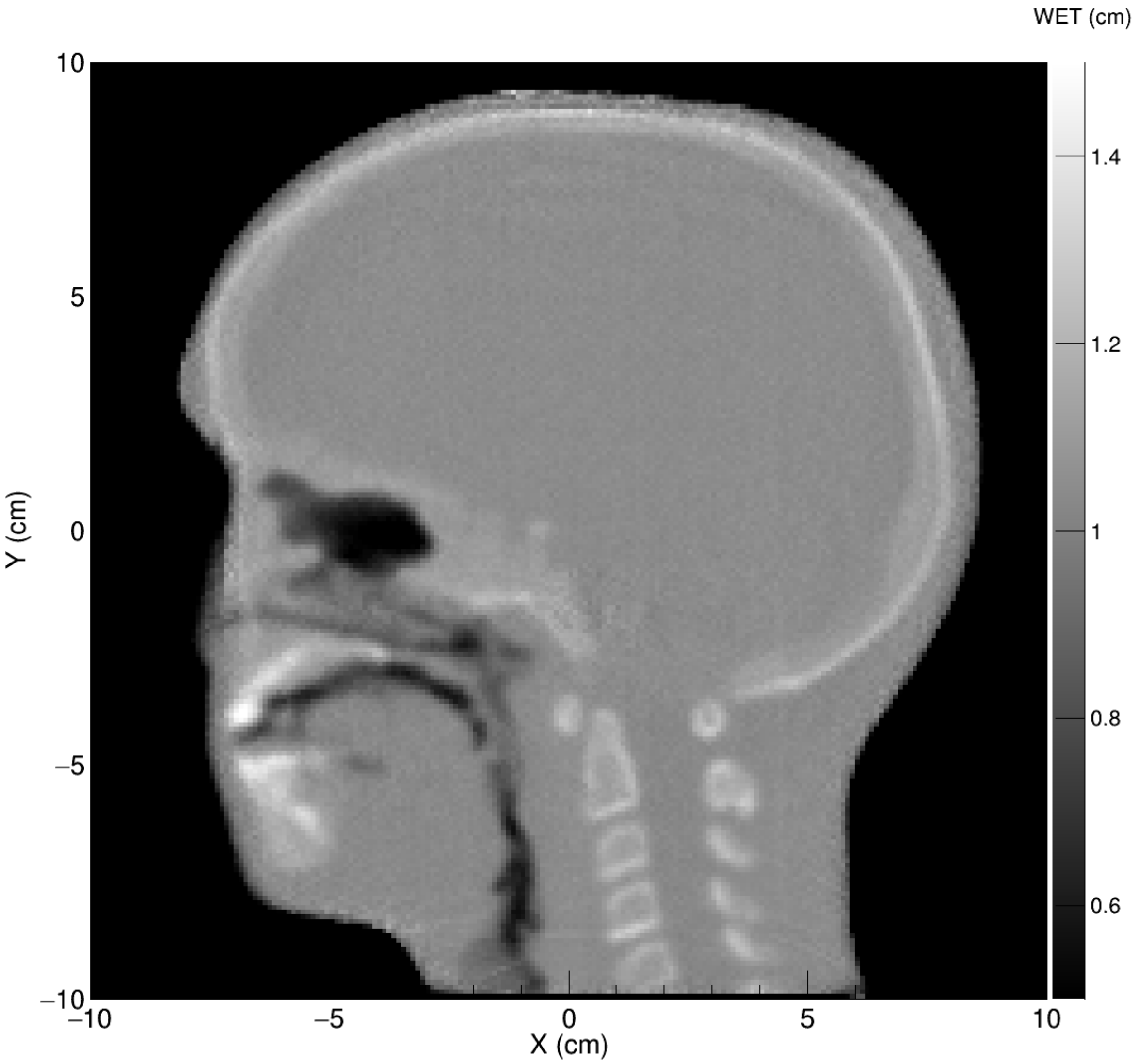

*Data taken from November 2021 fixed-beam room pCT scan

pRad Movie: 45 gantry angles

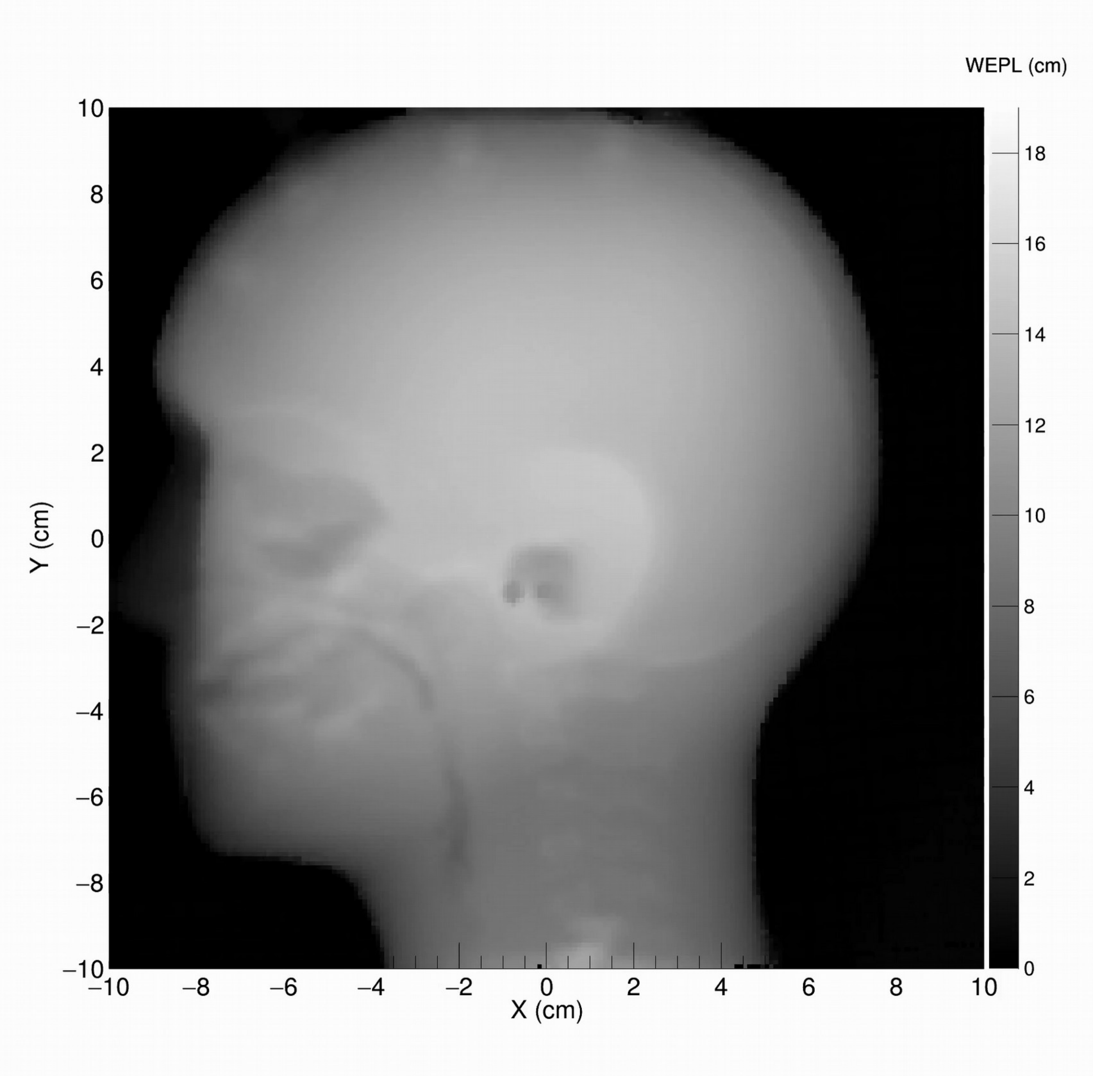

*Using separate beam-based position calibration at each angle

Sum of WEPL from all angles

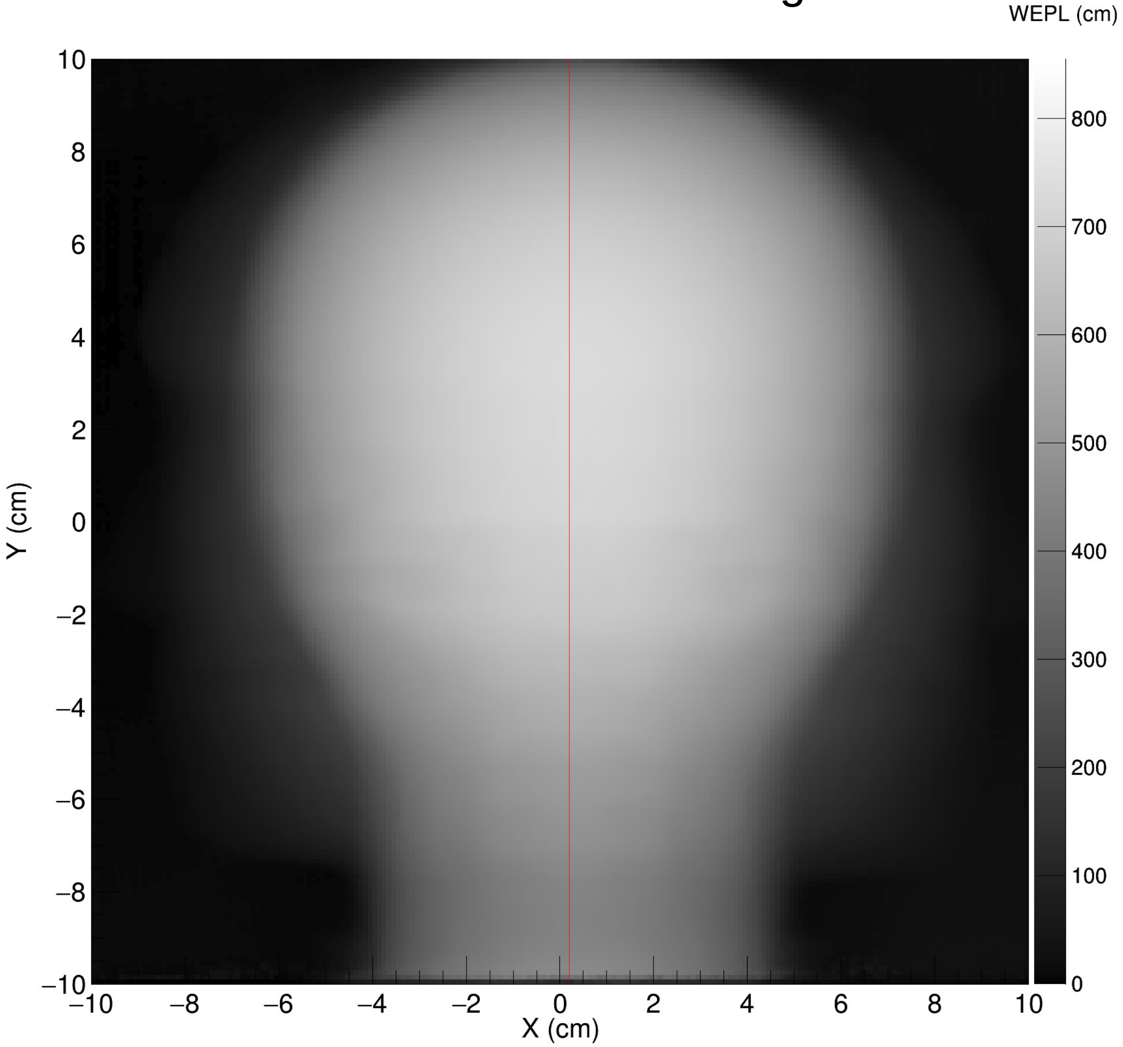

*Line of symmetry determines horizontal position of rotational axis to within 0.1 mm

1 mm pCT slices from gantry data

Vertical – from front of head

Vertical – from side of head

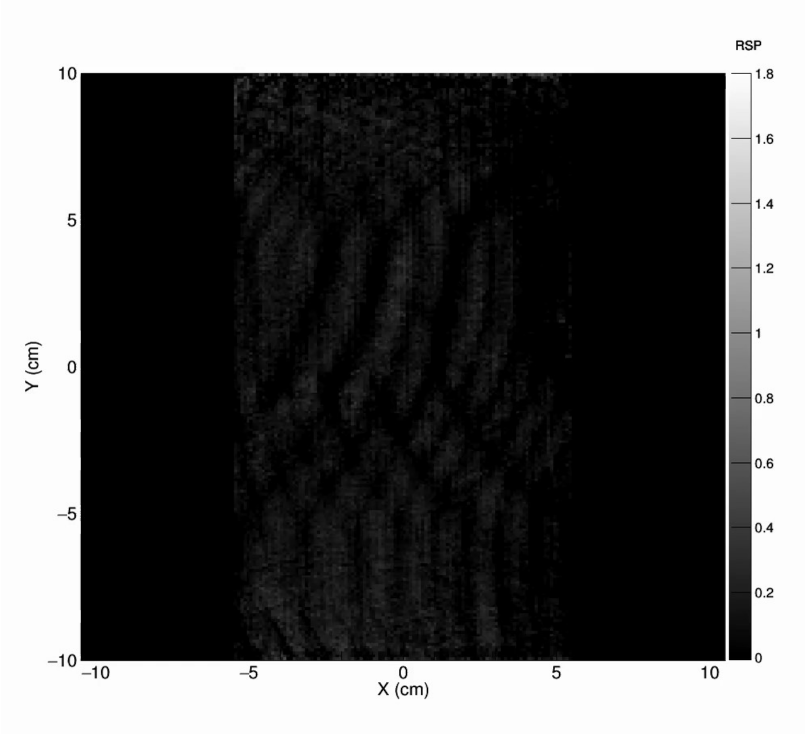

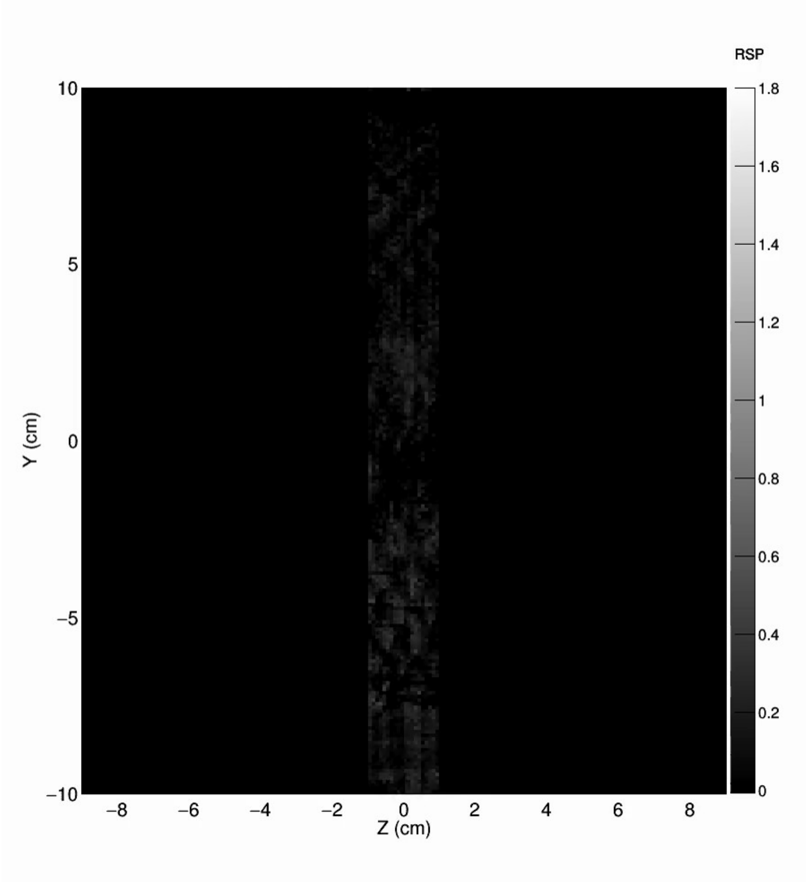

Horizontal

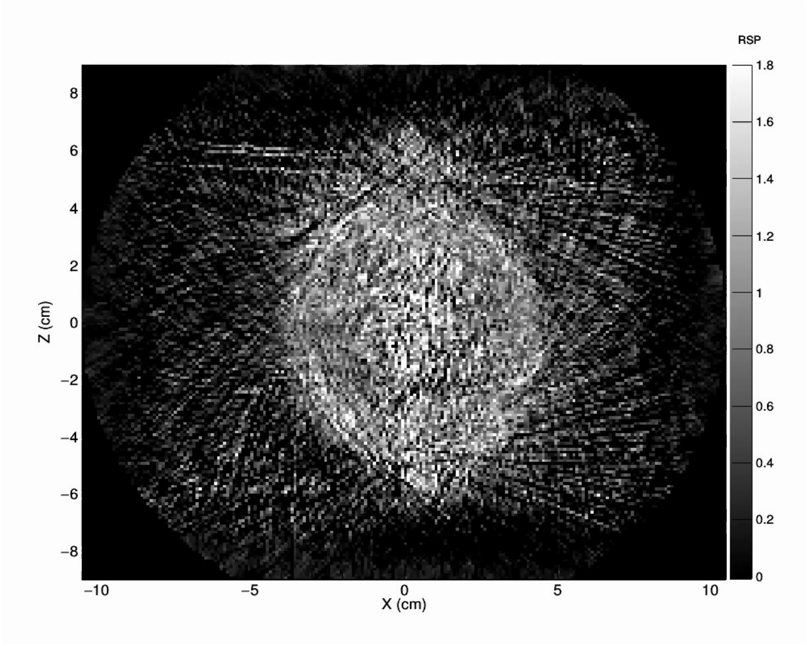

Gantry room data – 45 angles

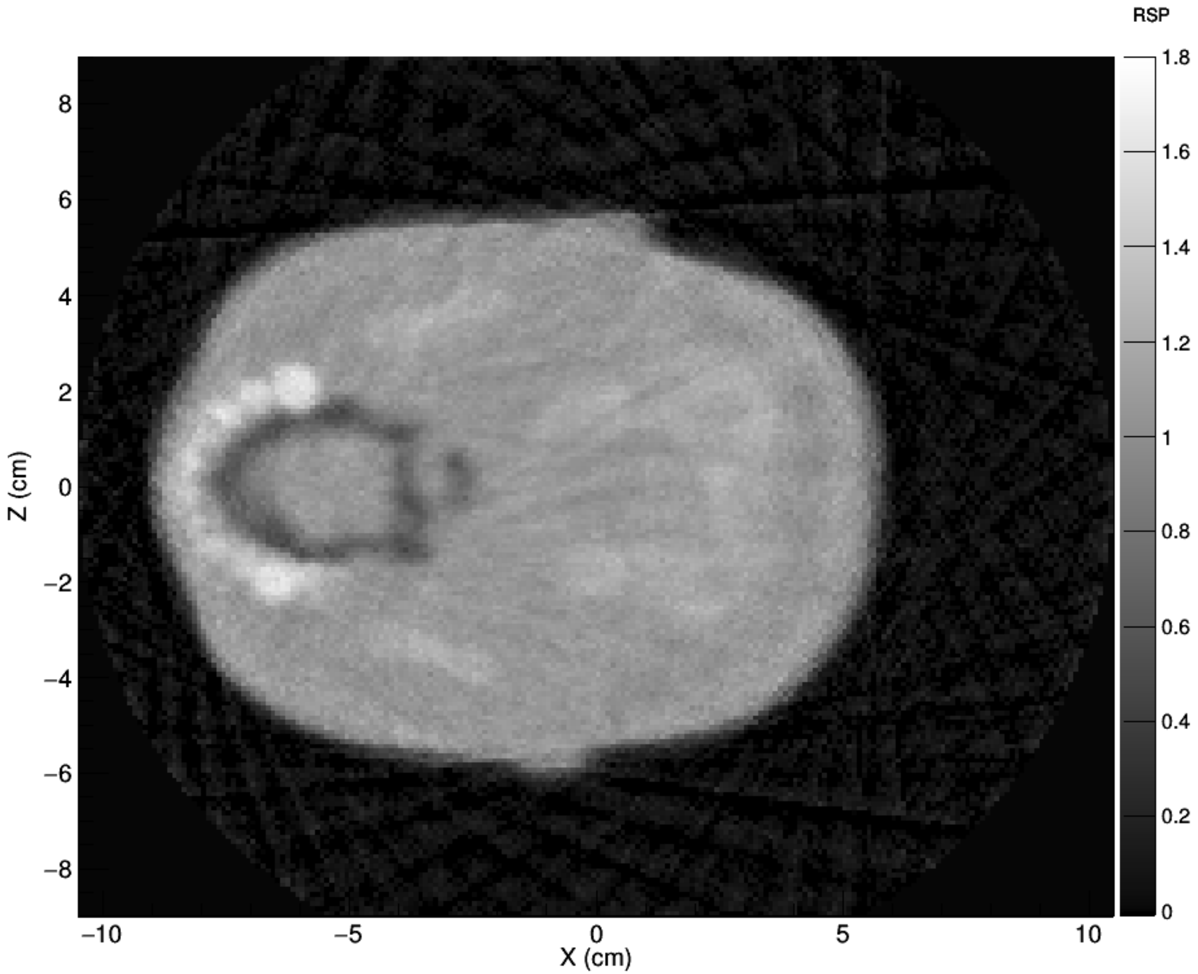

Fixed beam room – 180 angles

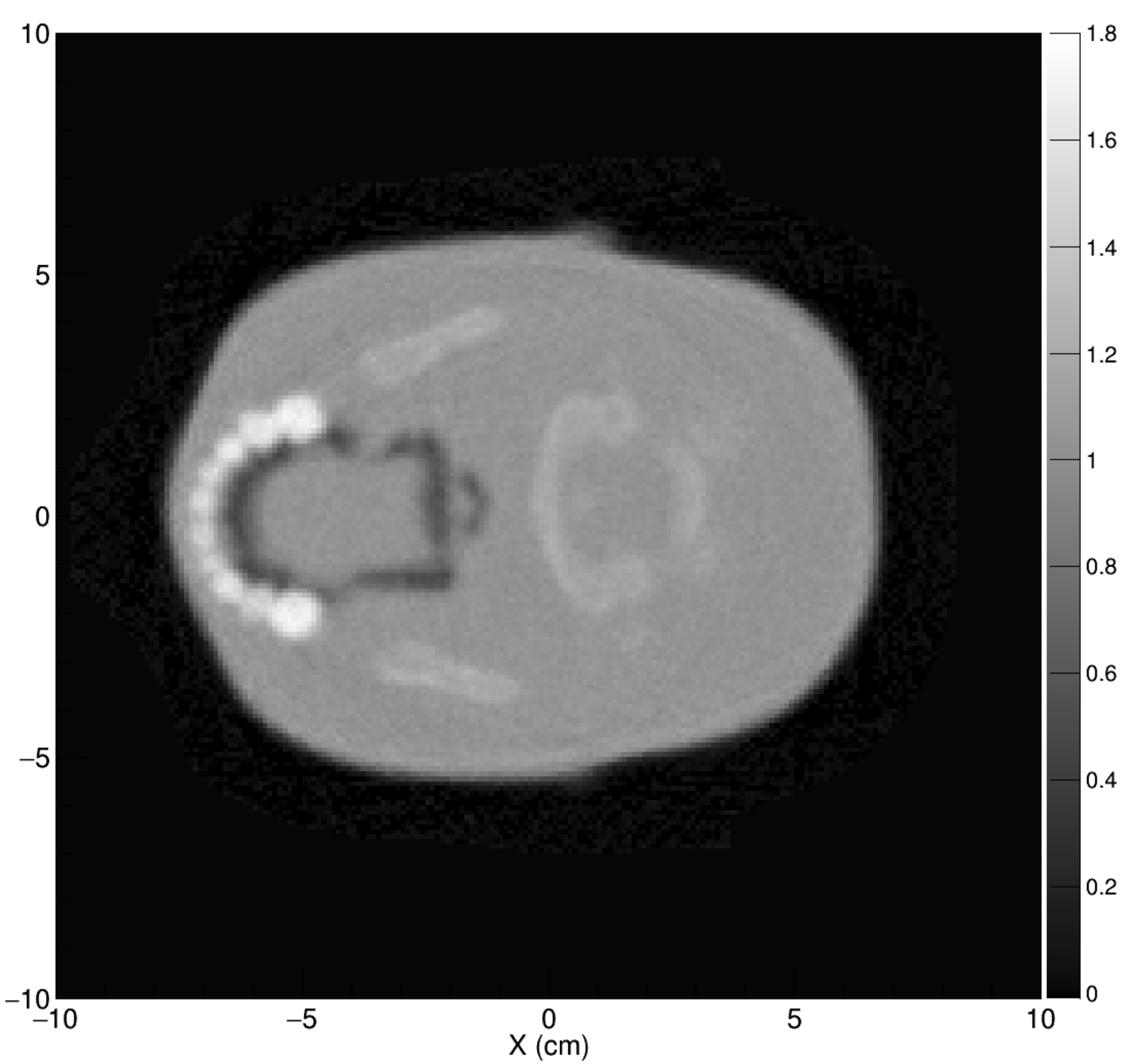

Gantry room data – 45 angles

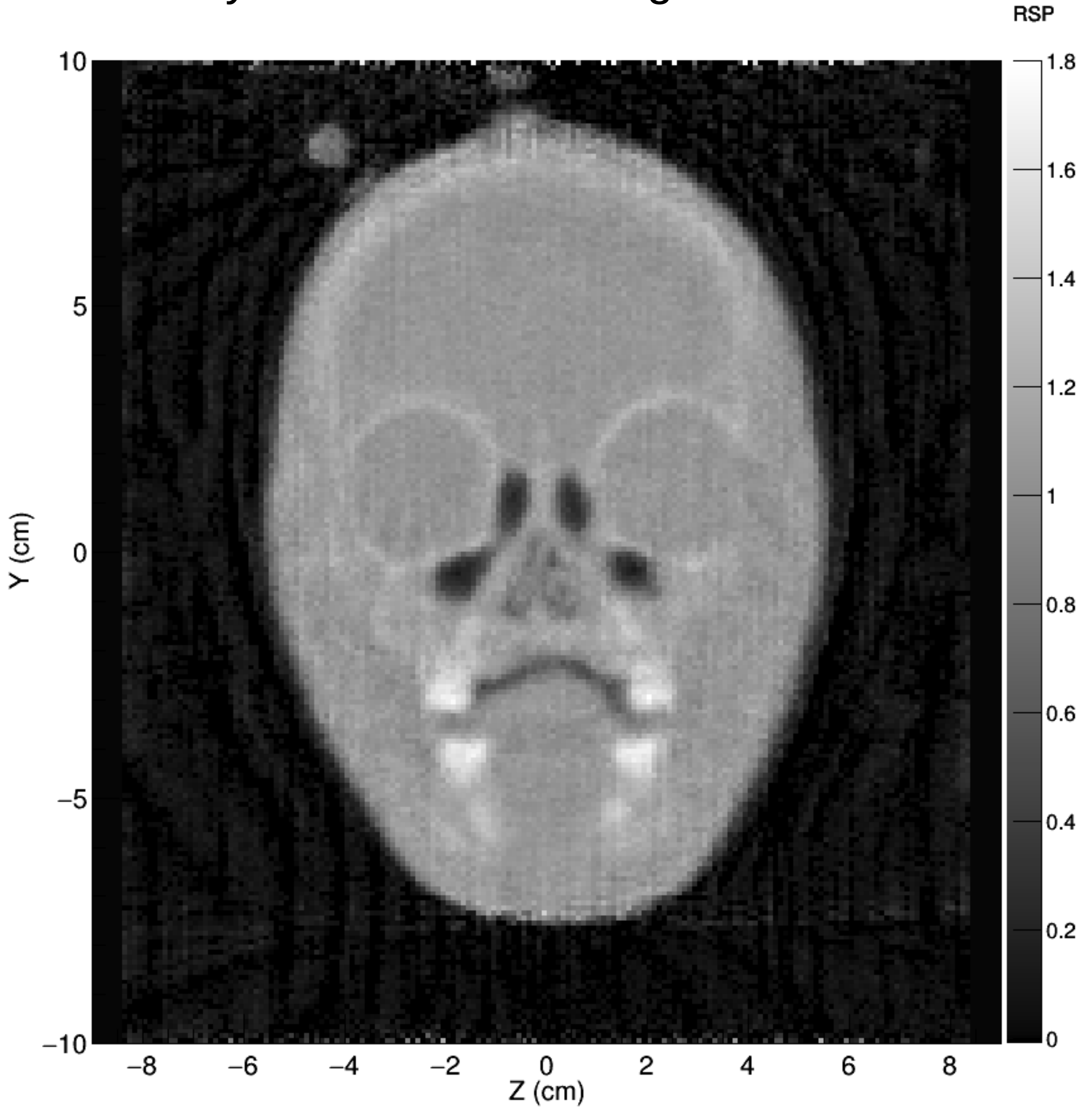

Fixed beam room – 180 angles

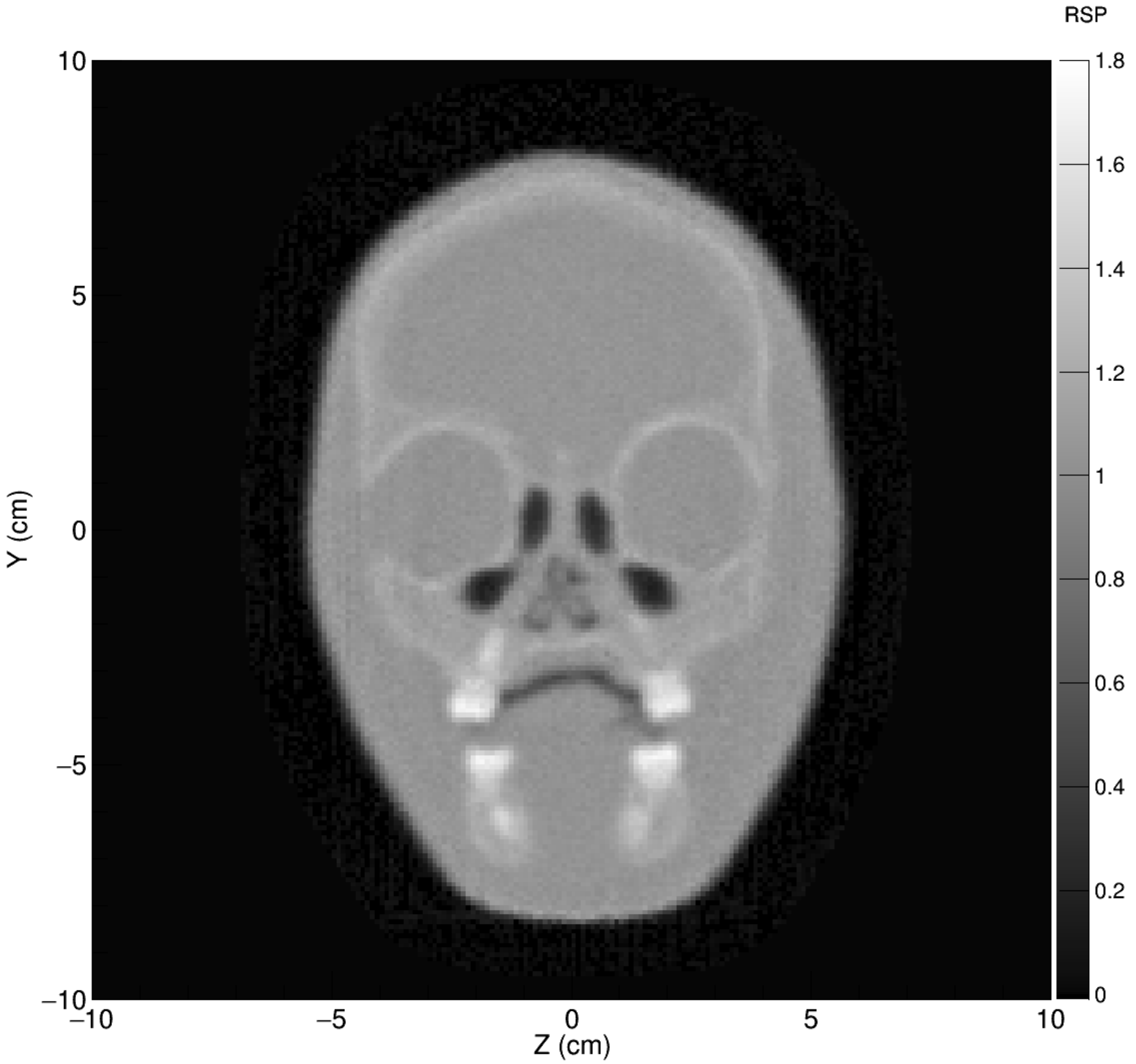

Gantry room data – 45 angles

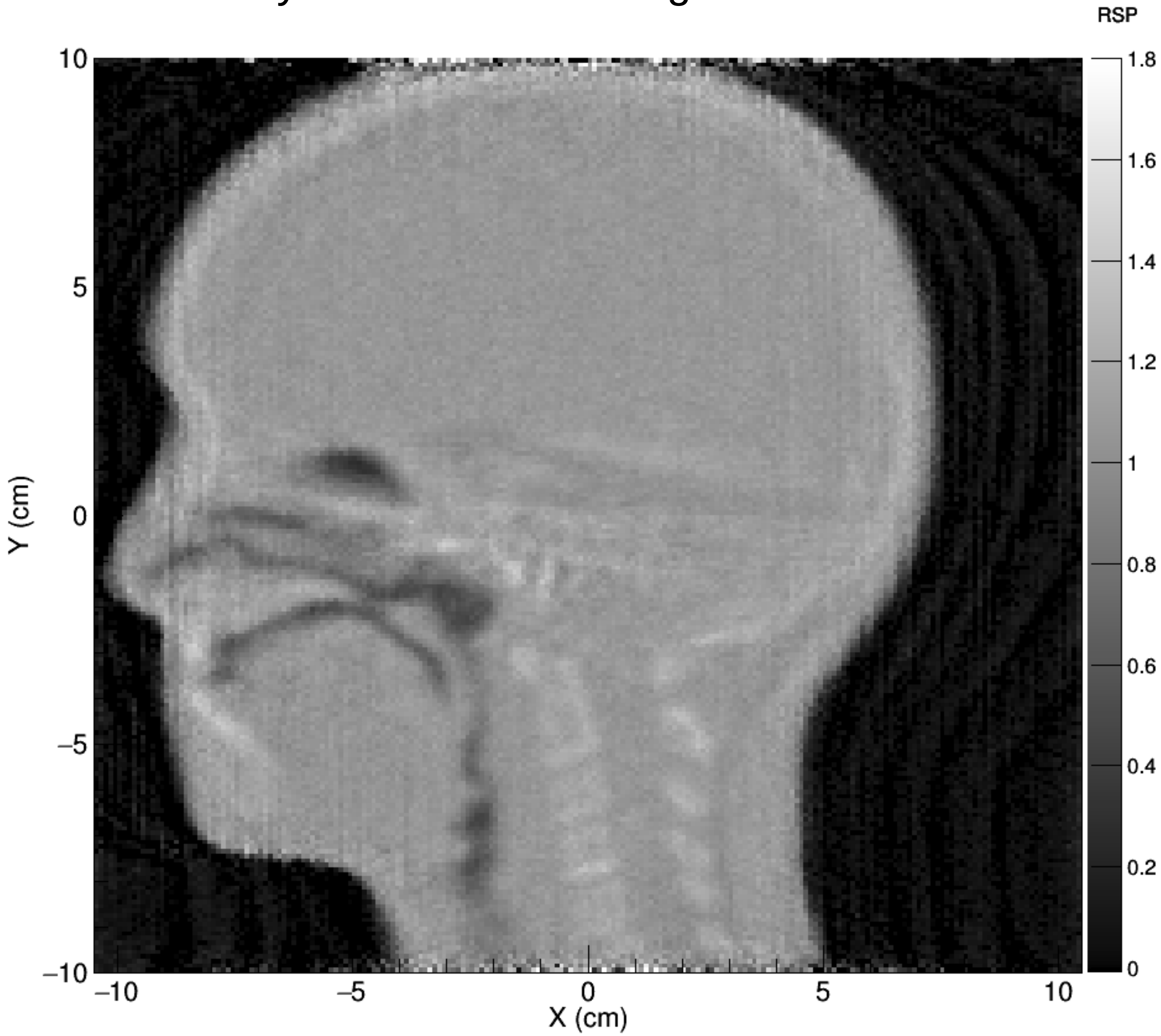

Fixed beam room – 180 angles

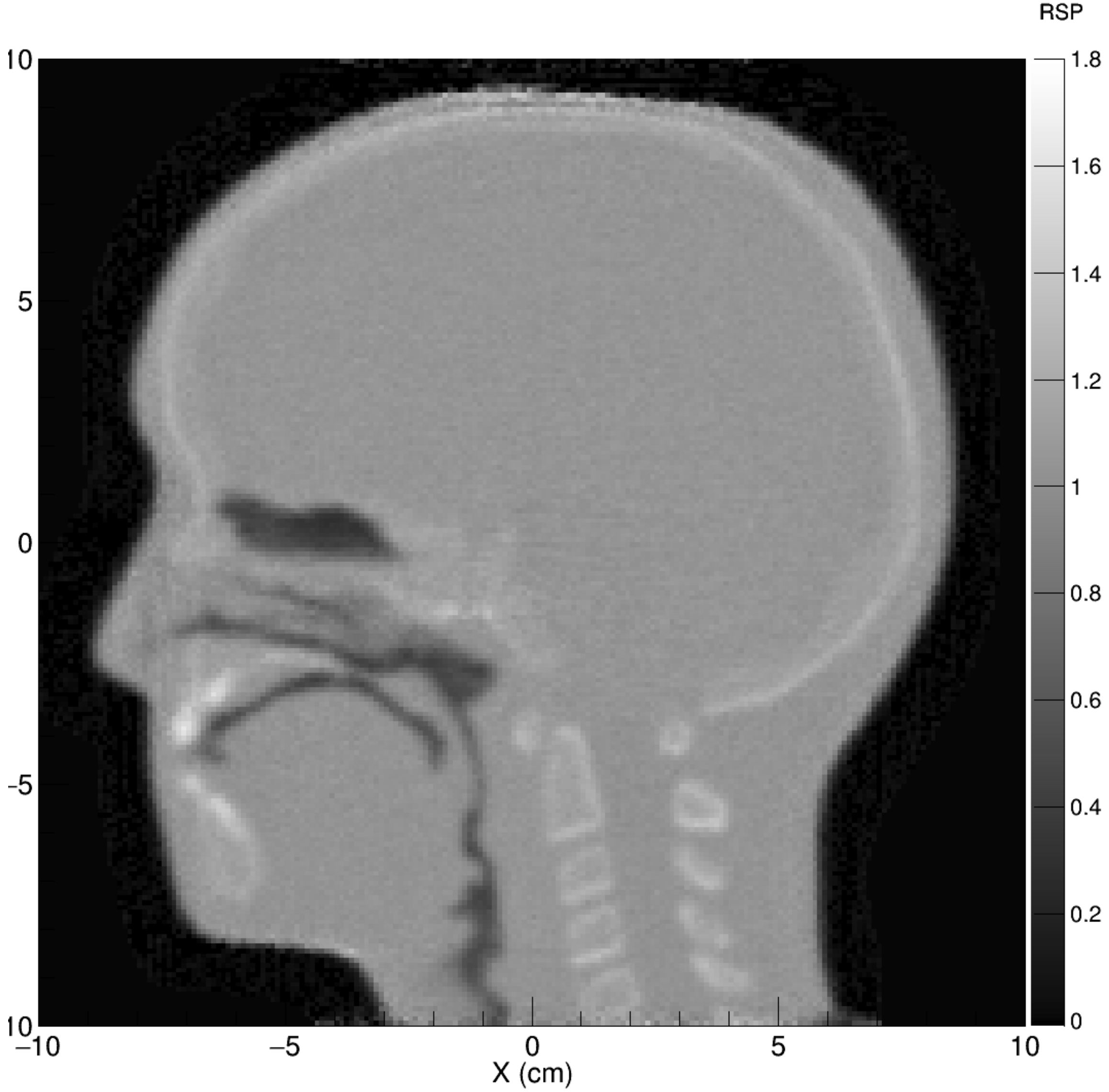

More tools to improve the image:

- Use of optical tracking markers to detect movement of trackers vs. patient

- 6D tracker alignment using beam spots – see talk by Kirk Duffin

- Apply angle-dependent position corrections to account for gantry sagging

- Angle-dependent range detector calibration

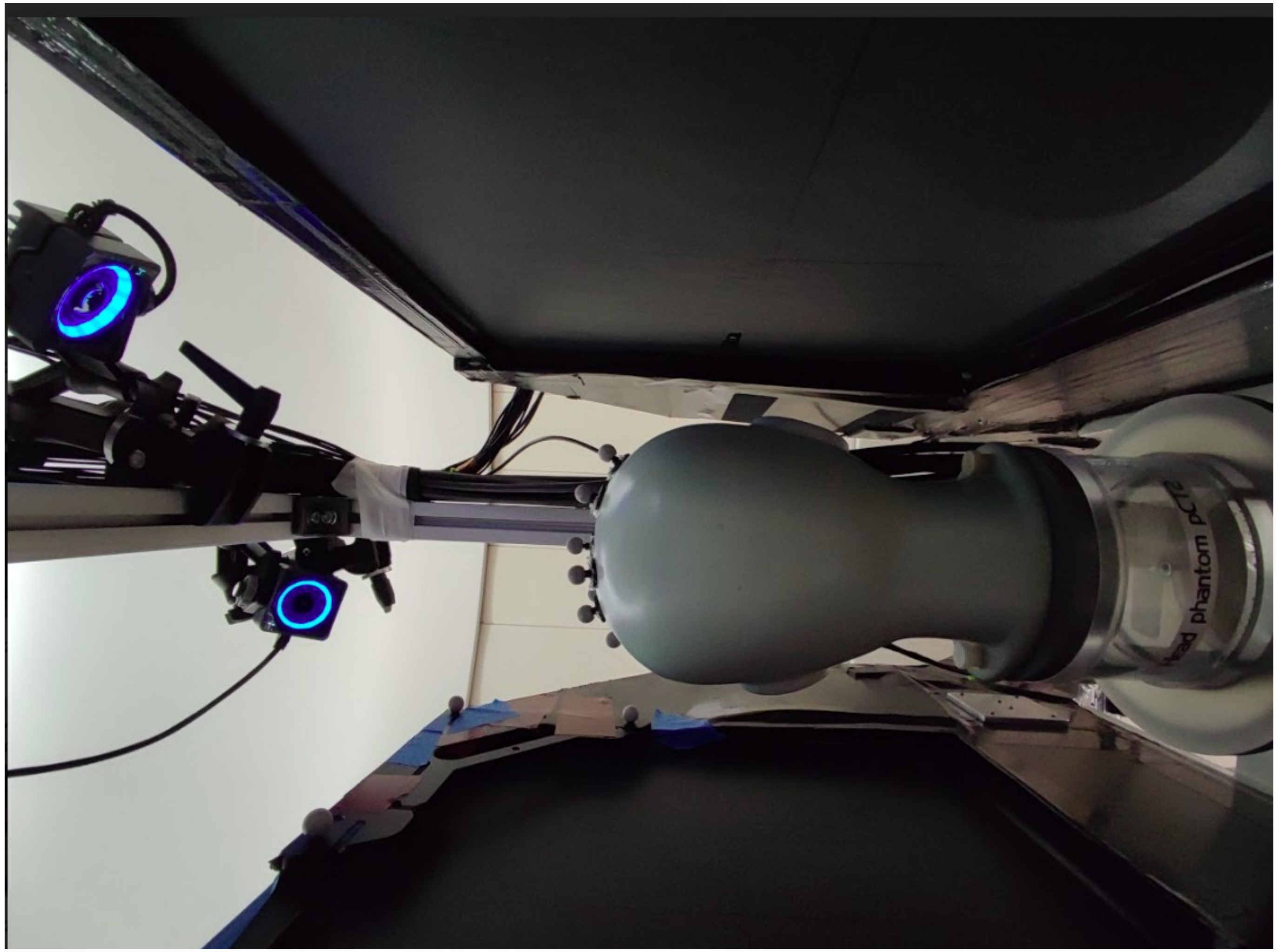

ProtonVDA

TRANSFORMING PROTON THERAPY

Conclusions:

Overall, a successful first test

We have demonstrated that pCT in a gantry system is challenging, but feasible.

Fixed-beam pCT is simpler due to:

- Single rotational axis
- Single detector alignment
- Single WEPL calibration

More work is needed to utilize all information in the image reconstruction.